

# An ESR Study of $\gamma$ -Irradiated Haemoglobin and DNA

A Thesis submitted by

**Nick Bartlett**

for the degree of

Doctor of Philosophy

in the

Faculty of Science

of the

University of Leicester

Department of Chemistry,  
The University,  
LEICESTER. LE1 7RH

DECEMBER 1985

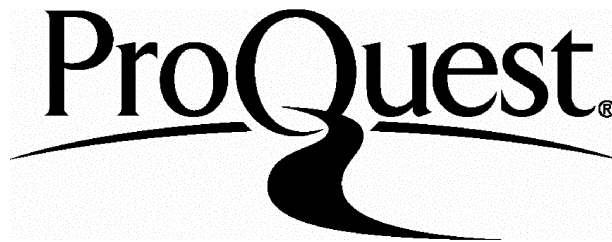
ProQuest Number: U360531

All rights reserved

INFORMATION TO ALL USERS

The quality of this reproduction is dependent upon the quality of the copy submitted.

In the unlikely event that the author did not send a complete manuscript and there are missing pages, these will be noted. Also, if material had to be removed, a note will indicate the deletion.



ProQuest U360531

Published by ProQuest LLC(2015). Copyright of the Dissertation is held by the Author.

All rights reserved.

This work is protected against unauthorized copying under Title 17, United States Code.  
Microform Edition © ProQuest LLC.

ProQuest LLC  
789 East Eisenhower Parkway  
P.O. Box 1346  
Ann Arbor, MI 48106-1346



*To my super Wife who has patiently supported and helped so much with the writing of this thesis. Also to my Mum, whose continual interest and encouragement enabled me to get there in the first place.*



STATEMENT

The accompanying thesis submitted for the degree of Ph.D. entitled "An ESR Study of  $\gamma$ -Irradiated Haemoglobin and DNA" is based on work conducted by the author in the Department of Chemistry of the University of Leicester mainly during the period between January 1981 and January 1984.

All the work recorded in this thesis is original unless otherwise acknowledged in the text or by references. None of the work has been submitted for another degree in this or any other university.

Signed: .....

Date: .....

## ACKNOWLEDGEMENTS

May I say what a pleasure it has been to work for such a brilliant and readily approachable man as Martyn Symons. I would like to thank him for all his help and endeavours during my time at Leicester. I would also like to thank Paul Cullis for all his help and support during the project.

I would like to say how lucky I was to have such a good work-mate and friend in Phil and how many good times were had in the company of Kleanthous and Rideout. In this context the name of George Eastland must not be excluded, who did so much to make life thoroughly enjoyable and interesting for us all.

I am indebted to Vicky and Ann who were responsible for converting some illegible piles of paper and graphs into a highly presentable document. Furthermore, I am so grateful for the accuracy of their excellent work which, of course, made my life so much easier.

Lastly, I would like to thank the Commission of the European Communities for the financial support that enabled me to pursue the research.

## LIST OF CONTENTS

Page No.

### CHAPTER 1 - HAEMOGLOBIN: THE STRUCTURE AND FUNCTION

References	23
------------	----

### CHAPTER 2 - ESR OF $\gamma$ -IRRADIATED HAEMOGLOBINS A, F AND MYOGLOBIN

Introduction	25
Experimental	34
Results	37
1. Frozen aqueous solutions of HbO <sub>2</sub> A	37
2. Frozen glassy solutions of HbO <sub>2</sub> A	39
3. Frozen aqueous glasses of HbO <sub>2</sub> F	49
4. Frozen aqueous glasses of oxymyoglobin	55
5. Deoxyhaemoglobin A	58
Discussion	63
References	69

### CHAPTER 3 - ELECTRON ADDITION TO THE (FeO<sub>2</sub>) UNIT OF OXYHAEMOGLOBIN GLYCERA

Introduction	73
Experimental Procedure	74
Results and Discussion	76
References	82

### CHAPTER 4 - ESR OF $\gamma$ -IRRADIATED DNA AND CONSTITUENTS

A. The Structure and Function of DNA	83
B. ESR of $\gamma$ -Irradiated DNA and Constituents	87
1. Guanine Compounds	88
2. Adenine Compounds	89
3. Cytosine Compounds	90
4. Thymine Compounds	91
5. DNA	93
References	100

### CHAPTER 5 - MODIFICATION OF $\gamma$ -INDUCED DNA DAMAGE IN THE PRESENCE OF ADDITIVES

Introduction	104
Experimental	114
Results and Discussion	115
Summary and Conclusions	142
References	145



# CHAPTER 1

**Haemoglobin: The Structure and Function**

Haemoglobin is the vital protein that conveys oxygen from the lungs to the tissues and facilitates the return of carbon dioxide from the tissues back to the lungs. Along with myoglobin they make up the respiratory haem proteins. The name 'haemoglobin' is given to these proteins when they are present in the blood of vertebrates, 'myoglobin' to those present in the smooth or striated muscles of all animals. The haemoglobin molecule consists of four polypeptide chains, two  $\alpha$  chains of 141 amino acid residues and two  $\beta$  chains of 146 amino acid residues each. Both chains, or subunits, have different amino acid sequences but similar tertiary structures. Each chain possesses one haem group, which is responsible for the red colour of blood. The haem consists of a porphyrin (protoporphyrin IX) ring with an Fe atom at its centre [Fig. 1]. The polypeptide chain, or globin, is made up of helical segments labelled A to H, the corners or non-helical segments are labelled AB, CD, EF, FG and GH whilst NA and HC denote the non-helical segments at the amino and carboxyl end of the chain; Figure 2 shows a sketch of the  $\beta$  subunit. The most significant difference between the two subunits is the absence of a D helix in the  $\alpha$  subunit. In the complete molecule the four subunits are closely joined to form a tetramer.

The other respiratory protein is myoglobin, its function is to combine with oxygen released by red cells, store it and transport it to the mitochondria where the oxygen generates chemical energy from the combustion of glucose. Myoglobin was the first protein whose three-dimensional structure was solved.<sup>1</sup> Its structure is analogous to that of the  $\beta$  subunit of haemoglobin and only consists of one polypeptide chain with one haem. In both proteins the oxygen binds to the ferrous iron atom at the centre of the porphyrin. As can be seen from Figure 1, the four porphyrin ligands are nitrogen atoms. The fifth bond from the haem is

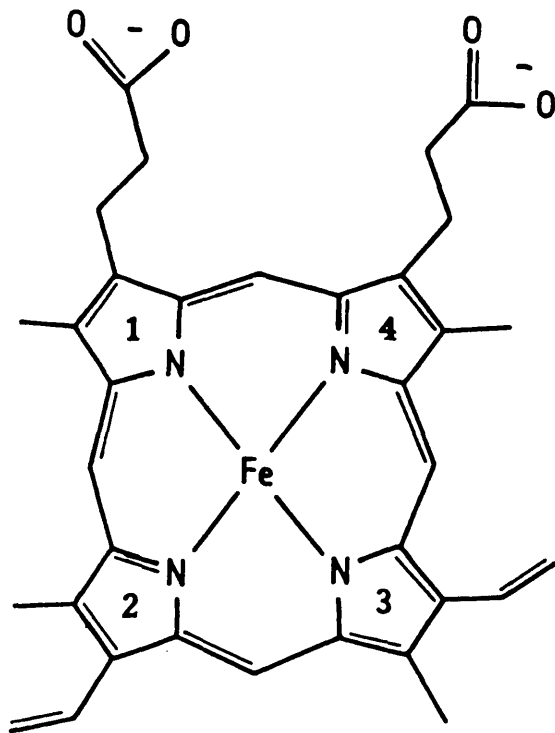


FIGURE 1

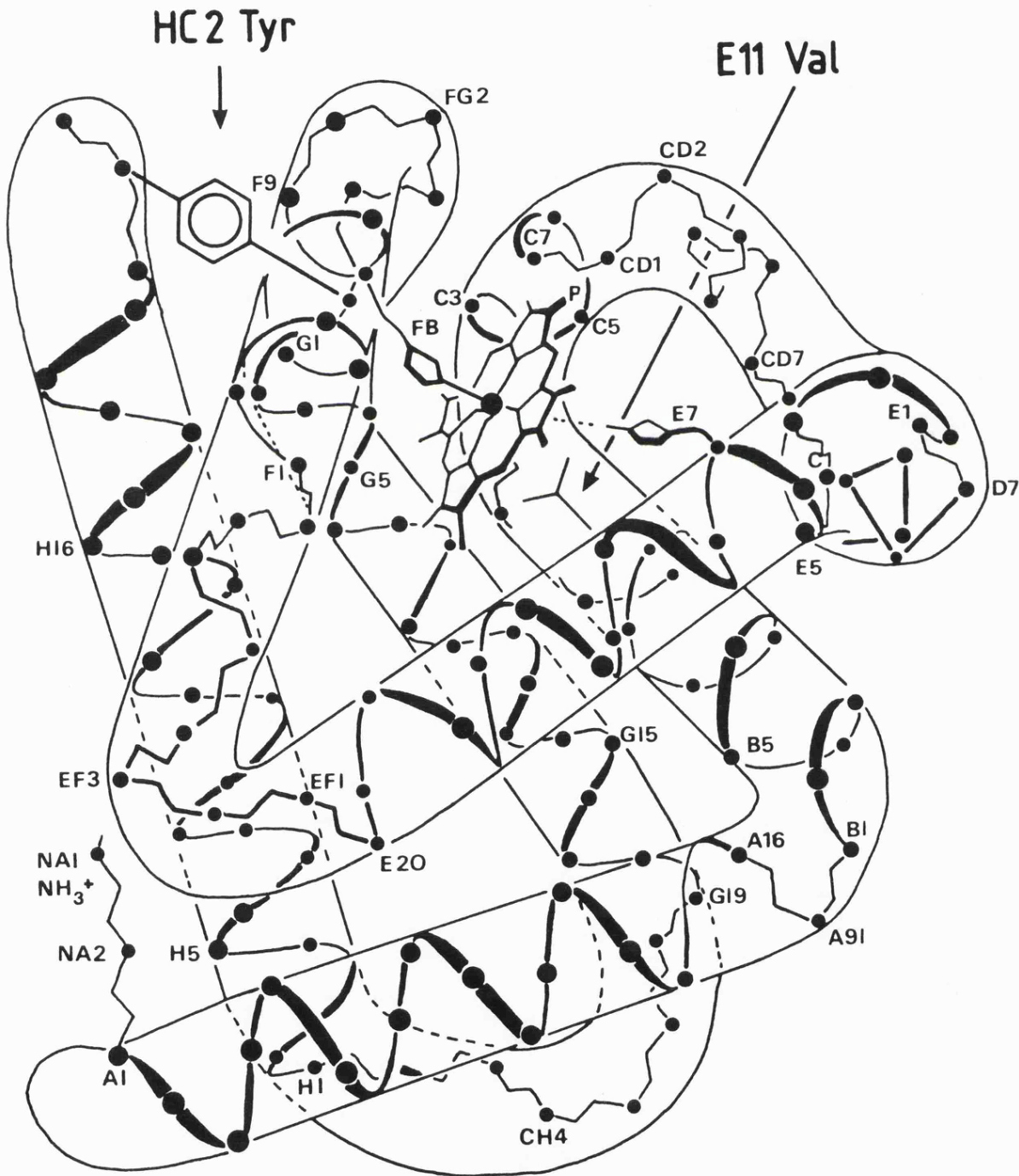
Structure of Proto Protoporphyrin IX.

attached to the globin via N<sub>ε</sub> of histidine (F8), called the proximal histidine, the sixth being to oxygen. In normal ferrous haem compounds the iron is oxidised on combination with oxygen yielding an Fe<sup>III</sup>-OH<sub>2</sub> complex formed via a bridged intermediate.<sup>2</sup> This is not the case in the two proteins as the folds of the polypeptide chain prevent the formation of the intermediate. The major difference in mechanism of oxygen binding between the two proteins becomes evident on plotting graphs of the ratio of oxygenated to deoxygenated protein against the partial pressure of oxygen, as shown in Fig. 3a. The myoglobin plot shows that at very low partial pressures the affinity of the molecule for oxygen is very high and that the molecule becomes saturated with oxygen at very low partial pressures.

In contrast, haemoglobin appears to have a very low affinity for oxygen at low partial pressures but once some oxygen is bound its

**FIGURE 2**

Secondary and tertiary structure showing  $\alpha$  carbons of the  $\beta$ -subunit of haemoglobin.



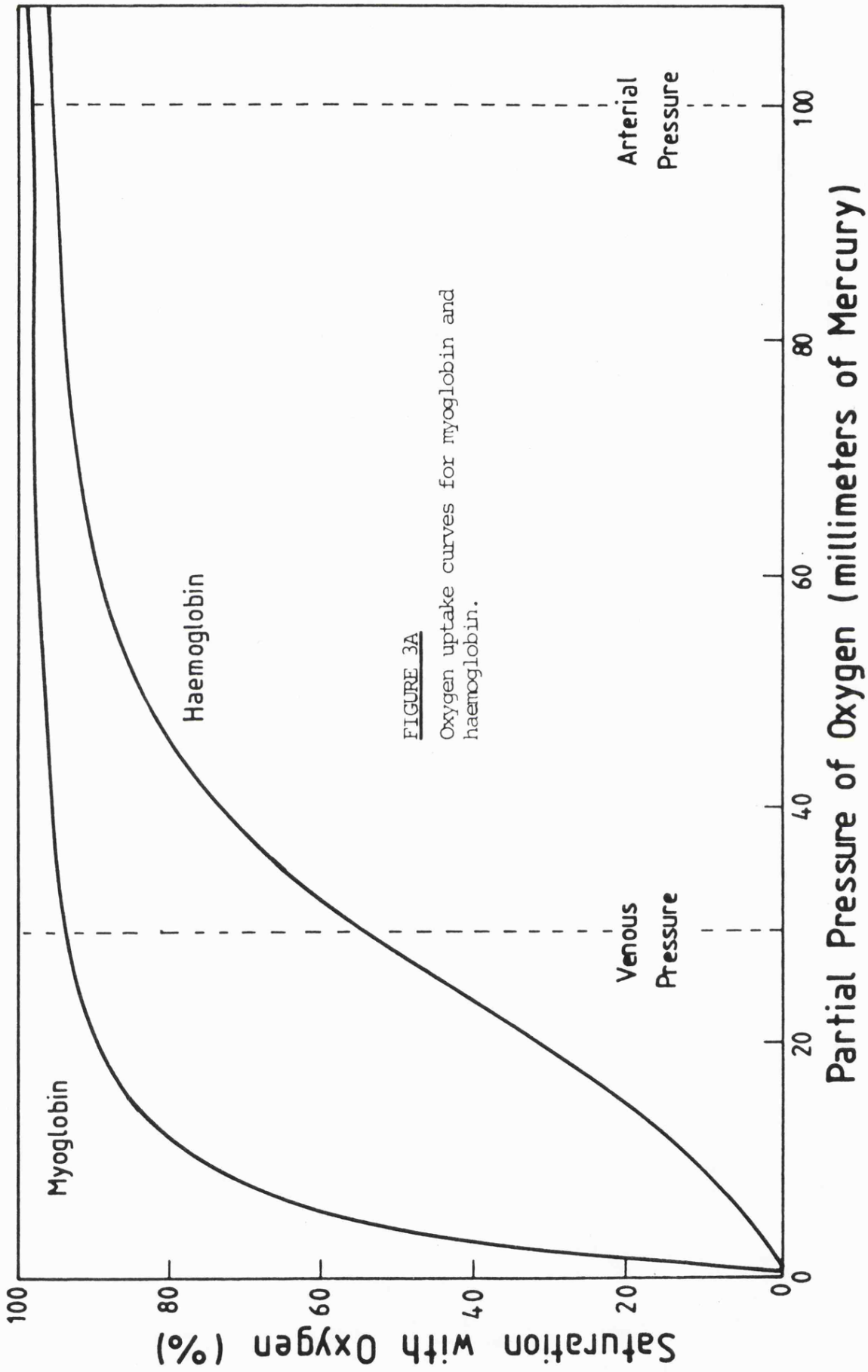
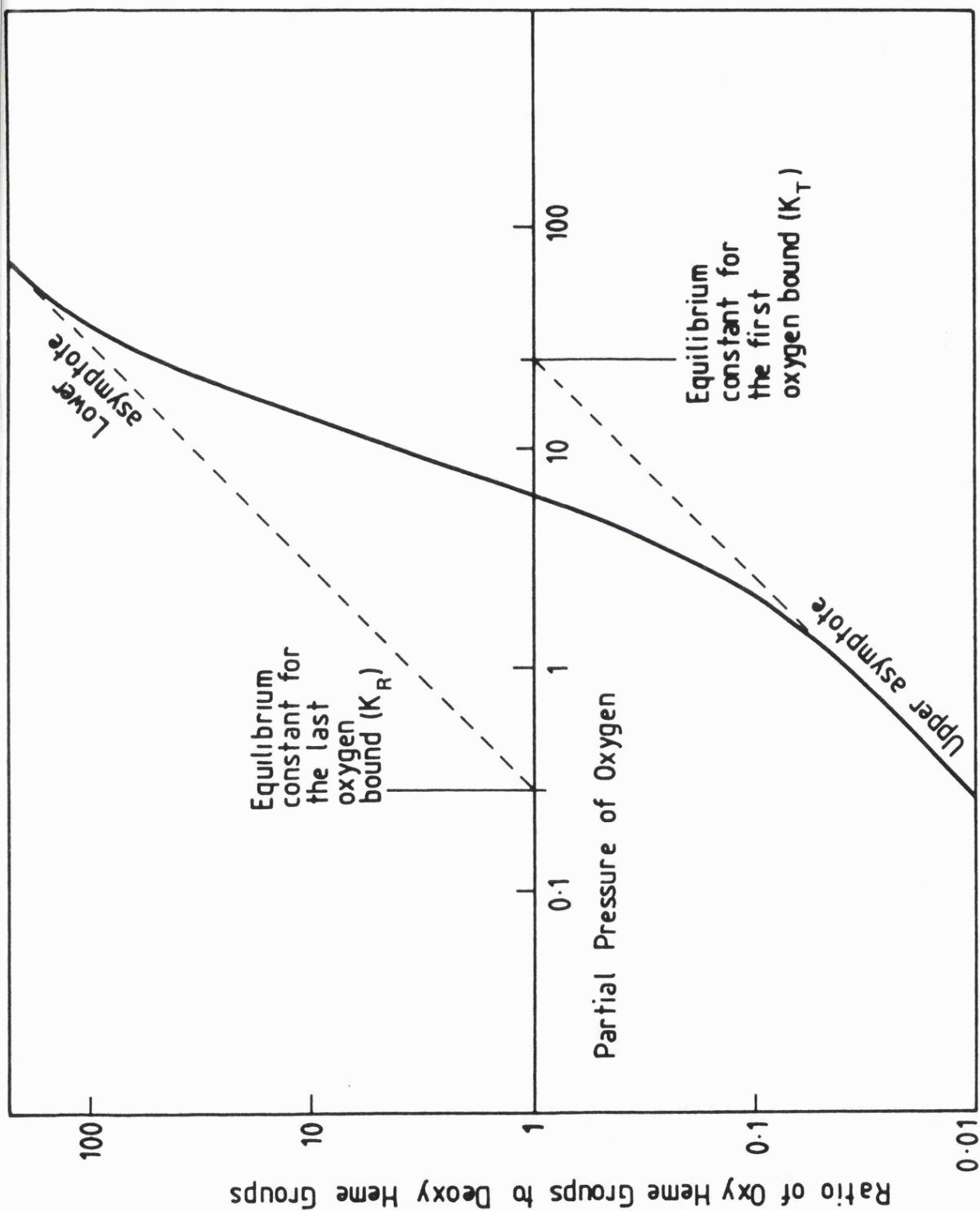


**FIGURE 3A**  
 Oxygen uptake curves for myoglobin and haemoglobin.

FIGURE 3B

A log plot of the oxygen uptake curves.



affinity increases according to the gradient of the slope and most of the oxygen is then taken up over a small range of oxygen partial pressure. It is thus evident that deoxygenated haemoglobin has a barrier to oxygen binding and this barrier becomes less as successive oxygen molecules bind to the subunits of the tetramer until, finally, the molecule becomes fully oxygen saturated. This suggests that there is some kind of communication between the haems of each molecule called haem-haem interaction or, more generally, cooperativity. The degree of cooperativity can be expressed in terms of Hill's coefficient which has a value of around 3 for oxyhaemoglobin and falls to unity with loss of cooperativity. This coefficient is the gradient of the line in the log plot of Fig. 3b and it stems from Hill's equation for the equilibrium  $\text{Hb}_n + n\text{O}_2 \rightleftharpoons \text{Hb}_n(\text{O}_2)$

$$Y = \frac{Kp^n}{1 + Kp^n}$$

where K and n are constants, Y is the fractional saturation of haemoglobin with oxygen and p is its partial pressure.

The cooperative oxygen binding of haemoglobin is vital for it to act efficiently. For the partial pressure of oxygen in the human tissues, where haemoglobin releases oxygen, is only 35 mmHg of mercury which would mean that only 10% of oxygen carried would be released if there was no cooperativity, i.e. if the oxygen uptake curve was hyperbolic as in myoglobin. Consequently, there is a need for certain factors to ensure that haemoglobin can readily lose oxygen in the tissues, i.e. its affinity for oxygen must be low. These factors came to light when it was discovered that Hill's coefficient and the oxygen affinity of the protein depend on the concentration of several chemical factors in the red blood cell; protons, carbon dioxide, chloride ions and 2,3-diphosphoglycerate (DPG). All these factors, if their concentration is increased shift the oxygen equilibrium curve to the right to lower affinity and

make it more sigmoid. None of these factors influence the oxygen equilibrium curves of myoglobin as it shows no cooperativity and has  $n=1$ . As myoglobin is structurally analogous to the  $\beta$  subunit and very similar to the  $\alpha$  subunit it seems clear that the tetrameric structure of haemoglobin is responsible in some way for its cooperativity as myoglobin is only a monomer. Furthermore, it was found that deoxyhaemoglobin crystallizes in a different form to oxyhaemoglobin as far back as 1938 by Felix Haurowitz in Prague. This has been verified by the X-ray diffraction results of Perutz and his colleagues at Cambridge,<sup>3-9</sup> the tertiary and quaternary structures changing between the oxy and deoxy forms.

In 1964 Jacques Monod, Jeffries Wyman and Jean-Pierre Changeux put forward their two state allosteric model of cooperativity.<sup>10</sup> Knowing that deoxy and oxyhaemoglobin were of different structure, they postulated that these structures should be distinguished by the arrangement of subunits and by the number and strength of the bonds between them. The state with fewer and weaker bonds between the subunits would be free to develop its full activity (i.e. oxygen affinity in haemoglobin case) and this they labelled R for "relaxed". The other structure they named T for "tensed" as its oxygen affinity would be reduced due to more and stronger bonds between the subunits. They then proceeded to describe a mathematical model that could fit the properties of allosteric enzymes and proteins which contained three independent variables,  $K_R$  and  $K_T$ , being the dissociation constants of oxygen in the two states respectively, and  $L$  the equilibrium constant for the  $R \rightleftharpoons T$  equilibrium. This model seemed to fit well for the haemoglobin case. The progressive increase in oxygen affinity could be explained by a switch from the low affinity T structure to the high affinity R structure. Furthermore, the chemical

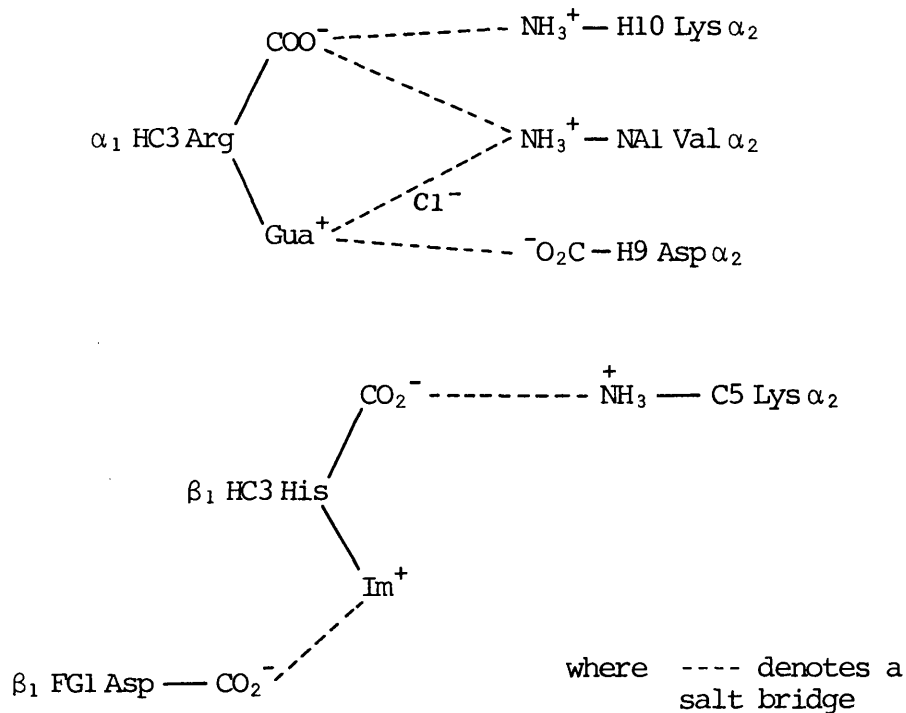
agents that altered the oxygen equilibrium curves (allosteric effectors) could do so by altering the  $R \rightleftharpoons T$  equilibrium in favour of the T [low affinity] structure. This would raise L, the fraction of molecules in the T structure without altering the oxygen equilibrium constants  $K_T$  and  $K_R$  of the two structures.

It was now left to experiment to confirm the theory and discover in detail the nature of the differences between the structures, to identify the bonds between them and the structural rôles of the allosteric effectors. The crystallographic data has been responsible for elucidating the detailed structures, the majority of which have been produced by Max Perutz who proposed a stereochemical model for the cooperative effects in 1970.<sup>11</sup> This model has been criticised in parts but the results are fundamental and unquestioned. Better resolution has enabled Baldwin and Chothia to put forward a more accurate analysis recently,<sup>12</sup> but a well-resolved map of oxyhaemoglobin has yet to be produced although one is shortly to be published.<sup>13</sup> The chief concern with X-ray data is, of course, that the results come from the solid phase whilst haemoglobin exists in vivo in solution. However, many other forms of experiment can be performed on haemoglobin in solution, a wide range of spectroscopy being now available. The results from Infra-Red, Optical, Nuclear Magnetic Resonance, Circular Dichroism and Electron Spin Resonance spectroscopy tend to back up the crystallographic data inferring that the situation is not far removed in the liquid state from the solid state. I shall now proceed to outline the main differences between the structures as discovered by Perutz<sup>11</sup> and Baldwin and Chothia<sup>12</sup> along with some of the liquid phase results. Also I shall describe the mechanisms of action of the allosteric effectors which are intricately linked with the  $R \rightleftharpoons T$  equilibrium as was earlier suggested in the Monod, Wyman and Changeux

model.<sup>10</sup>

So far the only ligand I have mentioned that binds to haemoglobin is oxygen - however, a number of others exist. Other ligands that bind to ferrous haemoglobin include carbon monoxide, which in fact has a higher binding constant than oxygen, hence its toxicity, and nitric oxide. There is further an oxidised form of haemoglobin called methaemoglobin that exists in the blood in small concentrations. In this form water is the sixth ligand rather than oxygen and the iron is in the ferric form. Water is not the only ligand that can combine to the ferric form, others being  $F^-$ ,  $CN^-$ ,  $N_3^-$  and  $NCS^-$  also denoted met but, in these cases, the ligand is specified, i.e. azidomet or fluoromet. All these liganded haemoglobins exist in the R state and their tertiary structures are very similar. Thus as no maps of oxyhaemoglobin were available, Perutz used horse methaemoglobin map as his model for the R structure.

The allosteric model of Monod, Wyman and Changeux predicted that the T state would be bound by strong bonds between the subunits which would be weaker or broken in the R state. Perutz correctly identified these bonds and called them salt bridges. These salt bridges were found to be broken in the R state. They occur at the C-terminal end of each chain in the T state. The carboxyl group of the  $\beta_1$  chain C-terminal group Histidine HC3 is salt-bridged to the  $\epsilon$  amino group of Lysine C5 in the  $\alpha_2$  chain whilst its imidazole is bridged to the carboxyl group of Aspartate FG1 in its own  $\beta_1$  chain. At the  $\alpha_1$  chain C-terminal the carboxyl group of Arginine HC3 $\alpha_1$  is salt-bridged to the  $\alpha$  amino end of two groups in the corresponding  $\alpha_2$  chain H10 $\alpha_2$  Lysine and NAl $\alpha_2$  Valine. The guanidium group of Arginine HC3 $\alpha_1$  is bridged to the carboxyl group of Aspartate H9 $\alpha_2$  and chloride bridged to the  $\alpha$  amino group of NAl Valine  $\alpha_2$ .

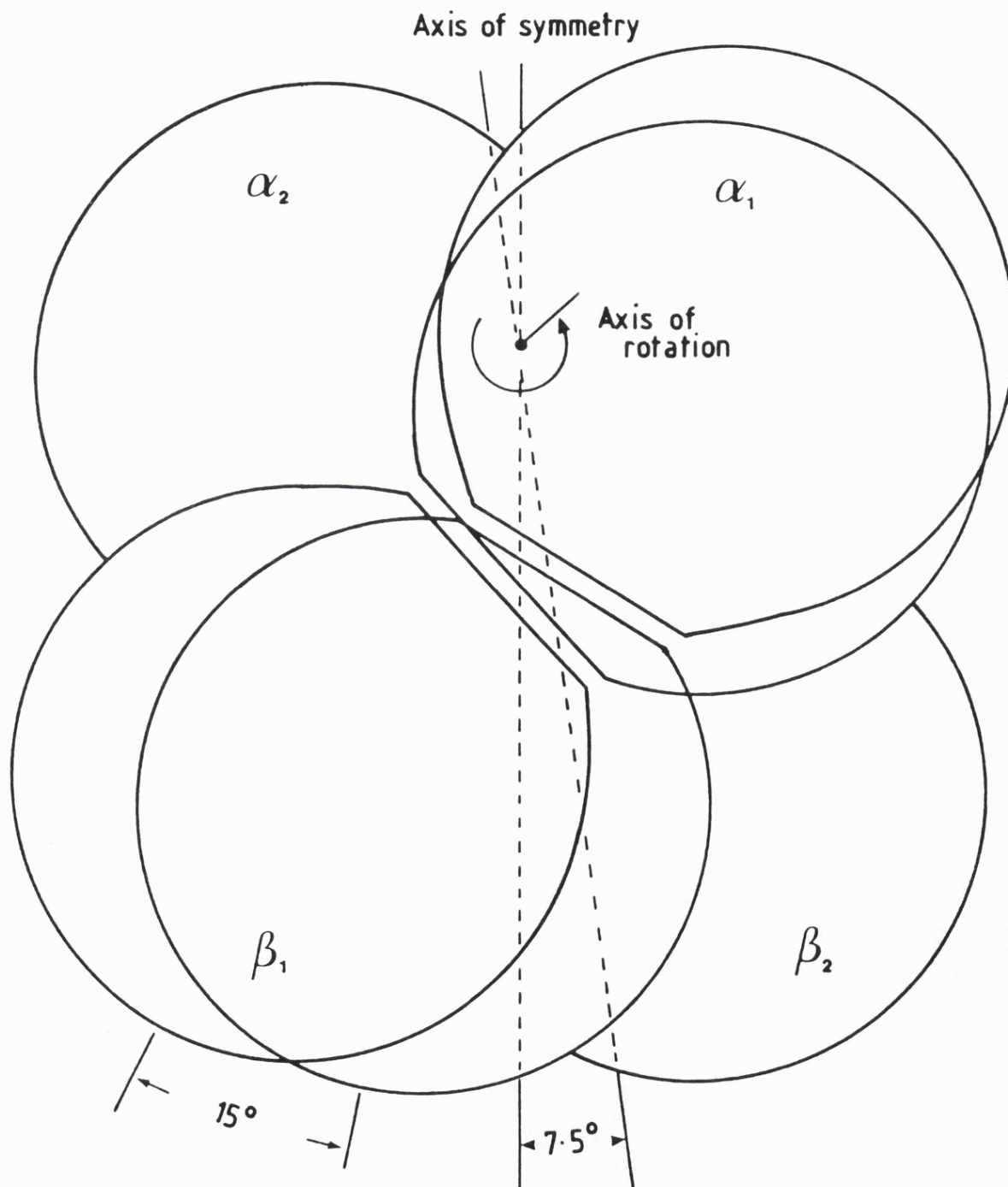


In haemoglobin the four subunits are arranged at the vertices of a tetrahedron around a twofold symmetry axis. Due to the twofold symmetry there are only four distinct contacts  $\alpha_1\beta_1$ ,  $\alpha_2\beta_2$ ,  $\alpha_1\beta_2$  and  $\alpha_2\beta_1$  as opposed to six. The  $\alpha_1\beta_1$ ,  $\alpha_2\beta_2$  contacts make up 60% of the total contact area, each contact comprises of about 35 amino acid residues tightly linked by from 17 to 19 hydrogen bonds. These bonds make the contacts so strong that liganded haemoglobin can be split into dimers of  $\alpha_1\beta_1$  and  $\alpha_2\beta_2$ . Consequently these contacts are hardly altered by a transition from one structure to the other.

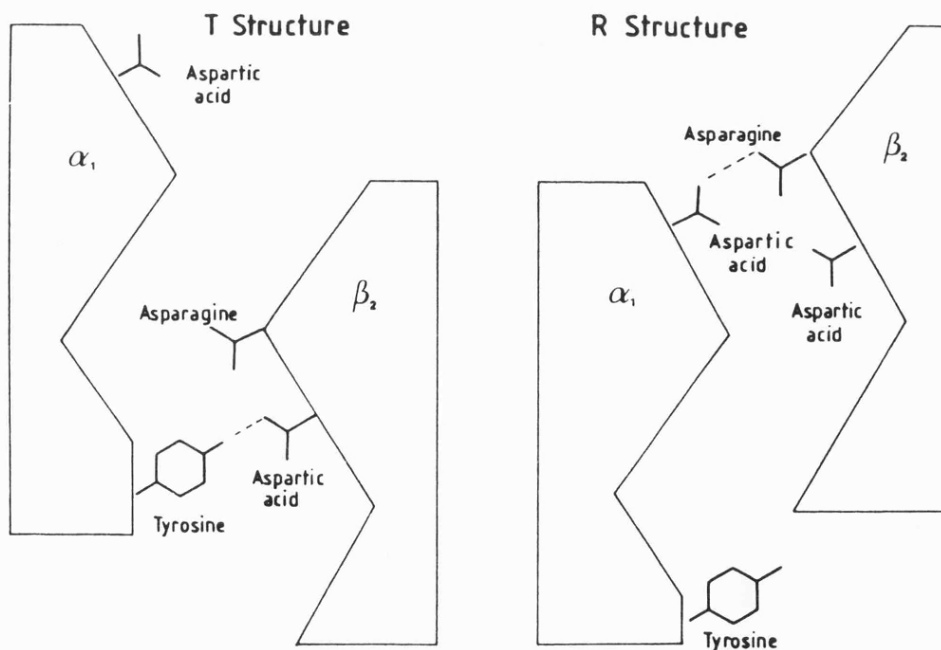
On the other hand, the  $\alpha_1\beta_2$  and  $\alpha_2\beta_1$  contacts shift by up to  $7 \text{ \AA}$  on the quaternary structural interchange [Fig. 4]. In both R and T states the  $\alpha_1\beta_2$  and  $\alpha_2\beta_1$  contacts are stabilised by van der Waal's contacts and hydrogen bonds. In each case the FG section of one subunit makes contact with the C helix of the other subunit and vice versa. The  $\alpha_1\beta_2$  contact in the T structure is held in position by a different set of hydrogen bonds from the contact in the R structure. The contact is dovetailed so

FIGURE 4

Rearrangement of subunits during the transition from the T structure to the R structure consists mainly in a rotation of one pair of subunits with respect to the other pair. Each alpha chain is bonded strongly to one beta chain, and the dimers formed in this way move as rigid bodies. If one dimer is held fixed, the other turns by 15 degrees about an off-centre axis and shifts slightly along it. The twofold symmetry of the molecule is preserved, but the axis of symmetry is rotated by 7.5 degrees.



that a turn of the C helix by one subunit fits into a V-shaped groove formed by the C $_{\alpha}$  of FG5 Val of the other subunit. Figure 5 shows the alternative hydrogen bonds formed between the subunits in the two structures. In the T structure the side chain of His  $\beta_2$ 97(FG4) packs between Thr  $\alpha_1$ 41(C6) and Pro  $\alpha_1$ 44(CD2) and the side chain of Asp  $\beta_2$ 99(G1) forms a hydrogen bond to the hydroxyl group of Tyr  $\alpha_1$ 42(C7). On ligation, however, His  $\beta_2$ 97 packs between Thr  $\alpha_1$ 38(C3) and Thr  $\alpha_1$ (41) and the side chain of Asp  $\beta_2$ 99(G1) no longer forms a hydrogen bond. This region has two distinct stable packing arrangements and any intermediate position would be unstable. The G helix in  $\beta_2$  now moves closer to the corresponding G helix of  $\alpha_1$  and O $_{\delta}$  of Asp  $\alpha_1$ 94(G1) hydrogen bonds to N $_{\delta}$  of Asn  $\beta_2$ 102(G4). This switch is shown in a very simplified manner in Figure 5. Of the two FG-C contacts that take place in the  $\alpha_1\beta_2$  contact it appears that the  $\alpha_1$ FG-C $\beta_2$  contact acts as a flexible joint on change



**FIGURE 5**

A diagrammatic view of the quaternary structural change at the  $\alpha_1\beta_2$  contact.

of structure as in both cases (R and T) the same side chains are involved but with different detailed contacts. The switch then occurs at the  $\alpha_1\text{C}-\text{FG}\beta_2$  section of the  $\alpha_1\beta_2$  contact. The steric barriers opposing the slide, which must take place at this section if a change of structure occurs, are concentrated where the side chains of His  $\beta 97(\text{FG4})$  have to pass the side chains Thr  $\alpha 41(\text{C6})$ .

I have now discussed the quaternary structures of the two states but what of the allosteric effectors that bias the equilibrium towards the low affinity T state? Their effects can be explained in terms of strengthening existing salt bridges or adding new inter- and intra-subunit bridges. The salt bridges explain both the lowering of the oxygen affinity by protons and the uptake of protons on oxygen release - a phenomenon known as the Bohr effect. The Bohr effect is only observed on change of quaternary structure. As it is dependent on proton concentration it is dependent on pH. At a pH above 6.0 haemoglobin takes up protons on release of haem ligands; this is known as the alkaline Bohr effect.

The alkaline Bohr effect has a twofold function. On liberation of oxygen haemoglobin neutralizes the protons released in the blood (by combining with them) from the reaction of carbon dioxide and water. The production of bicarbonate by this reaction enables the carbon dioxide to be transported from the tissues to the lungs. In the lung oxygen is bound and protons released driving the bicarbonate equilibrium towards the reformation of carbon dioxide which, not being very soluble, is then exhaled. On returning to the tissues, where the pH is more acidic, the Bohr effect is again functional, the proton concentration lowering the oxygen affinity of the protein. Below pH 6 the Bohr effect is reversed, protons being liberated on release of haem ligands. As pH's below 6 are

unlikely to occur in vivo this acid Bohr effect may have no physiological significance. Wyman showed that the Bohr effect could be attributed to ionizable groups with a pK close to 7.0 which might release or take up protons as a result of oxygenation of the iron atoms.<sup>14</sup> With the help of the higher resolution maps Perutz et al.<sup>15,16,17</sup> identified three groups responsible for the effect. Two of the three groups are salt-bridged groups whose environment alters on change of structure. All three groups are weak bases with pK's close to 7 which alter on change of quaternary structure. The first is Valine NAl $\alpha$  whose involvement was inferred after the discovery that blocking the  $\alpha$  amino groups of Val NAl $\alpha$  with cyanate inhibited about one quarter of the Bohr effect.<sup>16</sup> The pK's of the  $\alpha$  amino groups of the N-terminal residues are normal in liganded haemoglobin as they are free to rotate according to the electron density maps. However on deoxygenation or ligand loss these groups become salt-bridged to the C-terminal of the other  $\alpha$  chain. This linkage of the  $\alpha$  amino group of Valine to the  $\alpha$  carboxyl group of the neighbouring arginine raises the pK of the  $\alpha$  amino group in deoxyhaemoglobin. From the deoxyhaemoglobin map it can be seen that the  $\alpha$  amino group of Val NAl $\alpha_1$  is facing and in close proximity to the carboxyl of Arg 141 $\alpha_2$  whose negative charge will tend to affect the pK of the amino group.

In his 1970 paper<sup>17</sup> Perutz postulates that a second contributory effect from the  $\alpha$  chains comes from a change in the pK of histidines (122)H5 $\alpha_1$ . In liganded haemoglobin the centre of the histidine imidazole is 4.5 Å from the positively charged guanidinium group of Arg 141 $\alpha_2$  and 5.5 Å from the carboxyl group of Asp126 $\alpha_1$ , so it is subject to a slight net positive charge. In deoxyhaemoglobin these distances alter to 7.5 Å and 3 Å respectively; thus the imidazole is now subject to a negative charge resulting in a pK that is lowered in liganded and raised in unliganded

haemoglobin. However, on production of higher resolution maps of methaemoglobin<sup>18</sup> and deoxyhaemoglobin,<sup>8</sup> it was discovered that the  $\alpha$ 122 histidine interacted identically in both structures and, therefore, was unlikely to contribute to the Bohr effect. However in 1978 Nishikura<sup>19</sup> measured the pK for His 122 $\alpha$  and found it to be 6.6 in deoxyhaemoglobin and only 6.1 in carbon monoxyhaemoglobin (HbCO) showing that it contributes about 20% to the Bohr effect. Its involvement in the Bohr effect is indicated by the reduced alkaline Bohr effect of haemoglobin Tacoma<sup>20,21</sup> in which the neighbouring Arg B12(30) $\beta$  is replaced by Serine<sup>22</sup> and of the embryonic human haemoglobin Portland and Llama haemoglobin in which His H5 $\alpha$  is replaced by Aspartic acid.

The  $\beta$  chain contribution to the Bohr effect stems from His HC3(146) $\beta$ . Its imidazole changes pK on structure change as it is free in liganded haemoglobin and fixed in deoxyhaemoglobin. In deoxyhaemoglobin the imidazole of His HC3 $\beta$  forms a salt bridge with Asp 94 $\beta$  of the same chain. This raises the histidine's pK by interaction with the aspartate. The rôle of His 146 $\beta$  was confirmed by a 50% reduction in the alkaline Bohr effect in des- his 146 $\beta$  haemoglobin<sup>23</sup> (enzyme digested haemoglobins are written des- with the relevant digested amino acid residue in front). It has also been shown that its contribution to the alkaline Bohr effect is lost in abnormal haemoglobins where it has been replaced by Asp,<sup>24,25</sup> Arg<sup>26</sup> or Pro.<sup>27</sup> Its pKa values were discovered by nuclear magnetic resonance to be 8.0 in deoxyhaemoglobin and 7.1 in carboxyhaemoglobin,<sup>28</sup> whilst deuterium exchange gave values of 8.2 in deoxy- and 7.0 in oxyhaemoglobin.<sup>29</sup>

Carbon dioxide affects the R  $\rightleftharpoons$  T equilibrium by binding at a higher rate to deoxyhaemoglobin than to liganded haemoglobin. It binds by reacting reversibly with the  $\alpha$  amino groups to form carbamino compounds:

$\alpha\text{-NH}_2 + \text{CO}_2 \rightleftharpoons \alpha\text{-NHCO}_2^- + \text{H}^+$ . Its binding site was confirmed when it was shown that  $\text{CO}_2$  doesn't lower the affinity of  $\alpha_2 \beta_2$ , i.e. a haemoglobin which has both the  $\alpha$  and  $\beta$  chain  $\alpha$ -amino groups specifically blocked with cyanate.<sup>16</sup> The structural reason for greater  $\text{CO}_2$  affinity in deoxyhaemoglobin is probably due to the formation of a salt bridge between the negatively-charged carbamate group and a positively-charged group in the deoxy structure. In the  $\beta$  chain case the  $\alpha$ -amino group lies in a cavity lined with positively-charged groups and the  $\epsilon$ -amino group of Lysine  $\beta 82$ <sup>30</sup> is probably the positive group.

The third allosteric effector is the small molecule 2,3 DPG which exists in blood in about the same proportion as haemoglobin. Its significance wasn't realised until Benesch and Benesch stripped DPG from haemoglobin and showed that the oxygen affinity was lowered when it was put back. The Benesches measured the binding of DPG to oxy- and deoxy-haemoglobin and discovered that the association constant was reduced by over one hundred in oxy- compared to deoxy- haemoglobin. This accounted quantitatively for the lowering of the oxygen affinity.<sup>31</sup> Its site of binding was located by chemical<sup>32,33</sup> and crystallographic<sup>34</sup> means. One molecule of DPG forms salt bridges with an array of positively-charged groups in a cavity between the two  $\beta$  chains. On oxygenation this cavity contracts expelling DPG. Its binding site in oxyhaemoglobin is as yet unknown.

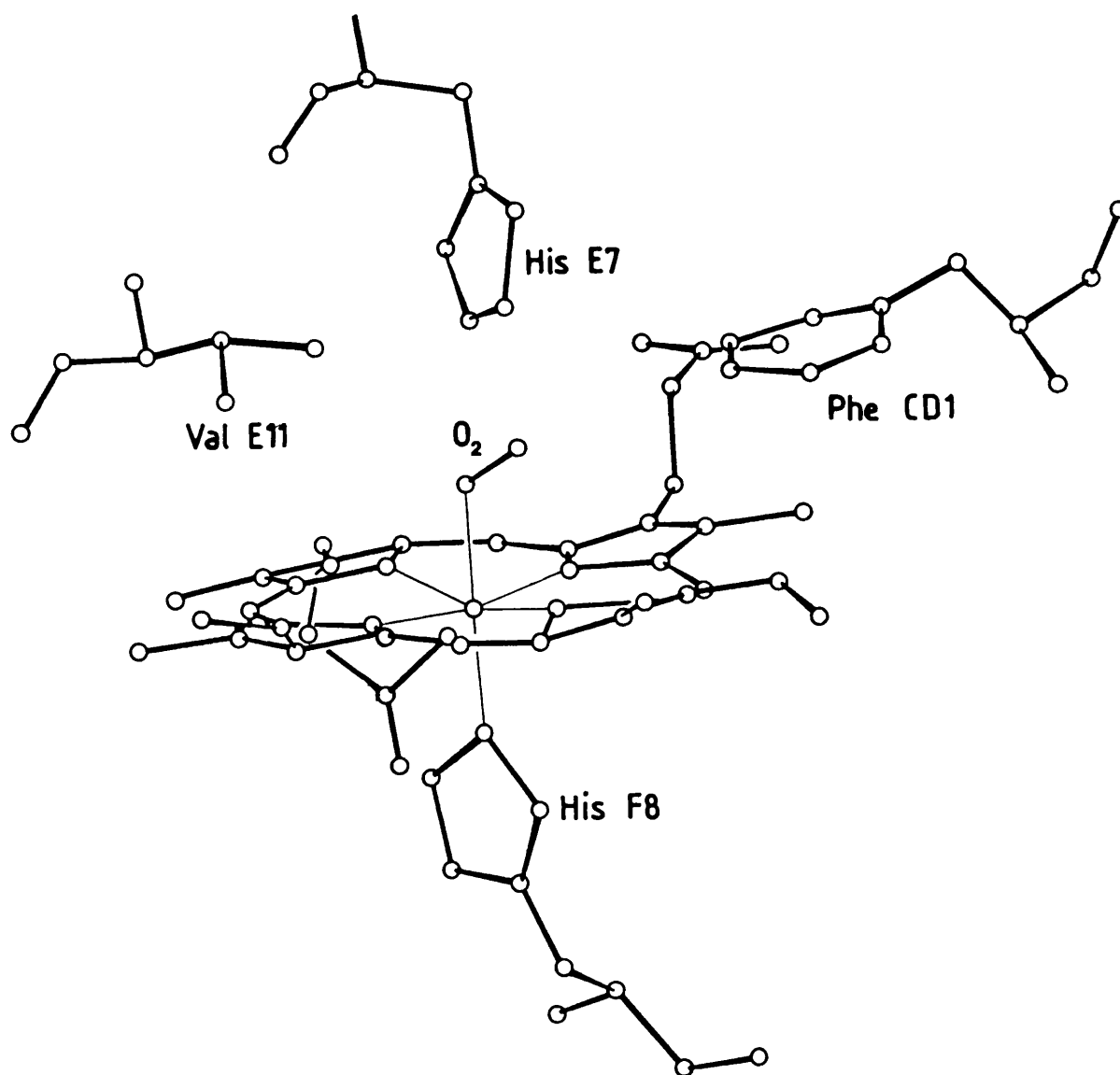
The effect on the oxygen affinity of haemoglobin of each of  $\text{H}^+$ ,  $\text{CO}_2$  or DPG will depend on pH. On the acid side of physiological pH DPG and proton binding will dominate as DPG binds to charged groups and increases the Bohr effect. On the alkaline side  $\text{CO}_2$  binding will tend to predominate because it binds mainly to uncharged amino groups and decreases the Bohr effect.

Having described the quaternary structure change on ligation and the rôle of the allosteric effectors, I will now describe the changes that take place at the site of ligand binding along with the main tertiary structure changes induced by ligand binding. The haem is attached to the polypeptide globin chain by a bond from iron to a nitrogen atom, N<sub>E</sub>, of His F8, the proximal histidine. This histidine is called proximal as this side of the haem is the proximal side, the distal side being the ligand binding side. On the distal side there is a pocket for the ligand surrounded by amino acid residues, the closest of these being distal valine E11, distal histidine E7 and distal phenylalanine CD1 (see Fig. 6). The distal histidine in fact forms hydrogen bonds to the ligand in aquomet, azidomethaemoglobin and, possibly, oxyhaemoglobin. In total the haem makes contact with 16 amino acid residues from seven segments of the chain and, with the exception of the histidines, the contacts are non-polar.

When the iron is six-coordinate, i.e. ligated, the iron atom lies almost in the plane of the porphyrin nitrogen atoms. However, on ligand loss, the iron atom drops below the plane to 0.6 Å in the α haems and 0.63 Å in the β haems.<sup>8</sup> Perutz<sup>11</sup> discovered that accompanying this movement of the iron into the plane of the porphyrin, on ligation, there was a movement of helix F towards helix H and the centre of the molecule. The narrowing of the F to H helices causes the rupture of a hydrogen bond that exists between the hydroxyl group of Tyr HC2 and the carbonyl of Val FG5 in deoxyhaemoglobin. This narrowing actually causes Tyr HC2 to be expelled from its pocket between the helices. Perutz then hypothesised that this pulls at the C-terminal salt bridges HC3 Arg or His and breaks them. He then put forward a mechanism of conformational change where oxygen is first bound to an α subunit [as the α ligand binding site is

FIGURE 6

Stereochemistry of the haem pocket with bound oxygen.



unobstructed whilst the  $\beta$  ligand binding site is obstructed by Valine Ell<sup>7</sup>], the corresponding tertiary changes then expel the penultimate Tyr HC2 and break the Arg HC3  $\alpha_1\alpha_2$  salt bridges. Next oxygen binds to the haem of  $\alpha_2$  and its salt bridges with  $\alpha_1$  are broken. At this point in the mechanism he assumed that the T to R transition takes place (although he correctly points out that this transition might take place at any point in the reaction depending on pH, CO<sub>2</sub> and phosphate concentration). On transition to the R form the  $\alpha_1\beta_2$  and  $\alpha_2\beta_1$  contacts slide over to their R conformation positions, breaking the remaining salt bridges and expelling 2,3 DPG as its cavity contracts. The oxygen affinity of the molecule has now increased and the  $\beta$  chains react with oxygen and break their internal HC2 Tyr to FG5 Val hydrogen bonds. In his mechanism Perutz has used the movement of the iron atom into the porphyrin plane as the trigger that initiates the T to R structural change on oxygen binding. The low oxygen affinity of the deoxy structure must be caused by a barrier which opposes the movement of the iron into the haem plane. Recently<sup>12</sup> Baldwin and Chothia have analysed the differences between carboxyhaemoglobin and deoxyhaemoglobin. Their results show that the proximal histidine is asymmetric relative to the haem plane in deoxy but nearly symmetric in carboxyhaemoglobin. The asymmetry of the histidine causes steric hindrance from the C<sub>ε</sub> with N1 of the porphyrin which prevents the approach of the imidazole to the porphyrin plane. Thus either the iron cannot move into the plane or the Fe-N<sub>ε</sub> bond has to be stretched or the N1 of the porphyrin plane must be pushed towards the distal side, all of which would lower the oxygen affinity. On comparison of the X-ray data of oxy<sup>13</sup> with deoxyhaemoglobin,<sup>8</sup> it appears that the Fe-N<sub>ε</sub> bond is not lengthened in oxy in the  $\alpha$  subunit nor is the N1 porphyrin pushed to the distal side. In the

$\beta$  subunit the Fe-N<sub>E</sub> bond is stretched by about  $\cdot 13 \text{ \AA}$ , in the T state, but the steric hindrance opposing iron's movement into the plane is less although there is the obstruction from C<sub>γ2</sub> of Val E11 as well. Thus it would appear that the position and tilt of the proximal histidine is responsible for the oxygen affinity of chains as well as the position of E11 Val in the  $\beta$  case.

Evidence to back up the theory that the proximal histidine is responsible for the restraint on the movement of the iron in the T structure comes from experiments on synthetic iron porphyrins. Two oxygen adducts of the picket-fence complex (2-methylimidazole)meso-tetra( $\alpha, \alpha, \alpha, \alpha$ -o-pivalamidophenyl)porphyrinato-Fe(II)<sup>35</sup> have been made, one having the sterically unhindered 1-methylimidazole as the fifth haem ligand, which might be regarded as a model for oxyhaemoglobin in the R structure and the other with the sterically unhindered 2-methylimidazole as the fifth ligand. The latter might be regarded as a model of oxyhaemoglobin in the T structure because repulsion between the methyl group in the 2-position and the porphyrin nitrogens appears to mimic the restraints of the globins. In both structures the bonds from the iron to the porphyrin nitrogens are  $0.09 \text{ \AA}$  shorter than in the oxygen free complexes. In the unhindered complex the iron atom is in the porphyrin plane whilst it is  $0.08 \text{ \AA}$  below the plane (towards the methylimidazole) in the hindered case which has an Fe-O bond  $0.15 \text{ \AA}$  longer, consistent with its lower oxygen affinity. This theory is also backed up by the calculations of Gelin and Karplus<sup>36</sup> who find that non-bonding contacts between the proximal histidine and the haem are responsible for the strain produced on transition to the T structure.

The pull exerted by the F helix on the iron on ligand loss can be demonstrated by the case of nitrosohaemoglobin. Switching to the T

structure (by the addition of Inositol Hexaphosphate) caused the appearance of a second infrared band, of equal intensity to the first, characteristic of five-coordinated haems.<sup>37</sup> Similarly the e.s.r. spectrum of nitrosylhaemoglobin in the R state shows a spectrum akin to that of six-coordinate nitrosyl haems whilst the T state spectrum is a composite of five- and six-coordinate nitrosyl haems.<sup>38</sup> Resonance Raman spectra of five- and six-coordinate nitrosyl haems show similar results on comparison with T and R state nitrosylhaemoglobins.<sup>39,40</sup> These results all point to the breakage of the Fe-N<sub>c</sub> bond on transition to the T structure in the  $\alpha$  chain. The lengthening of the Fe-N<sub>porph</sub>, movement of iron out of the plane and change to high spin are all changes synonymous with the change of quaternary structure from R to T.

In their analysis of the changes that take place on ligand binding, Baldwin and Chothia<sup>12</sup> report that both haems move further into their haem pockets whilst the F helix translates across the haem plane in the CH(2)-CH(4) direction and tilts towards the haem plane. In the  $\beta$  subunit the E helix also shifts and this, coupled with the F helix movement and the haem tilt, removes the obstruction of Val E11. The translation and tilt of the F helix brings the proximal histidines into positions where their imidazole rings become closer and symmetrical relative to the haem planes pushing the iron atoms into the haem planes. Movement of the F helix will, in turn, move the FG segment which forms part of the  $\alpha_1\beta_2$  ( $\alpha_2\beta_1$ ) contact. The  $\alpha_1\beta_2$  contact is stable at the same time as the  $\alpha_2\beta_1$  contact when the two FG segments are the correct distance apart for either quaternary structure. Consequently, movements in the tertiary structure, i.e. in the F helix and therefore the iron are directly coupled to movements in the quaternary structure. Work by Anderson<sup>41</sup> on ligated haemoglobin constrained in the T state and by Perutz<sup>11</sup> on

deoxyhaemoglobin constrained in the R state correlate well with results of Baldwin and Chothia.<sup>12</sup> Anderson<sup>41</sup> found from a difference Fourier analysis of deoxy to methaemoglobin (in T structure) that the iron, on ligation, moves towards the porphyrin plane causing a tilt of the haem. The F and E helices move slightly disturbing the  $\alpha_1\beta_2$  contact where the Tyr C7(42) $\alpha$ -Asp G1(99) $\beta$  hydrogen bond is loosened. The penultimate Tyrosines HC2 are seen to be loosened in their pockets but the salt bridges are intact. Changes in the met minus deoxy-BME-haemoglobin (liganded haemoglobin constrained in the T structure) maps of Perutz<sup>11</sup> tend to be similar but opposite in nature to those of Anderson's.

Thus it can be seen that the tertiary structure changes are intimately linked with the quaternary structure. Therefore, as ligands successively bind the ligand affinity is increased by the molecule changing its quaternary structure as is borne out by the oxygen binding curves.

Myoglobin, on the other hand, is unable to undergo a quaternary structure change and its tertiary structure changes, on ligation, are less than in haemoglobin. The ligand affinity of deoxymyoglobin is greater than that of deoxyhaemoglobin as its proximal histidine is symmetrical relative to the haem plane. On the other hand, the oxygen affinity of oxymyoglobin is less than that of oxyhaemoglobin as its iron oxygen bond is weaker, the iron atom being further from the haem plane than in oxyhaemoglobin.

## REFERENCES FOR CHAPTER 1

1. Kendrew, J.C., Dickerson, R.E., Strandberg, B.E., Hart, R.G., Davies, D.R., Phillips, D.C., Shore, V.C., Nature, 1960, 185, 422.
2. Cohen, J.A., Caughey, W.S., Biochemistry, 1968, 7, 636.
3. Cullis, A.F., Muirhead, H., Perutz, M.F., Rossmann, M.G., Proc. Roy. Soc. A, 1962, 265, 161.
4. Perutz, M.F., J. Mol. Biol., 1965, 13, 646.
5. Muirhead, H., Cox, J.M., Mazzarella, L., Perutz, M.F., J. Mol. Biol., 1967, 28, 117.
6. Perutz, M.F., Muirhead, H., Cox, J.M., Goaman, L.C.G., Nature, 1968, 219, 131.
7. Bolton, W., Perutz, M.F., Nature, 1970, 228, 551.
8. Fermi, G., J. Mol. Biol., 1975, 97, 237.
9. Ten Eyck, L.F., Arnone, A., J. Mol. Biol., 1976, 100, 3.
10. Monod, J., Wyman, J., Changeux, J.P., J. Mol. Biol., 1965, 12, 88.
11. Perutz, M.F., Nature, 1970, 228, 726.
12. Baldwin, J., Chothia, C., J. Mol. Biol., 1979, 129, 175.
13. Shaanan, B., Nature, 1982, 296, 683.
14. Wyman, J., J. Biol. Chem., 1939, 127, 581.
15. Perutz, M.F., Muirhead, H., Mazzarella, L., Crowther, R.A., Greer, J., Kilmartin, J.V., Nature, 1969, 222, 1240.
16. Kilmartin, J.V., Rossi Bernardi, L., Nature, 1969, 222, 1243.
17. Perutz, M.F., Nature, 1970, 228, 734.
18. Ladner, R.C., Heidner, E.J., Perutz, M.F., J. Mol. Biol., 1977, 114, 385.
19. Nishikura, K., Biochem. J., 1978, 173, 651.
20. Idelson, L.I., Didkowsky, N.A., Casey, R., Lorkin, P.A., Lehman, H., Acta Haematol., 1974, 52, 303.
21. Hayashi, A., Suzuki, T., Stamatoyannopoulos, G., Biochim. Biophys. Acta, 1974, 351, 453.
22. Tucker, P.W., Perutz, M.F., J. Mol. Biol., 1977, 114, 415.
23. Kilmartin, J.V., Wootton, J., Nature, 1970, 228, 766.
24. Imai, K., Arch. Biochem. Biophys., 1968, 127, 543.
25. Perutz, M.F., Pulsinelli, P.D., Ten Eyck, L.F., Kilmartin, J.V., Shibata, S., Iuchi, I., Miyaji, T., Hamilton, H.B., Nature New Biol., 1971, 232, 147.
26. Wajeman, H., Kilmartin, J.V., Najman, A., Labie, D., Biochim. Biophys. Acta, 1975, 400, 354.

27. Barem, G.H., Bromberg, P.A., Alben, J.O., Brimhall, B., Jones, R.T., Mintz, S., Rother, I., Nature, 1976, 259, 155.
28. Kilmartin, J.V., Breen, J.J., Roberts, G.C.K., Ho. C., Proc. Natl. Acad. Sci. U.S.A., 1973a, 70, 1246.
29. Ohe, M., Kajita, A., J. Biochem. (Japan), 1977a, 81, 431.
30. Arnone, A., Nature, 1974, 247, 143.
31. Baldwin, J.M., Prog. Biophys. Mol. Biol., 1975, 29, 225.
32. Bunn, H.F., Briehl, R.W., J. Clin. Invest., 1970, 49, 1088.
33. Benesch, R.E., Benesch, R., Renthal, R.D., Maeda, N., Biochemistry, 1972, 11, 3576.
34. Arnone, A., Nature, 1972, 237, 146.
35. Collman, J.P., Gagne, R.R., Reed, C.A., Robinson, W.T., Rodley, G.A., Proc. Natl. Acad. Sci. U.S.A., 1974, 71, 1326.
36. Gelin, B.R., Karplus, M., Proc. Natl. Acad. Sci. U.S.A., 1977, 74, 801.
37. Maxwell, J.C., Caughey, W.S., Biochemistry, 1976, 15, 388.
38. Szabo, A., Perutz, M.F., Biochemistry, 1976, 15, 4427.
39. Szabo, A., Barron, L.D., J.A.C.S., 1975, 97, 660.
40. Burke, J.M., Daly, P., Strong, J.P., Wright, P., Spiro, T.G., J.A.C.S. (in press) 1985.
41. Anderson, L., J. Mol. Biol., 1973, 79, 495.

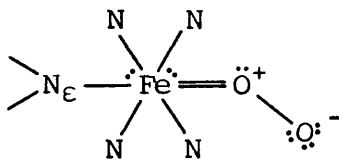


# CHAPTER 2

**ESR of  $\gamma$ -irradiated Haemoglobins A, F and Myoglobin**

## INTRODUCTION

The structural formula for the FeO<sub>2</sub> unit in oxyhaemoglobin (HbO<sub>2</sub>) was originally proposed by Pauling<sup>1,2</sup> to be:-



a spin-paired low-spin diamagnetic complex. This agreed with the measured zero magnetic moment discovered by Pauling and Coryell in 1936.<sup>3</sup> In 1964 Weiss<sup>4</sup> proposed the superoxo structure, Fe<sup>III</sup>O<sub>2</sub><sup>-</sup>, considering the two unpaired electrons to be "antiferromagnetically" coupled. Both these structures give a singlet ground state for HbO<sub>2</sub>. However, in 1977, Cerdonio et al.<sup>5</sup> reported magnetic susceptibility measurements of frozen aqueous solutions of HbO<sub>2</sub> in the range 25-250 K. They found a temperature dependent behaviour typical of a thermal equilibrium between a singlet ground state and an excited triplet state, separated by 146 cm<sup>-1</sup>, for two electrons per haem. Shortly afterwards Pauling published a paper<sup>6</sup> claiming that the paramagnetism observed by Cerdonio et al. was due to partial dissociation of oxygen in the samples. Meanwhile Cerdonio et al.<sup>7</sup> measured the magnetic susceptibility of HbO<sub>2</sub> at room temperature and confirmed their earlier results.

The question of the nature of the low-lying triplet state in terms of the bonding in the FeO<sub>2</sub> unit was subsequently investigated by various workers using quantum mechanical calculations. Herman and Loew<sup>8</sup> used semi-empirical INDO-SCF-CI calculations on a model oxyhaem complex and obtained a singlet diamagnetic ground state with a low lying paramagnetic triplet state 150 cm<sup>-1</sup> above it. They found that the singlet ground state had considerable Fe<sup>III</sup>O<sub>2</sub><sup>-</sup> character due to charge delocalisation but not due to transfer of spin density. The coupled singlet state of

Weiss was found to be a highly excited state. On the other hand Makinen<sup>9</sup> concluded, from polarized single crystal optical studies of oxymyoglobin (MbO<sub>2</sub>), that the low-lying excited state could not be the  $\psi[{}^3E; Fe(II)]-\phi[{}^3\Sigma_g^-; O]$  triplet triplet configuration. He went on to suggest that both the  $\psi[{}^1A_1; Fe(II)]\phi[{}^1A_g; O_2]$  singlet singlet and the  $\psi[{}^2E; Fe(III)]-\phi[\Pi_g; O_2^-]$  charge transfer configurations provided the most important contributions to the oxygen binding in HbO<sub>2</sub> and MbO<sub>2</sub>. However Goddard and Olafson,<sup>10</sup> using ab initio calculations on haem models, obtained a singlet ground state with an excited triplet state about 3000 cm<sup>-1</sup> above it in MbO<sub>2</sub>. The discrepancies between the results of these and other calculations probably arises as a result of the different haem models used, as the X-ray structures of MbO<sub>2</sub><sup>11</sup> and HbO<sub>2</sub><sup>12</sup> have only recently been resolved. However these calculations do support the findings of Cerdonio et al. They also imply some form of charge delocalisation as is suggested by the liberation of superoxide in the autoxidation of HbO<sub>2</sub>,<sup>13</sup> from X-ray fluorescence studies<sup>14</sup> and further from infrared studies,<sup>15</sup> polar solvent effects<sup>16</sup> and Mössbauer studies.<sup>17</sup>

Despite its measured magnetic moment, HbO<sub>2</sub> has no detectable ESR spectrum and thus only the ferrous haemoglobins with paramagnetic ligands, such as NO or O<sub>2</sub><sup>-</sup>, can be studied. However the oxidised ferric forms methaemoglobin (MetHb) and metmyoglobin (MetMb) are paramagnetic. These oxidised forms were the first to be studied by ESR and in 1957 Bennett et al.<sup>18</sup> performed a single crystal study on MetMb using the axial symmetry to align the crystal. Since then a variety of ferric haemoglobin and myoglobin complexes have been studied by ESR, a review being recently compiled by Dickinson and Symons.<sup>19</sup> Another approach is to replace the ferrous d<sup>6</sup> ion with the paramagnetic cobalt d<sup>7</sup> ion as was first achieved by Hoffman and Petering.<sup>20</sup> This haemoglobin, which also binds oxygen reversibly, is prepared by substituting cobalt protoporphyrin

IX for iron protoporphyrin IX in haemoglobin or myoglobin. This then provides the ESR spectroscopist with three ESR-sensitive systems closely related to the native system. The majority of the ESR studies of these systems have been performed at liquid nitrogen temperatures as the spectral resolution is significantly better at lower temperatures. In the irradiated HbO<sub>2</sub> case the electron adduct formed, (FeO<sub>2</sub>)<sup>-</sup>, is not stable at high temperatures as it converts to Methb above 220 K.<sup>21</sup>

Nitrosyl haemoglobin (HbNO) and nitrosyl myoglobin (MbNO) have been extensively studied as their ESR spectra are sensitive to the R ⇌ T quaternary structure change and the spectra of the α and β subunits are quite distinct. Rhein et al.<sup>22</sup> noted that the addition of inositol hexaphosphate (IHP) caused a change in the spectrum of HbNO. As mentioned in Chapter 1 infra red,<sup>23</sup> visible<sup>24</sup> and resonance raman<sup>25</sup> spectroscopy have been used to study the reaction of HbNO with IHP, the conclusion being that the α chains are only five-coordinate in the T structure (as the Fe-N<sub>E</sub> His F8 bond is broken in the T form), whilst the β chains retain their coordination number of six. The ESR results were interpreted in these terms<sup>26-33</sup> but ESR is not sensitive enough to allow the conclusion that the Fe-N<sub>E</sub> His F8 bond is broken. It may simply be stretched to reduce the hyperfine coupling.

Höhn et al.<sup>34</sup> did a <sup>14</sup>N and <sup>1</sup>H ENDOR (electron nuclear double resonance spectroscopy) study of HbNO. They found that in the isolated α<sup>NO</sup> subunits the Fe-N<sub>E</sub> His F8 coupling was lost in acid pH whilst that of the isolated β<sup>NO</sup> subunits was unaffected by pH. In the HbNO tetramer the N<sup>14</sup> His F8 coupling changed on going to acid pH in the presence of IHP to reveal a coupling identical with the β<sup>NO</sup> isolated chain coupling. This is good evidence for the breakage of the Fe-N<sub>E</sub> His F8 bond in the α chain on quaternary structure change (R → T). Further work<sup>35</sup> with hybrids of the

type  $\alpha^{\text{NO}}\beta^{\text{X}}$  and  $\alpha^{\text{X}}\beta^{\text{NO}}$  (where X = deoxy or carbonmonoxy) shows that in the hybrid  $\alpha^{\text{NO}}\beta^{\text{X}}$ , the  $\alpha$  signal is pH dependent but is unaffected by the ligation state of the  $\beta$  chain. However the hybrid  $\alpha^{\text{X}}\beta^{\text{NO}}$  does show a  $^{14}\text{N}$  coupling which is affected both by the  $\alpha$  chain ligation state and by pH.  $^1\text{H}$  ENDOR spectra of HbNO show an exchangeable coupling attributed to a possible hydrogen bond to the  $\text{N}_\epsilon$  of the distal histidine (E7) and a non exchangeable coupling probably due to one of the methyl protons  $\text{C}_{\gamma_1}$  of valine E11. The exchangeable proton coupling is found in HbNO, in the separated chains as well as in MbNO.

The transition to the T structure (HbNO, pH6 + IHP) sees only a very small change in the coupling (reduced by 0.05 MHz) in the tetramer. Lowering the pH in the  $\alpha^{\text{NO}}$  single chain causes a dramatic change in the proton couplings, that of the distal histidine proton being lost, whilst the  $\beta^{\text{NO}}$  chain couplings are hardly affected by pH. From the hybrid work it appears that the  $\beta^{\text{NO}}$  distal histidine coupling is affected both by pH and by the ligation state of the  $\alpha$  chain (low pH only) in the tetramer. As with the single chains the distal histidine proton coupling in  $\alpha^{\text{NO}}\beta^{\text{X}}$  is lost on going to acid pH but is unaffected by the ligation state of the  $\beta$  chain.

Other important studies are the single crystal studies of MbNO<sup>36-38</sup> and HbNO.<sup>39,40</sup> Dickinson and Chien<sup>36,37</sup> reported the FeNO angle to be  $108-110^\circ$  in MbNO, as was found by Chien in HbNO,<sup>39</sup> quite different, however, from the reported value of  $145^\circ$  obtained from the X-ray diffraction of HbNO by Deatherage and Moffat.<sup>41</sup> They also calculated the unpaired electron spin density distribution over the atoms using  $^{57}\text{Fe}$  and  $^{15}\text{N}$  isotopes, finding nearly half on the  $^{57}\text{Fe}$ , the rest being on the  $^{15}\text{NO}$  ligand with a very small amount delocalised onto the  $\text{N}_\epsilon$  of the proximal histidine. The small delocalisation onto the proximal histidine  $\text{N}_\epsilon$  atom

along with the small magnitude of  $\Delta g$  ( $g$ -shift from the free spin value) accord well with a  $\sigma^*$  type radical in which the unpaired electron is delocalised over the  $3d_{z^2}$  iron orbital, the  $sp$  hybrid antibonding orbital of the NO and slightly over the  $N_C(\sigma)$  orbital of the proximal histidine. The nature of the bonding in FeNO has been discussed both in  $\sigma^*$  and  $\pi^*$  terms. It is important that the nature of the orbital containing the unpaired electron is correctly assigned as this can lead to misinterpretation of the single crystal results. Hori *et al.*<sup>38</sup> have performed a single crystal study on MbNO at ambient and cryogenic temperatures. They concluded from their results that the ligand orientation changes on freezing the crystal. However their interpretation has been criticized by Dickinson and Symons,<sup>19</sup> in particular their choice of  $g_{\min}$  as the direction of the Fe-N(NO) bond. Although they have incorrectly interpreted their results, their conclusion is backed up by the fact that another species was evident in low concentration on freezing. In an early investigation on separated nitrosyl chains Shiga *et al.*<sup>42</sup> noted that both chains show marked departure from their room temperature axial symmetry on freezing. Morse and Chan<sup>43</sup> studied the interchange of two species found in a frozen solution study of MbNO between 30 and 180 K. Unfortunately they didn't take their study above the freezing point of the crystal, but by factor analysis they deconvoluted the spectra to show that one species was predominant at higher temperatures (180 K) interconverting to the second species on decreasing the temperature.

Single crystal studies of oxycobaltmyoglobin ( $\text{CoMbO}_2$ )<sup>44-47</sup> show that about 90% of the spin density is on the dioxygen ligand and that there are two distinct ligand orientations at 77 K, one being about  $90^\circ$  from the other.<sup>45</sup> On comparison with the X-ray diffraction results<sup>48</sup> it can

be seen that both orientations are rotations of about  $50^\circ$  from the room temperature ligand orientation. Furthermore Dickinson and Chien<sup>45</sup> found that the two oxygen atoms were inequivalent in their species II whilst the atoms appeared equivalent in species I using  $O_2^{17}$  enriched  $CoMbO_2$ . They interpreted the inequivalence of the oxygen atoms in species II to be due to possible hydrogen bonding with the distal histidine since the O-O axis is directed towards the histidine in this species. Earlier Gupta et al.<sup>49</sup> had found non-equivalent oxygen atoms in their frozen solution studies on  $CoHbO_2^{17}$ . The question of hydrogen bonding had been raised earlier in studies by Yonetani et al. who noticed a line narrowing in  $D_2O^{50}$  and a pH effect<sup>51</sup> in their spectra of  $CoMbO_2$ . For comparison they used the monomeric cobalt haemoglobin Glycera, which has a leucine residue replacing the distal histidine, and found no pH or deuterium substitution effects, supporting their hydrogen bond postulate. Höhn and Hüttermann published an ENDOR study of  $CoHbO_2^{52}$  in which they found two types of proton coupling, one-exchangeable, the other non-exchangeable. The exchangeable coupling was assigned to a hydrogen bond from the outer oxygen to the  $N_\epsilon H$  of the distal histidine, as in  $HbNO$ . The other coupling was assigned to a non-polar interaction with a methyl proton on distal valine (E11).

The third ESR sensitive system is the  $(FeO_2)^-$  unit, which is formed in  $HbO_2$  on gamma irradiation. Symons first reported the formation of two paramagnetic centres in gamma irradiated  $HbO_2$  in 1975.<sup>53</sup> Through work with electron scavengers in frozen ethylene glycol glasses, Symons and Petersen showed that the centres were electron adducts formed at the  $FeO_2$  centres.<sup>21</sup> They reported a similar centre formed in  $MbO_2$  on gamma irradiation at 77 K. By separating the haemoglobin tetramer into its monomeric subunits they showed that the two centres corresponded to

$(\text{FeO}_2)^-$  centres formed in the individual chains. On warming the samples above 77 K they noted various new centres formed from the original ones. Further warming resulted in an increased MethHb signal at  $g = 6$ . Furthermore, they showed that the oxygen atoms of the  $(\text{FeO}_2)^-$  unit were inequivalent using  $\text{O}^{17}$  isotopically enriched oxygen, and that about 70% of the spin density was located on the two oxygen atoms, the rest being on the iron atom. Later Symons and Petersen published a single crystal study of irradiated  $\text{MbO}_2$ <sup>54</sup> which placed the projection of  $g_{\text{max}}$   $10^\circ$  towards N(2) from the bisector of N(1) FeN(2), however the results were slightly ambiguous and have been re-interpreted by Dickinson and Symons.<sup>19</sup> A further single crystal study of irradiated  $\text{MbO}_2$  has been performed by Nietsche,<sup>55</sup> which places the projection of  $g_{\text{max}}$ , the O-O direction, towards N(2) from the bisector of N(3) FeN(2) (using the pyrrole numbering of Fermi<sup>56</sup>) which is close to the position in native  $\text{MbO}_2$ <sup>11</sup>.

In their postulated mechanism of MethHb formation from irradiated  $\text{HbO}_2$  Symons and Petersen<sup>21</sup> suggested that the reaction proceeded via proton transfer from the hydrogen bonded distal histidine to the outer oxygen atom of the ligand. The next step involved loss of  $\text{HO}_2^-$  leaving  $\text{Fe}^{\text{III}}$ , which quickly reacted with water to form MethHb. The mechanism of this reaction is important as it is analogous to the in vivo autoxidation of  $\text{HbO}_2$  to MethHb. The ability of haemoglobin to bind oxygen reversibly without the  $\text{Fe}^{\text{II}}$  complex undergoing oxidation to  $\text{Fe}^{\text{III}}$  is critical to the protein's physiological function in that the oxidised Met form is unable to bind oxygen. However a small amount of MethHb is formed in normal erythrocytes and is reduced back to  $\text{Fe}^{\text{II}}$  enzymatically.<sup>57</sup> Unusually high amounts of MethHb of clinical importance can result from an abnormal amino acid substitution (M-type haemoglobin)<sup>58</sup> or exposure to

certain drugs or toxic agents.<sup>59</sup> It has been shown that the globin chain prevents the oxidation taking place via a peroxide-bridged dimer, which is the mechanism in protein-free iron(II) porphyrin complexes.<sup>60</sup> A number of workers<sup>13,61-64</sup> have interpreted the observed ability of autoxidising solutions of haemoglobin to reduce cytochrome C or oxidise epinephrine as evidence for the formation of superoxide in these reactions. The autoxidation reaction has also been shown to be dependent on the concentration of anions such as chloride.<sup>65</sup> Furthermore, the reaction in the presence of anions was found to be both pH and anion nucleophilicity dependent.<sup>66</sup> Wallace and Caughey<sup>66</sup> proposed that the autoxidation reaction involved the nucleophilic displacement of superoxide from a protonated intermediate, the nucleophile being the chloride ion in the erythrocyte. In 1975 they proposed a mechanism for the autoxidation reaction in the presence of toxic agents which also applied to abnormal haemoglobins.<sup>67</sup> This involved the two-electron reduction of oxygen, one electron coming from the external donor and one from the ferrous ion with the subsequent production of peroxide. Peroxide has been shown to be released on addition of phenols to HbO<sub>2</sub><sup>67</sup> and has been found present in erythrocytes following exposure to oxidising drugs.<sup>68</sup> In the case of the mutant haemoglobins (HbM), in which a tyrosine residue replaces either the proximal or the distal histidine, there is a phenol residue which can act as an external electron donor allowing the two-electron reduction of oxygen to proceed readily.

In the following Chapter I have studied the differences in the ESR spectra of haemoglobins A, F and myoglobin, on change of pH and temperature. Also I have studied frozen aqueous HbO<sub>2</sub> solutions at low oxygen partial pressures finding that the  $\alpha$  and  $\beta$  chains have equal affinities. Various workers have addressed this problem using different

techniques. Asakura and Lau, using a nitroxide spin label attached to the haem group of either chain, reported equal oxygen affinities of the two chains in the absence of organic phosphates but found a preference for the  $\alpha$  chain in the presence of 2,3 DPG or IHP.<sup>69,70</sup> In a similar study using a spin label Ogata and MacConnell<sup>71,72</sup> reported that the  $\alpha$  subunit was preferentially oxygenated in the presence of organic phosphates, in agreement with Asakura and Lau. Using high resolution  $^1\text{H}$  nuclear magnetic resonance (NMR) Johnson and Ho showed<sup>73</sup> that oxygen exhibited a slight preferential binding to the  $\alpha$  haems in the absence of organic phosphates. However, their method of assignment of the  $\alpha$  and  $\beta$  NMR peaks, which were used to monitor the ligation state of the  $\alpha$  and  $\beta$  haems, has been questioned by Ikeda-Saito *et al.*<sup>74</sup> Later, Huang and Redfield<sup>75</sup> performed the same experiment over a wider range of conditions, finding no evidence for any large difference in the relative oxygen affinities of the two subunits, both in the presence and absence of organic phosphates. Lindstrom and Ho,<sup>76</sup> using  $^1\text{H}$  NMR, reported equal binding to the chains in the absence of organic phosphates, but they noted a preference for  $\alpha$  chain binding with IHP or 2,3 DPG. Using  $^{19}\text{F}$  NMR studies on haemoglobin labelled with trifluoroacetyl groups at  $\beta 93$  cysteine Huestis and Raftery<sup>77</sup> reported that, on average,  $\alpha$  chain ligation exceeded  $\beta$  ligation by approximately 10% throughout most of the range. However it was suggested that the  $^{19}\text{F}$  trifluoroacetyl group was more likely to be a probe of the transition of the quaternary conformers ( $\text{R} \rightleftharpoons \text{T}$ ) instead of the ligation of the  $\beta$  subunits.<sup>78</sup> Makino and Sugita<sup>79</sup> used hybrid-haem haemoglobins containing proto and mesohaems in their study of oxygen binding to haemoglobin. From their study they concluded that the  $\beta$  chains have a slightly higher affinity for the first oxygen molecule than the  $\alpha$  chains. Nagai<sup>80</sup> has measured the oxygen

affinities of the ferrous subunits in valency hybrid haemoglobins finding that if the ferric chain is high spin then the  $\beta$  ferrous subunit has a greater oxygen affinity than the  $\alpha$  ferrous subunit. On the other hand, the oxygen affinities of the ferrous subunits are equal if the ferric chains are low spin. Very recently Wada et al.<sup>81</sup> have used high performance multi-dimensional spectroscopy to study the problem. This spectroscopic technique makes it possible to continuously assimilate sets of data at several wavelengths on one sample whilst increasing or decreasing the partial pressure of oxygen. They concluded from their results that the  $\beta$  subunit is preferentially oxygenated, the effect being more marked if IHP is present.

#### EXPERIMENTAL

Haemoglobins A and F were obtained according to the method of Rossi Fanelli et al.<sup>82</sup> The blood was diluted to five times its volume with a 1% saline solution and centrifuged at 4,000 r.p.m. for five minutes at 10°C. The clear supernatant layer was discarded and the process repeated a further four times. After the last centrifugation the red cells were suspended in three volumes of cold, doubly-distilled water, the resulting solution being sonicated for ten seconds (setting 10  $\mu$ m) at 4°C for cell lysis. Cell debris was removed by centrifugation at 18,000 r.p.m. at 4°C for one hour, the pellet being discarded. Deuterated haemolysates were prepared in the same manner using D<sub>2</sub>O and deuterated saline solutions.

Fresh oxymyoglobin was prepared from a horse's heart by the method of Yamazaki et al.<sup>83</sup> All procedures were carried out in a cold room at 2°C. The heart muscle was freed from fat and ligaments and homogenized with one gallon of water, the pH being adjusted from around 6.0 to 7.5 with 2M aqueous ammonia. The homogenate produced was squeezed through a

cloth by hand as far as possible, the extract being 70% saturated with ammonium sulphate on addition of the solid salt. The pH was again adjusted to 7.5 with 2M aqueous ammonia. The resulting precipitate was centrifuged at 6,000 r.p.m. for 15 minutes to obtain a pellet which, containing mostly haemoglobin, was discarded. The supernatant was then 100% saturated with ammonium sulphate and the pH re-adjusted to 7.5. This precipitated down the myoglobin which was then filtered off. The resulting precipitate was dissolved in the minimum amount of distilled water, dialysed against two volumes of distilled water and then against 0.005 M Tris-HCl buffer at pH 8.4. The dialysed solution (ca. 100 ml) was placed on a column (4×20 cms) of DEAE cellulose (20 gms) which had been equilibrated with 0.005 M Tris buffer, pH 8.4. In this chromatography the oxymyoglobin separated into two main fractions, one slow the other fast moving. The faster moving fraction was eluted with 0.05 M Tris buffer, the slow fraction remaining on the column. Any haemoglobin still left in the solution remained tightly adsorbed at the top of the column. The eluted oxymyoglobin was then concentrated in an Amicon ultrafiltration cell using a YM50 filter under nitrogen pressure, after which the visible spectrum was checked. For acid and neutral pH runs the solution was dialysed for 24 hours at 4°C against mixed phosphate buffer at pH 5.8 and 7.4 respectively.

Commercially prepared freeze-dried myoglobin powder was purchased from Sigma Chemical Company. As this was predominantly in the ferric form it was reduced with dithionite in a nitrogen atmosphere and then oxygen bubbled.

Deoxyhaemoglobin was prepared by purging the haemolysate solution with oxygen-free nitrogen under a nitrogen atmosphere for five hours.

The frozen aqueous solutions were prepared, at the desired pH, by the

addition of 100 mM mixed phosphate buffer and frozen in liquid nitrogen. Frozen glassy solutions were prepared by the addition of up to 50% (v/v) ethylene glycol to the buffered solution. Deuterated frozen glasses were obtained using deuterated haemolysates and fully deuterated ethylene glycol (C.E.A., France). Variation in pH/pD was achieved using 50% citrate/phosphate buffer.

The solutions were either injected into quartz tubes and frozen or were frozen into small glass beads by pipetting into liquid nitrogen. The samples were irradiated at 77 K in a  $^{60}\text{Co}$   $\gamma$ -cell for 2 hours at a dose rate of 0.96 Mrad/hour.  $\gamma$ -Irradiations at  $-78^\circ\text{C}$  were performed in a  $\text{CO}_2$ /acetone bath.

The X-band spectra were recorded on a Varian E-109 spectrometer at 77 K in a glass Dewar flask. Electrons trapped in the glycol glass matrix were photobleached with an incandescent lamp. Samples were annealed either by using the Varian V6040 variable temperature system or by warming the samples in the Dewar flask without liquid nitrogen, simultaneously monitoring the spectrum until a change occurs at which point the sample is quickly recooled to 77 K.  $g$ -Values were calculated using an HP 5246C frequency counter in conjunction with a Bruker B-H1ZE field calibrant.

## RESULTS

### 1. Frozen aqueous solutions of HbO<sub>2</sub>A

#### (i) Neutral and alkaline pH's

At 77 K two signals, well removed from free spin, with rhombic symmetry are detected. These have  $g$ -values (Table 1) which are very similar to those reported by Symons and Petersen<sup>21</sup> and are certainly the centres they identified as electron adducts at the iron oxygen site, denoted  $(\text{FeO}_2)^-$ . In the absence of a glass former the two centres are equal in yield as noticed by Symons in his preliminary communication.<sup>53</sup> The central region of the spectrum around the free spin  $g$ -value contains the asymmetric doublet, characteristic of hydroxyl radicals trapped in ice,<sup>84</sup> as well as signals from organic radicals formed in the globin chain. At  $g=6$  a small amount of MetHb was detectable along with a small signal at  $g=4$ , which is attributable to a rhombically distorted high spin  $\text{Fe}^{\text{III}}$  signal. The  $g_x$  and  $g_y$  signals of the  $(\text{FeO}_2)^-$  units of the  $\alpha$  and  $\beta$  units were verified using apoglobin.<sup>85</sup>

Warming above 77 K produces changes in these centres as well as the loss of the hydroxyl radical signal. Between 100 and 130 K the  $\alpha$  peak increases in yield by about 50% with the concurrent loss of 50% of the yield of the  $\beta$  peak (Figure 1a). The next change occurs at 130 K when the  $\beta$  peak starts to broaden, shifting to a new centre,  $\beta'$ . At 140 K the species  $\gamma_1$  (formerly called  $\gamma^{21}$ ) appears as well as a very small amount of a species called  $\delta$ , visible on the low-field side of  $\alpha$ . Further warming the sample to 170 K produces a growth in  $\gamma_1$  as a result of the loss of  $\beta'$  and  $\alpha$ . Thereafter, at about 200 K,  $\gamma_1$  broadens and shifts to a new signal  $\gamma_1'$  upon the final decay of  $\alpha$  and  $\delta$ . At 220 K the composite broad peak of  $\gamma_1$  and  $\gamma_1'$  decays to zero and a concurrent increase in the high-spin ferric MetHb signal at  $g=6$  is seen.

TABLE 1

g-Values for the various species formed  
from irradiation of HbO<sub>2</sub>A

Species	g <sub>x</sub>	g <sub>y</sub>	g <sub>z</sub>
α	2.2148	2.1198	1.9650
β	2.2504	2.1460	1.9650
β'	2.2594	2.1540	1.9650
δ	2.2315	2.1320	1.9650
γ <sub>1</sub>	2.3071	2.1770	1.9460
γ <sub>1</sub> '	2.3130	2.1840	1.9296
γ <sub>2</sub>	2.3650	2.2080	1.9090

TABLE 2

Variation in yield and g-value of α and β  
species of HbO<sub>2</sub>A in frozen aqueous glasses

pH	β	α	β/α	g <sub>x</sub> β	g <sub>x</sub> α
5.10	64	62	1.03	2.2494	2.2199
5.14	55	55	1.00	2.2490	2.2195
5.38	67	60	1.12	2.2491	2.2190
5.50	82	68	1.21	2.2495	2.2187
5.58	75	61	1.23	2.2505	2.2174
5.75	74	52	1.42	2.2497	2.2174
5.82	97	65	1.50	2.2496	2.2173
5.98	86	53	1.62	2.2508	2.2169
6.24	115	62	1.85	2.2499	2.2168
6.45	112	51	2.17	2.2502	2.2163
6.64	114	49	2.33	2.2494	2.2162
6.76	115	46	2.50	2.2506	2.2160
6.92	114	43	2.62	2.2491	2.2160
7.18	127	45	2.82	2.2497	2.2158
7.40	131	42	3.12	2.2501	2.2148
7.44	128	41	3.13	2.2497	2.2136
7.68	130	40	3.25	2.2491	2.2137
7.74	129	40	3.23	2.2496	2.2134

## (ii) Acid pH

Reducing the pH below neutral has no effect on the 77 K spectrum, i.e. the peak heights of the  $\alpha$  and  $\beta$  species remain equal. Annealed samples show the same transitions as found in neutral and alkaline samples.

## 2. Frozen glassy solutions of HbO<sub>2</sub>A

Irradiating frozen aqueous glasses of HbO<sub>2</sub>A (containing up to 50% EG), at 77 K, results in the formation of the same  $\alpha$  and  $\beta$  centres. However, under these conditions the peaks are in unequal yields, the  $\beta/\alpha$  ratio being approximately 2.5:1 at neutral pH.<sup>91</sup> Photobleaching the electrons trapped in the glass at 77 K had no effect on these centres.

The changes that occur on warming neutral and alkaline solutions were very similar to those found in frozen aqueous solutions. Notable differences being the greater yield of the  $\delta$  species (arising from decay of  $\beta$ ), the clarity of the  $\beta \rightarrow \beta'$  shift and the predominance of the formation of  $\gamma_1$  from  $\beta'$ , (Figure 1b).

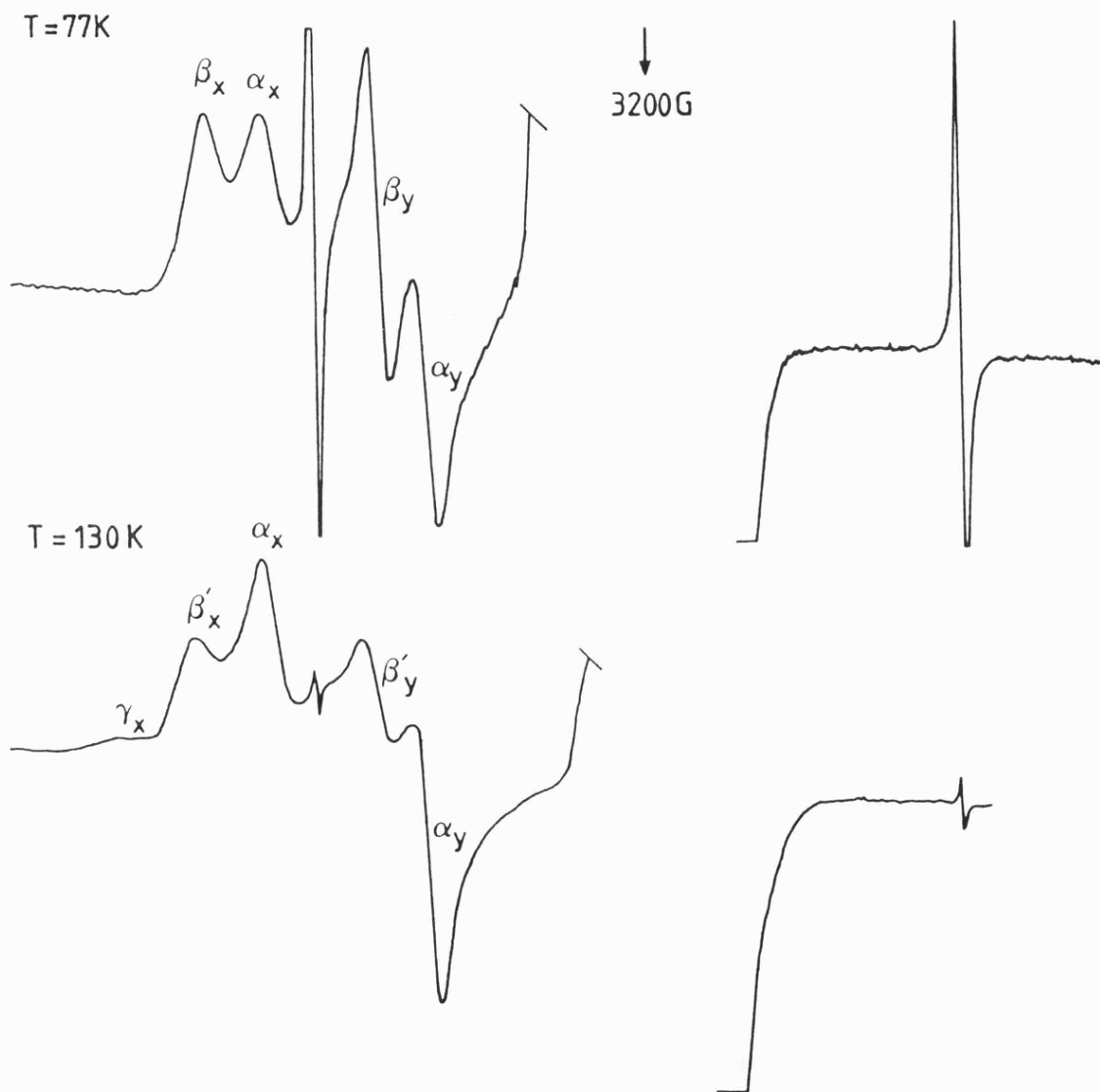
### (i) pH effect

As reported by Symons and Petersen<sup>91</sup> only the  $\beta$  yield is sensitive to pH, decreasing with pH. Thus the  $\beta/\alpha$  ratio varies with pH falling from 3:1 to nearly 1:1 in acid solution (Table 2). Further to the variation in  $\beta$  yield there is a variation in the  $g$ -value of the  $\alpha$  peak (Figure 6).

In the case of the glassy solutions, depression of pH alters the mechanism for the decay of the  $\alpha$  and  $\beta$  species on anneal above 77 K. At low pH's a further  $\gamma$ -type species, denoted  $\gamma_2$ , is formed, in competition with  $\gamma_1$ , from the decay of  $\alpha$ ,  $\beta'$  and  $\delta$ .  $\gamma_2$  is first seen around pH 6.7 (being formed above 140 K), its yield increasing with

FIGURE 1a

ESR spectrum of irradiated  $\text{HbO}_2\text{A}$  in frozen aqueous solution.



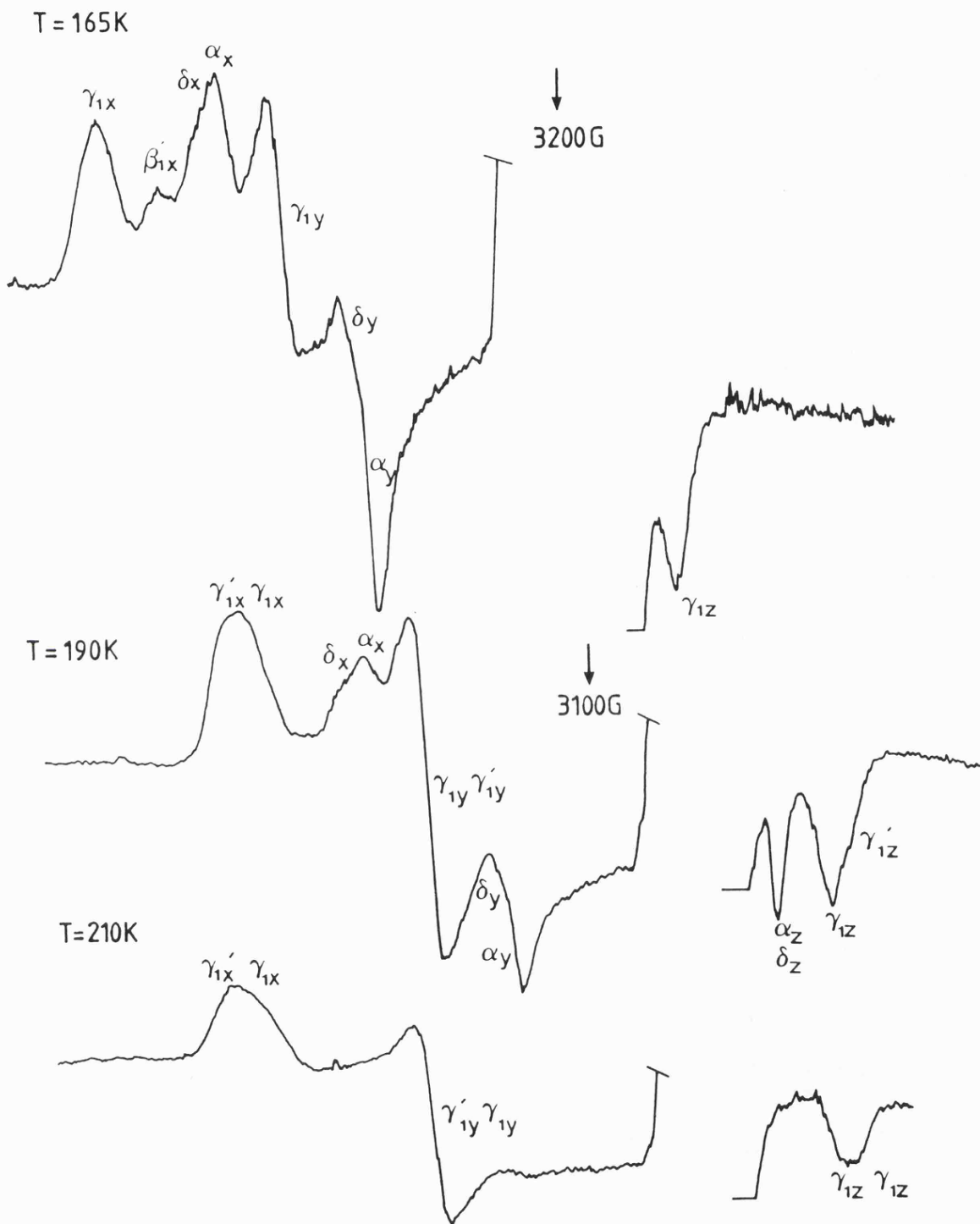


FIGURE 1a (Continued)

FIGURE 1b

ESR Spectra of irradiated  $\text{HbO}_2\text{A}$  in EG glass.

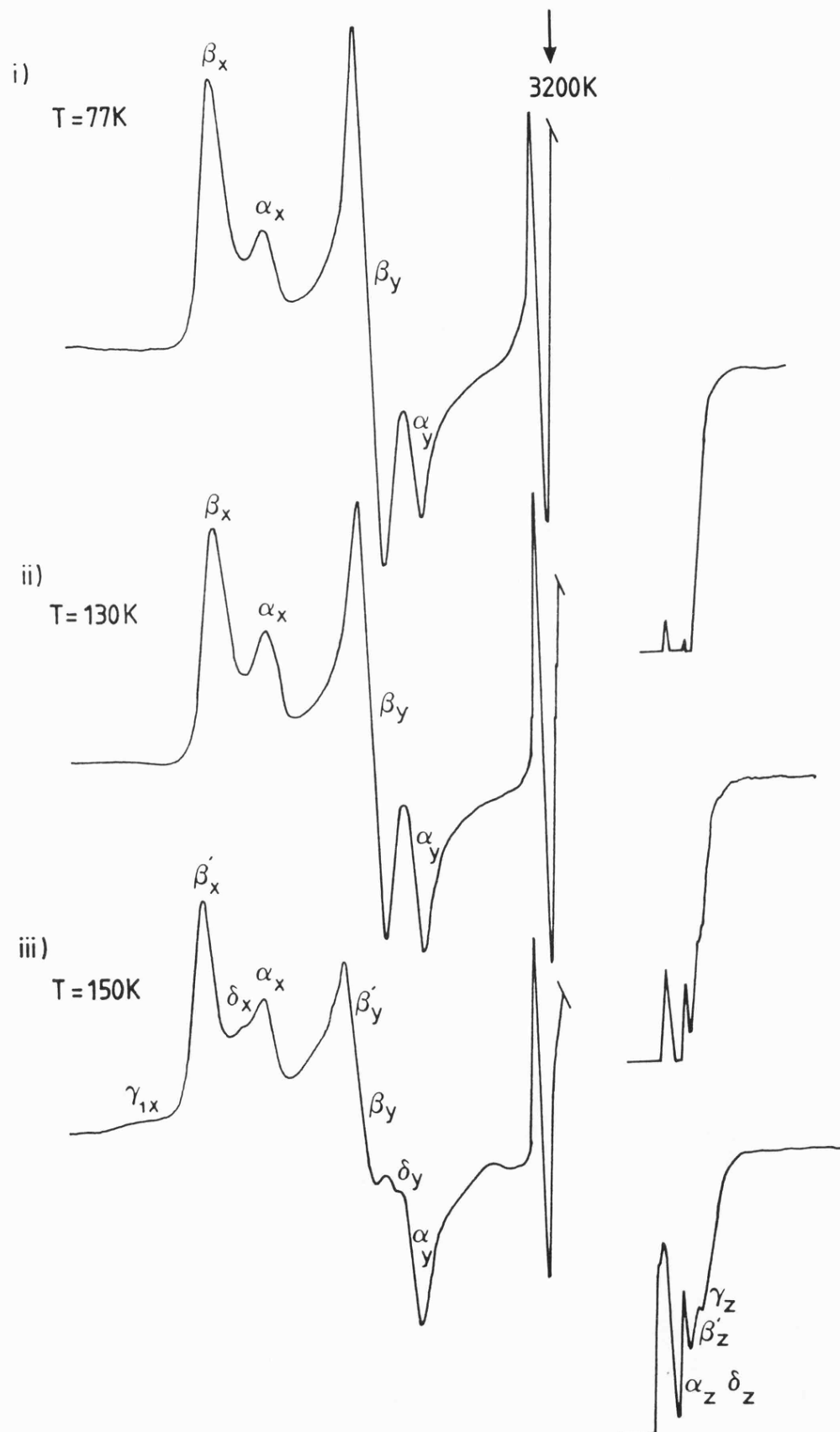
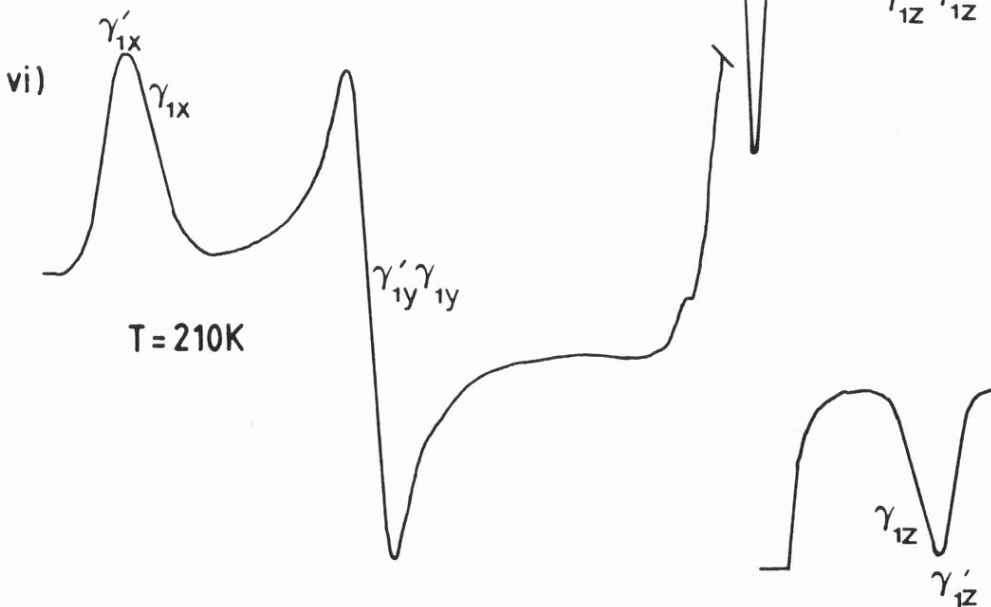
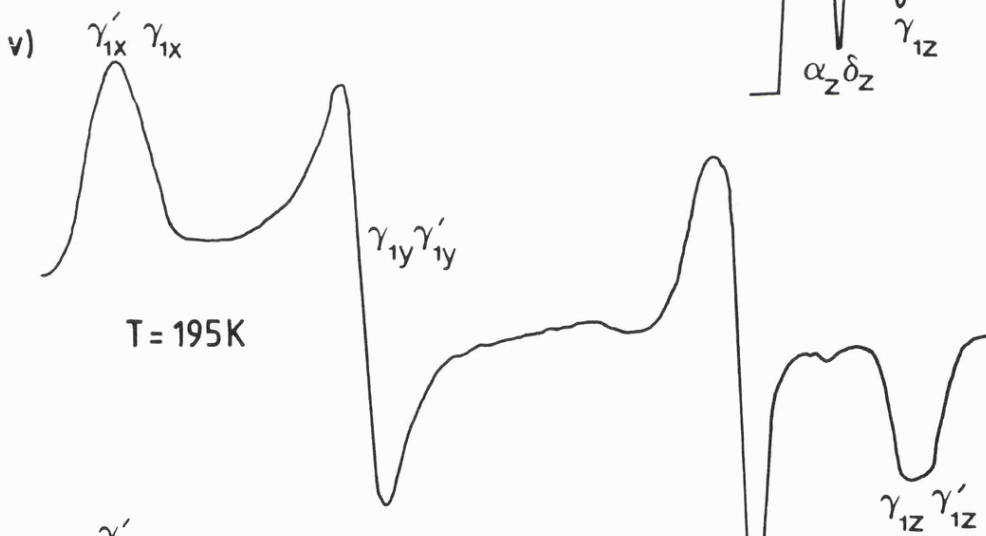
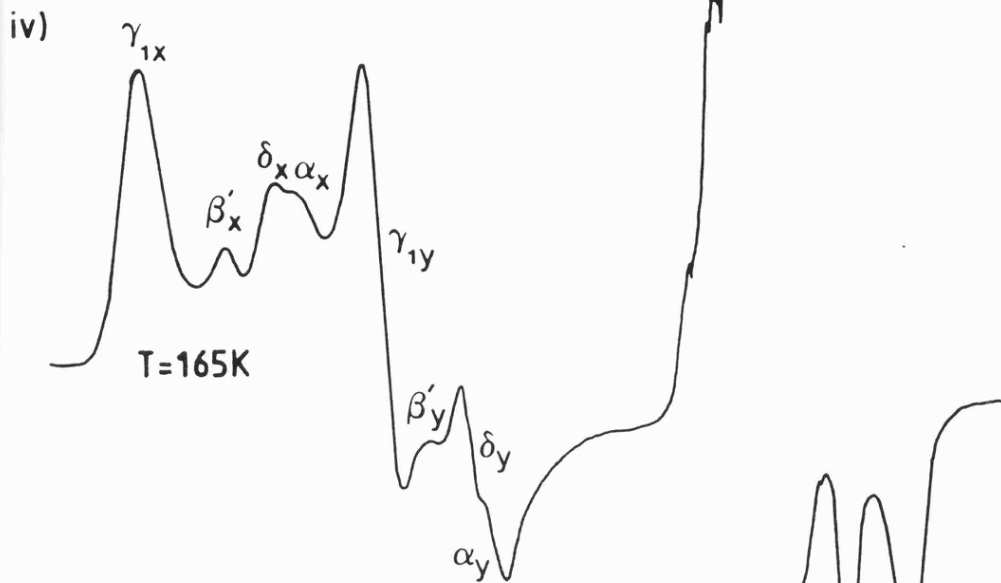


FIGURE 1b (Continued)

↓  
3200 K



decreasing pH, and at pH 6.5 all three  $\gamma$  species ( $\gamma_1$ ,  $\gamma_1'$  and  $\gamma_2$ ) are simultaneously present at 200 K. Below pH 6 the  $\gamma_1 \rightarrow \gamma_1'$  conversion ceases to occur, high temperature spectra comprising of  $\gamma_1$  and  $\gamma_2$  co-existing in a pH dependent equilibrium, pure  $\gamma_2$  spectra being obtained at pH 5.5 (Figure 2).

(ii) Deuterated glasses

As there is a pH variation in the  $\alpha$  and  $\beta$  yields, I examined fully deuterated glassy solutions, at different pH's at 77 K, to see if there was any evidence of coupling to any exchangeable protons. Figures 3a and 3b show graphs of the  $\alpha_x$  and  $\beta_x$  yields at 77 K in protonated and deuterated glycol glasses respectively. The graphs are very similar with no evidence of any change in splitting as a result of deuterium substitution. Also, no change in linewidths of the high temperature species were noted.

(iii) Matrix effect

The addition of a glassifying agent, ethylene glycol, clearly has a significant effect on the HbO<sub>2</sub>A spectra. The question thus arises as to whether the results are due to the effect of the glycol itself on the HbO<sub>2</sub>A or whether they are due to the formation of a glass. Therefore, I studied the effect of concentration of ethylene glycol (and other glass formers) on the 77 K spectra of HbO<sub>2</sub>A. The results shown in Figure 8 and Table 6 indicate that the  $\beta/\alpha$  ratio is most effected by increasing concentration up to 20% v/v. In the cases of ethylene and propylene glycol the  $\beta/\alpha$  ratio again increases above 40% v/v as the concentrations approach denaturing values of around 60% v/v.<sup>86</sup> In the case of polyethylene glycol, at high concentration (50% v/v), the species  $\delta$  is present even at 77 K and further increases in yield on warming to higher temperatures. In samples containing CH<sub>3</sub>OH the  $\gamma_1$  species is

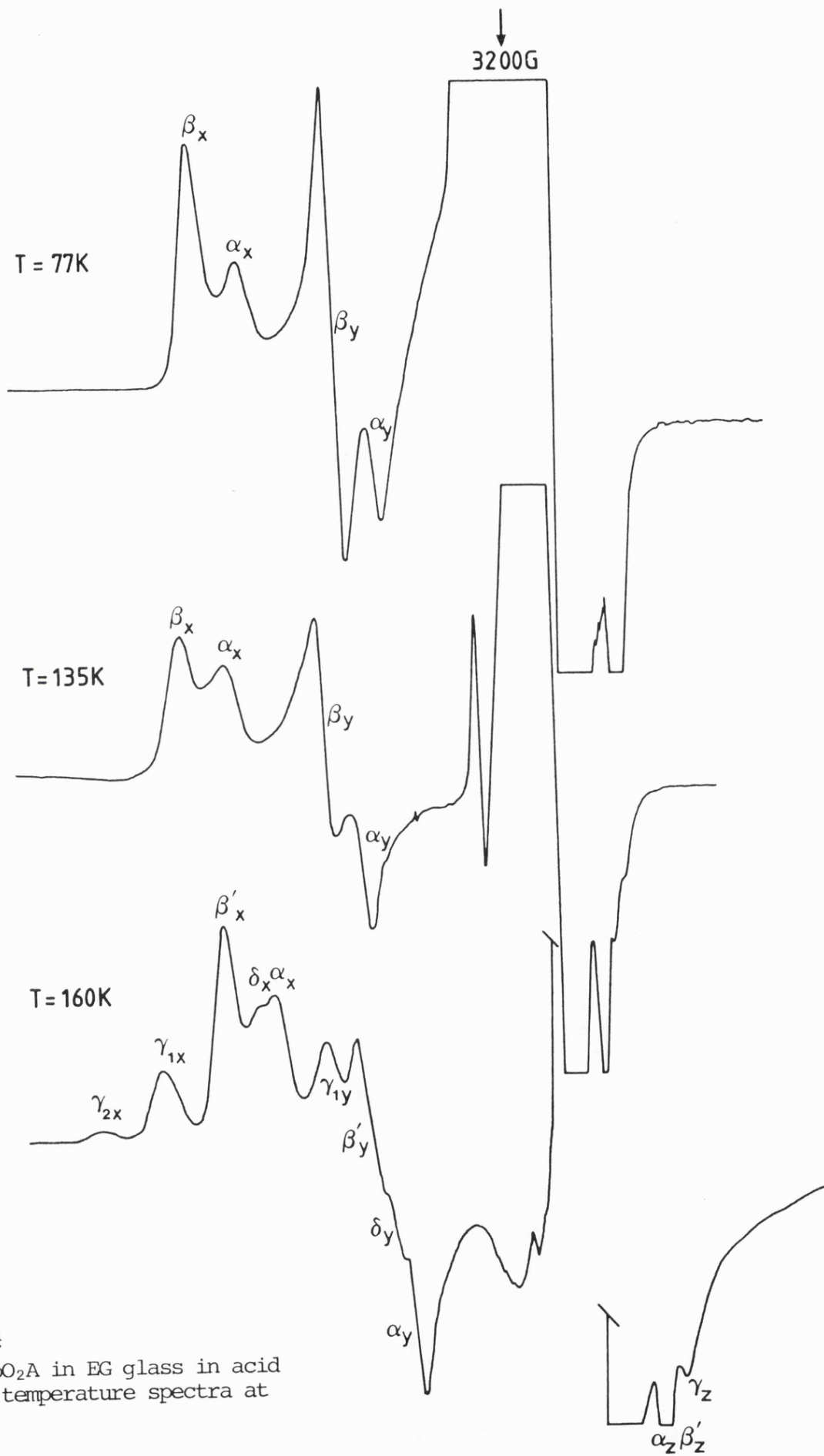
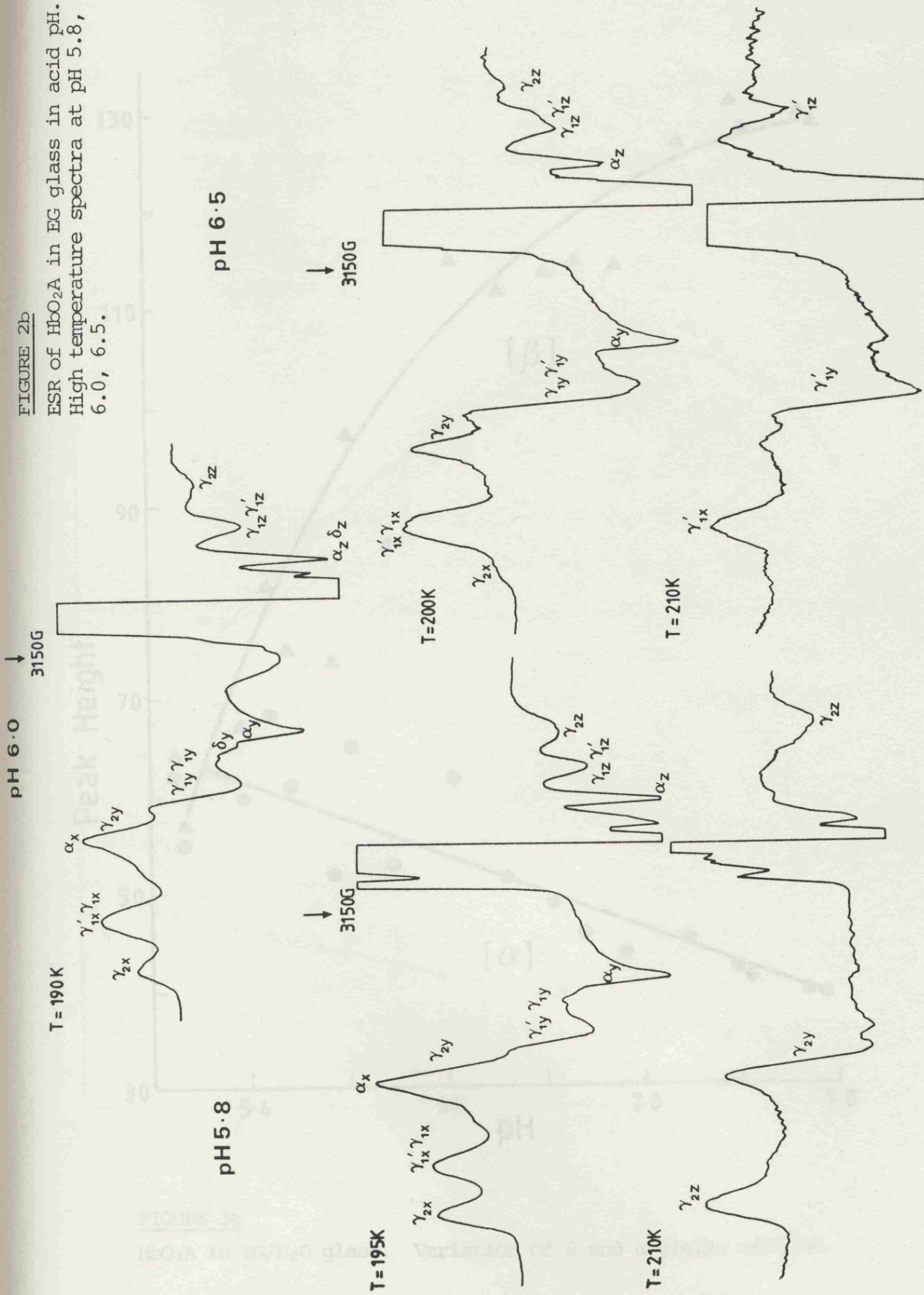


FIGURE 2a

ESR of  $\text{HbO}_2\text{A}$  in EG glass in acid pH. Low temperature spectra at pH 6.0.

FIGURE 2b

ESR of  $\text{HbO}_2\text{A}$  in EG glass in acid pH.  
 High temperature spectra at pH 5.8,  
 6.0, 6.5.



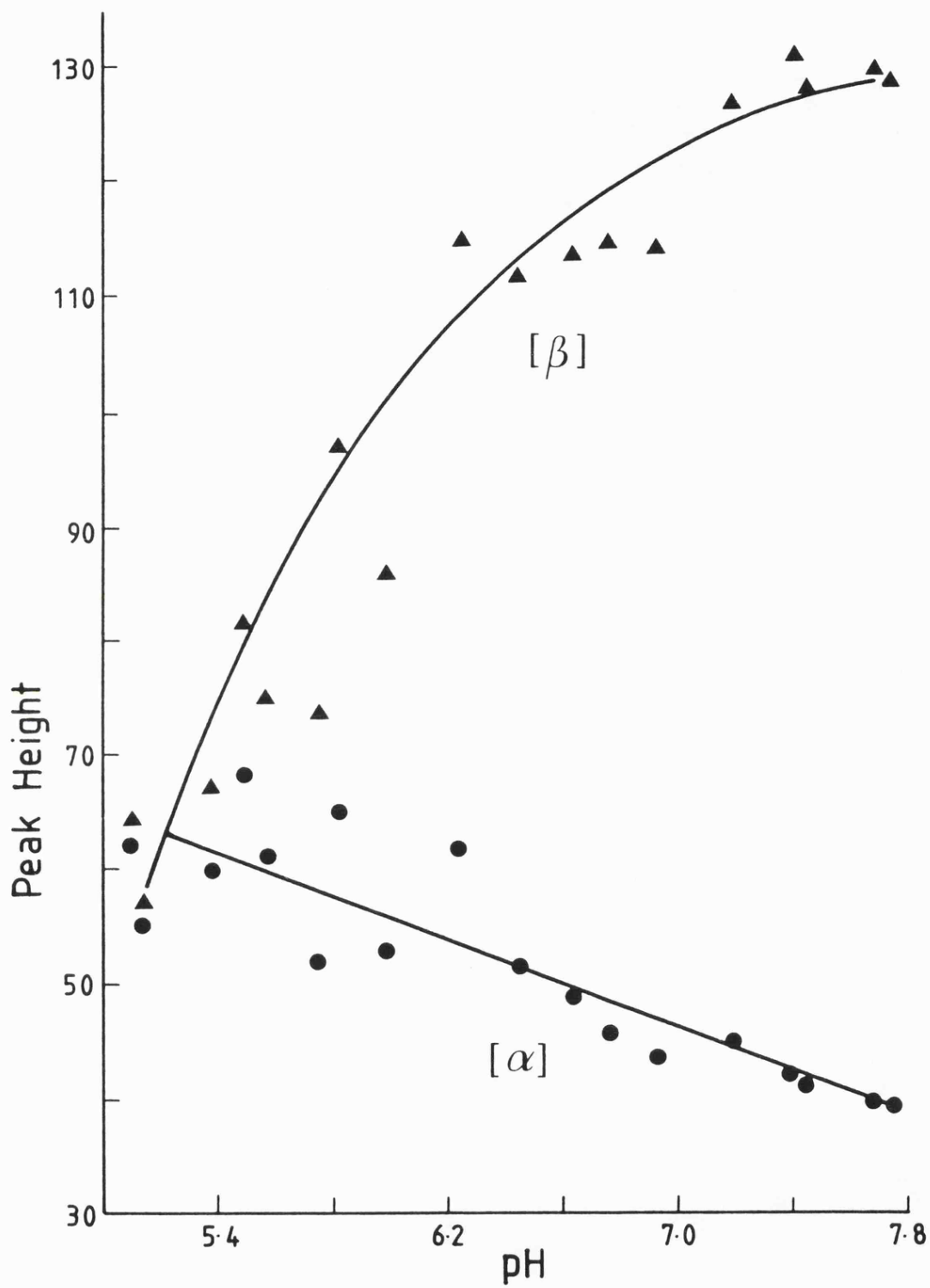
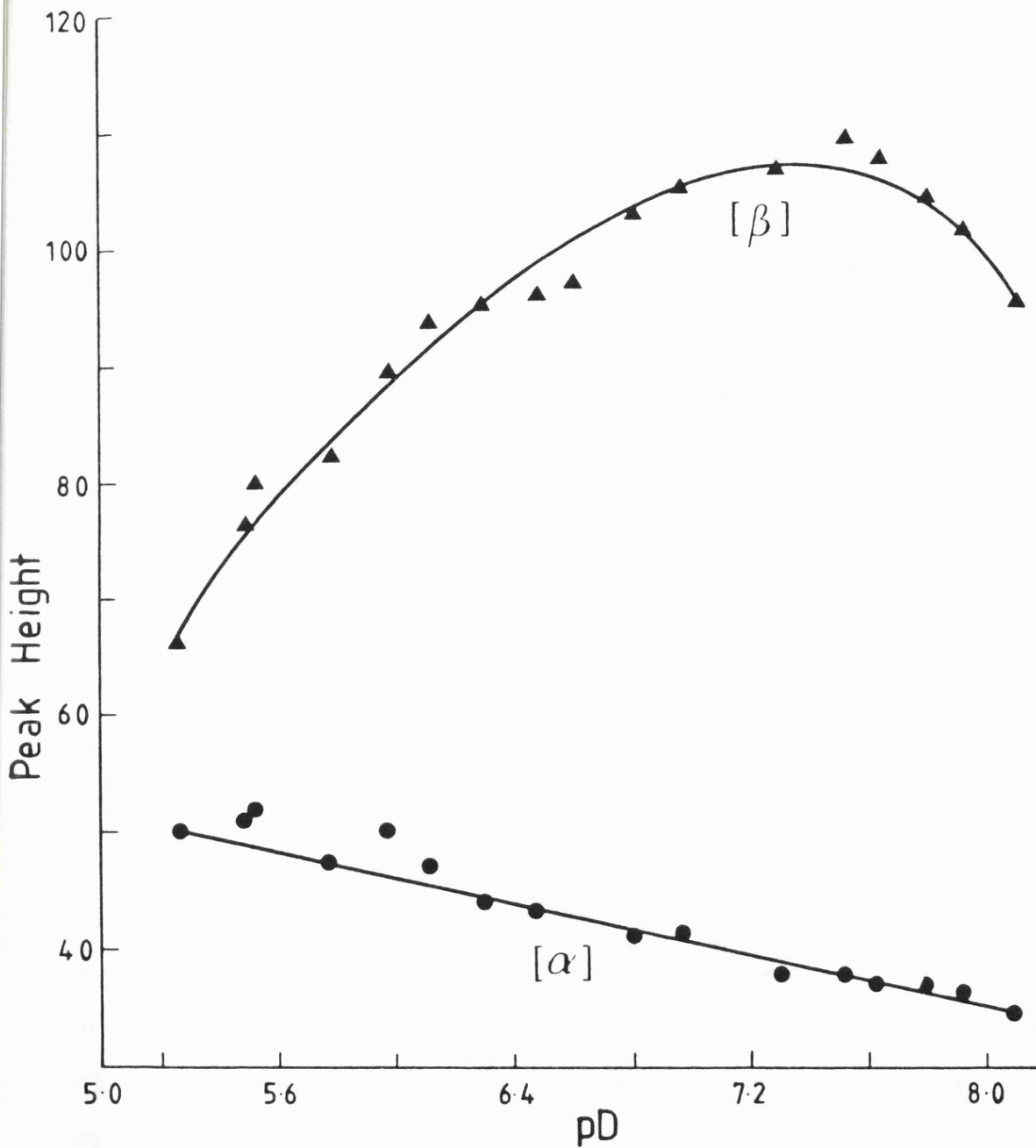


FIGURE 3a

HbO<sub>2</sub>A in EG/H<sub>2</sub>O glass. Variation of β and α yields with pH.

FIGURE 3b

HbO<sub>2</sub>A in deuterated EG/D<sub>2</sub>O glass. Variation of  $\beta$  and  $\alpha$  yields with pD.



evident even at 77 K! On annealing these spectra similar changes occur to those found in ethylene glycol glasses (with the exception that the  $\delta$ -species isn't formed), but at lower temperatures. Isopropanol did not appear to be a very efficient glass former influencing the  $\beta/\alpha$  ratio to a lesser degree. Only low concentrations were used as alcohols readily cause denaturation of HbO<sub>2</sub>A at higher concentrations.<sup>86</sup>

### 3. Frozen aqueous glasses of HbO<sub>2</sub>F

Foetal haemoglobin has the same  $\alpha$  chains as HbA but its  $\beta$  chains (known as  $\gamma$ ) differ at 39 points.<sup>87</sup> The oxygen affinity of HbF is higher in vivo than that of the adult HbA, which facilitates the transfer of oxygen across the placenta. However, when isolated and stripped of organic phosphates, its affinity becomes lower than that of HbA.<sup>88,89</sup> The former effect was attributed solely to the replacement of histidine 143 $\beta$  by serine in the  $\gamma$  chain at the 2,3 DPG binding site. Frier and Perutz,<sup>90</sup> in their X-ray study of HbF, suggested that the lower affinity of stripped HbF may be due to the substitutions Glu 7 $\beta$   $\rightarrow$  Asp  $\gamma$  and Leu 3 $\beta$   $\rightarrow$  Phe  $\gamma$  which draw the A and E helices closer together in much the same way as the organic phosphates do in HbA.

Three main changes are evident on comparison of spectra of irradiated frozen glasses of HbO<sub>2</sub>F with those of HbO<sub>2</sub>A. The  $g_x$  value of the  $\beta$  peak has shifted upfield from 2.250 to 2.2474 (I will refer to the  $\gamma$  chains of HbF as  $\beta$  chains herein, to avoid confusion with the nomenclature of the ESR species  $\gamma$ ) whilst the  $g_x$  value of the  $\alpha$  peak has shifted downfield (Figure 6) and the  $\beta/\alpha$  ratio is significantly lower than in the case of HbO<sub>2</sub>A (Table 4). Spectral changes on annealing above 77 K are very similar to those in HbO<sub>2</sub>A (Figure 4). The only differences being that no  $\delta$  is formed and that  $\beta'$  decays, in part, into  $\gamma_1$  and, in part, shifts into an analogous centre  $\beta''$  ( $g_x = 2.656$ ,  $g_y = 2.1606$  and  $g_z = 1.957$ ).

TABLE 3

Variation in yield and g-value of  $\alpha$  and  $\beta$  species of  $\text{HbO}_2\text{A}$  in frozen deuterated glasses

pD	$\beta$	$\alpha$	$\beta/\alpha$	$g_x \beta$	$g_x \alpha$
5.26	66	50	1.20	2.2500	2.2181
5.48	76	51	1.50	2.2493	2.2178
5.52	80	52	1.54	2.2497	2.2177
5.78	82	47	1.75	2.2495	2.2174
5.98	90	50	1.84	2.2491	2.2165
6.11	94	47	2.00	2.2499	2.2162
6.29	95	44	2.17	2.2497	2.2160
6.48	96	43	2.24	2.2498	2.2160
6.60	97	42	2.32	2.2496	2.2163
6.80	103	41	2.52	2.2499	2.2157
6.96	105	41	2.54	2.2503	2.2155
7.30	107	38	2.82	2.2501	2.2140
7.52	110	38	2.89	2.2494	2.2131
7.63	108	37	2.92	2.2497	2.2125
7.80	105	37	2.84	2.2491	2.2122
7.92	102	36	2.79	2.2496	2.2120
8.10	96	34	2.78	2.2499	2.2117

TABLE 4

Variation in yield and g-value of  $\alpha$  and  $\beta$  species of  $\text{HbO}_2\text{F}$  in frozen aqueous glasses

pH	$\beta$	$\alpha$	$\beta/\alpha$	$g_x \beta$	$g_x \alpha$
5.20	40	53	0.75	2.2467	2.2222
5.52	41	55	0.74	2.2470	2.2226
5.75	53	59	0.90	2.2478	2.2214
5.90	50	49	1.03	2.2469	2.2216
6.00	58	55	1.05	2.2476	2.2210
6.38	67	49	1.37	2.2477	2.2194
6.43	84	59	1.41	2.2470	2.2200
6.55	75	49	1.55	2.2480	2.2203
6.75	82	50	1.65	2.2478	2.2190
6.92	84	43	1.95	2.2470	2.2174
7.09	101	46	2.19	2.2480	2.2175
7.29	108	42	2.57	2.2479	2.2163
7.56	103	42	2.48	2.2470	2.2153
7.82	106	44	2.49	2.2469	2.2152
7.88	109	42	2.52	2.2472	2.2140

TABLE 5

g-Values for the various species formed on irradiation of  $\text{MbO}_2$

Species	$g_x$	$g_y$	$g_z$
Mb (acid)	2.2200	2.1180	1.9590
Mb (neutral)	2.2215	2.1186	1.9580
Mb (alkaline)	2.2240	2.1190	1.9580
Mb'	2.2450	2.1340	1.9586
My	2.3190	2.1860	1.9363

TABLE 6

Yield of  $\beta/\alpha$  as a function of solvent concentration

Concentration (% v/v)	Ethylene Glycol ( $\beta/\alpha$ )	Polythene Glycol ( $\beta/\alpha$ )	Isopropanol* ( $\beta/\alpha$ )	Methanol* ( $\beta/\alpha$ )
0	1.02	1.02	1.02	1.02
10	1.65	1.39	1.13	1.93
20	2.04	1.48	1.24	2.32
30	2.09	1.50	-	-
40	2.08	1.69	-	-
50	2.71	1.96	-	-

[\* Denatures above 20% v/v]

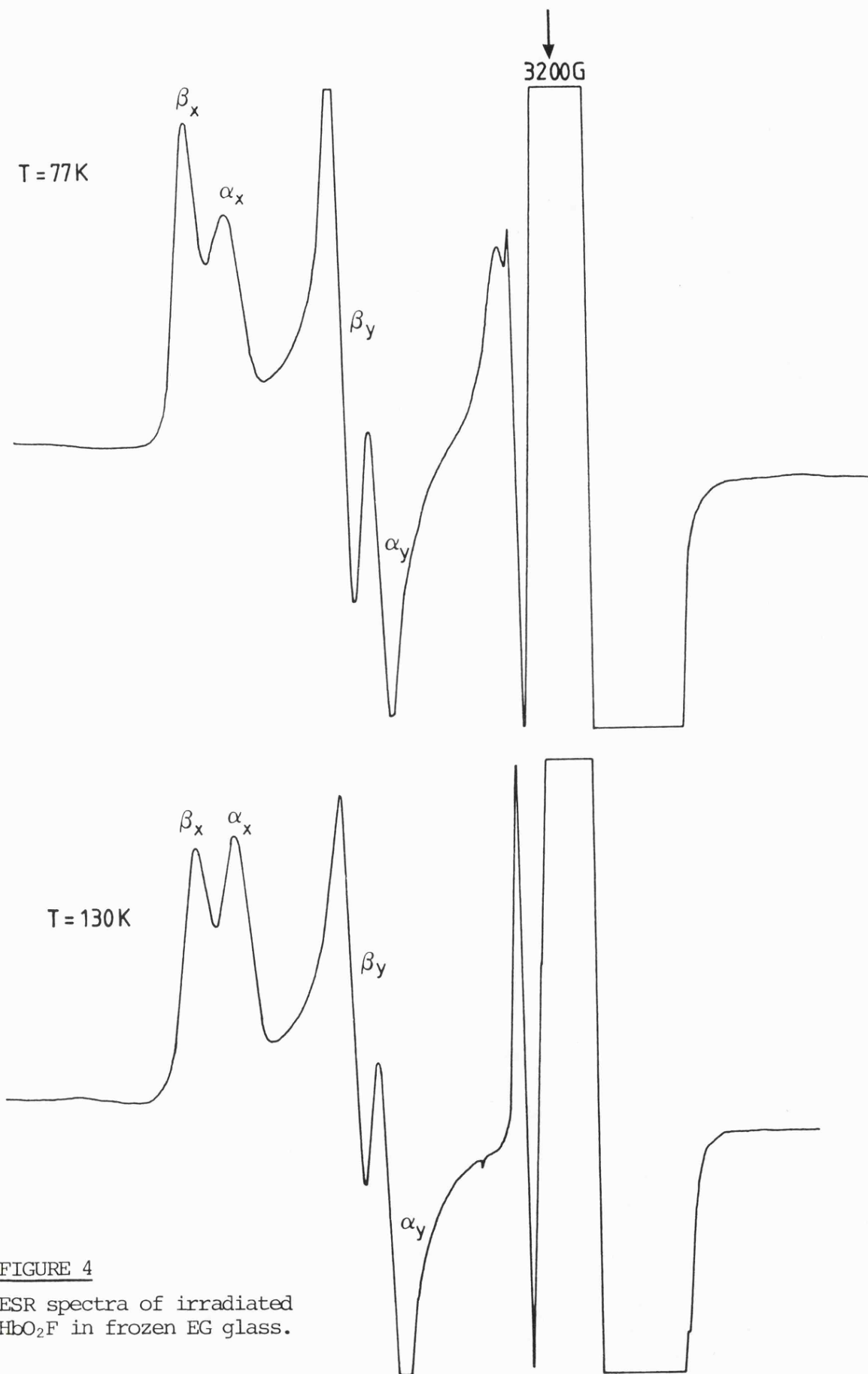


FIGURE 4

ESR spectra of irradiated  $\text{HbO}_2\text{F}$  in frozen EG glass.

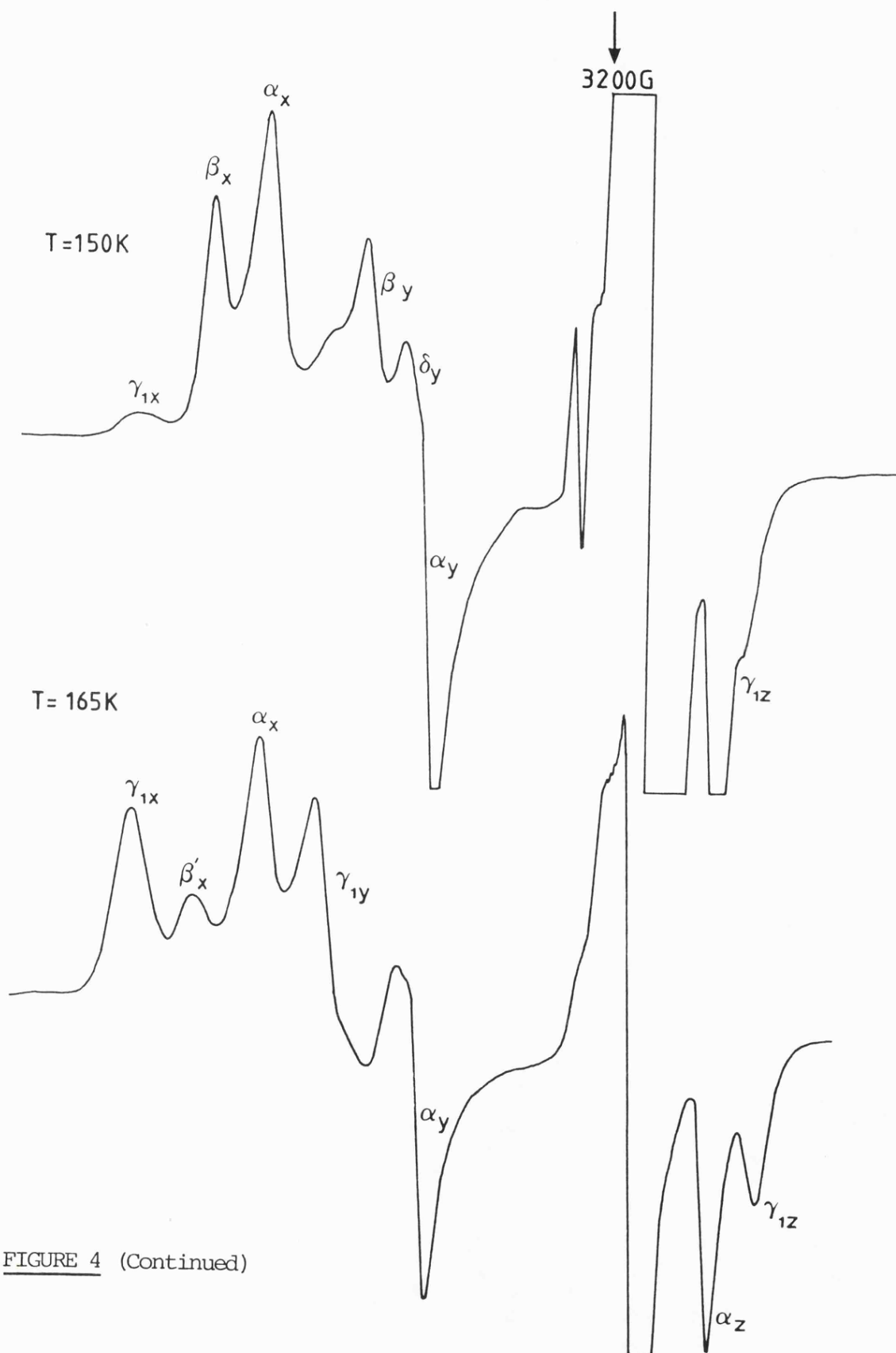


FIGURE 4 (Continued)

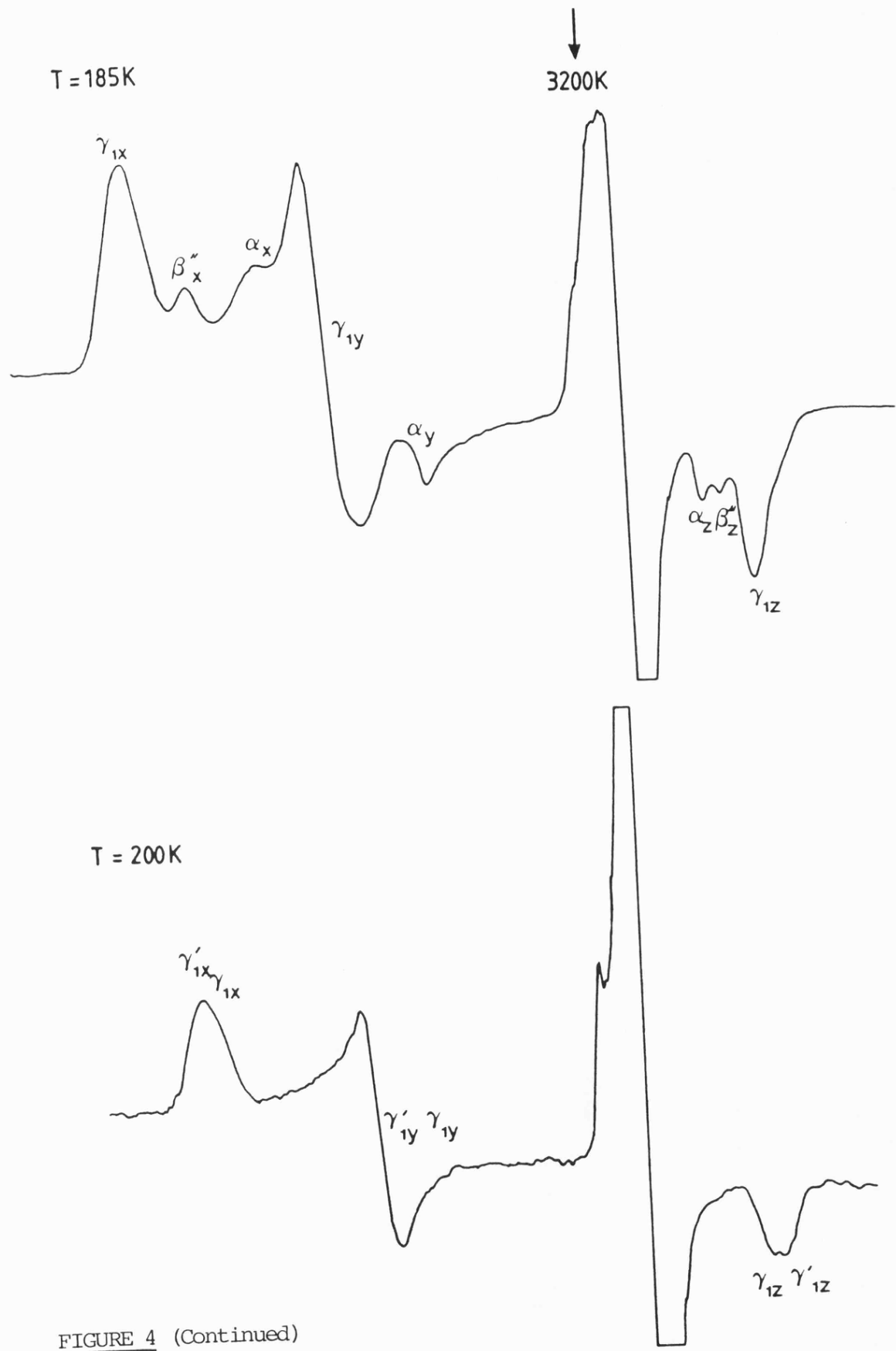


FIGURE 4 (Continued)

Finally residual  $\alpha$  and  $\beta''$  along with  $\gamma_1$  decay into  $\gamma_1'$ .

(i) pH effect

The effect of pH is similar to the case in HbO<sub>2</sub>A in that the  $\underline{g}$  value of the  $\alpha$  chain varies with pH whilst the  $\underline{g}$ -value of the  $\beta$  chain is insensitive to pH. This effect is depicted graphically in Figure 6, which also shows the difference in  $\underline{g}$ -value of the chains in the two HbO<sub>2</sub> types as well as their sensitivity/insensitivity to pH. Figure 5 is a plot of the variation of the  $\alpha$  and  $\beta$  yields at 77 K in HbO<sub>2</sub>F. This plot shows that the situation is again similar to HbO<sub>2</sub>A, in that the  $\beta$  yield is pH sensitive whilst the  $\alpha$  yield is relatively insensitive. However, in contrast to HbO<sub>2</sub>A, the yield curves actually cross near pH 6 and the  $\beta/\alpha$  ratio becomes less than one below this pH (Table 4).

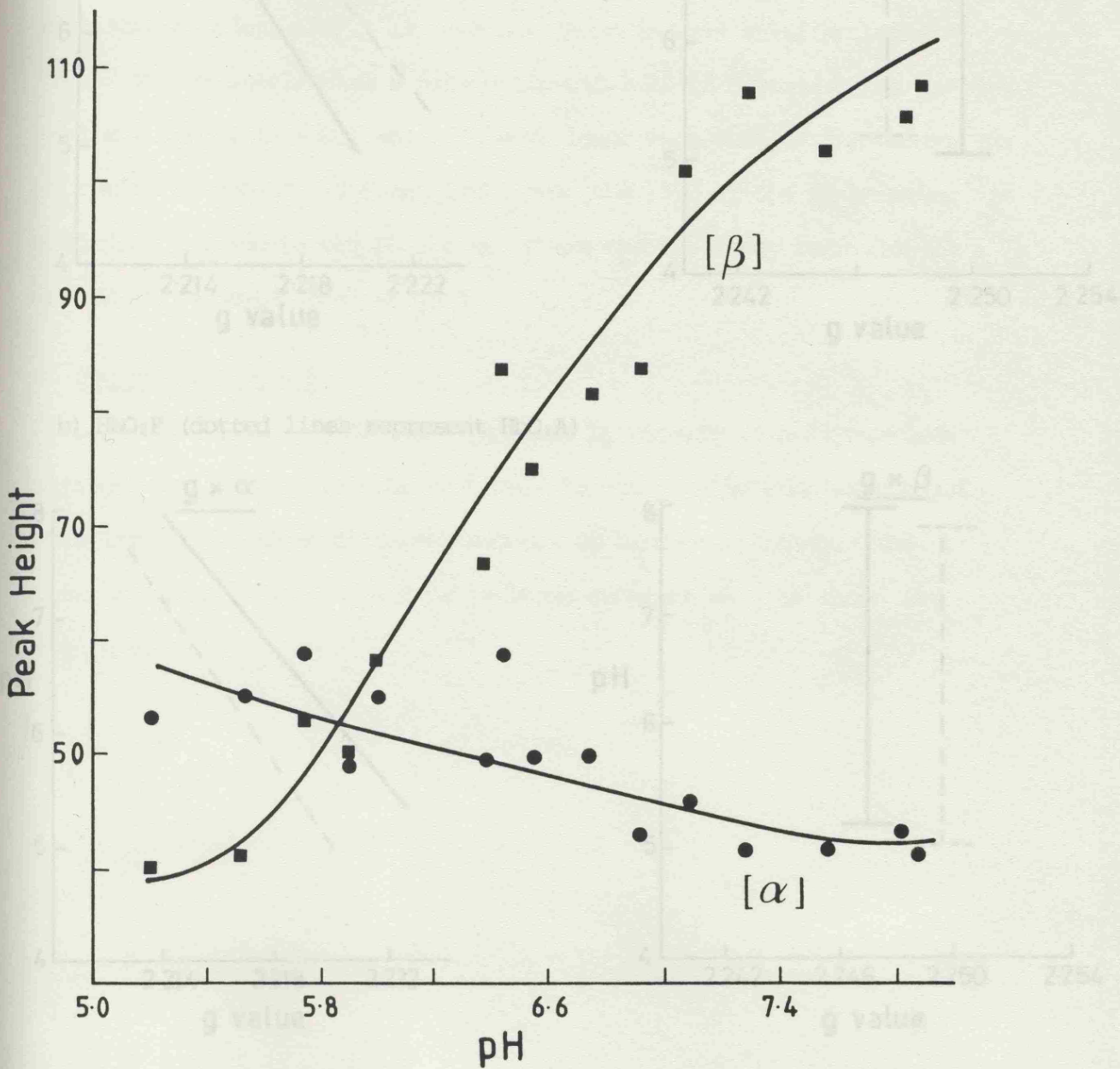
The effect of pH on the samples, on anneal, is identical to that of HbO<sub>2</sub>A in that the species  $\gamma_2$  is found, in a pH dependent equilibrium with  $\gamma_1$ , below pH 6 whilst alkaline spectra are identical with those at neutral pH.

4. Frozen aqueous glasses of oxymyoglobin

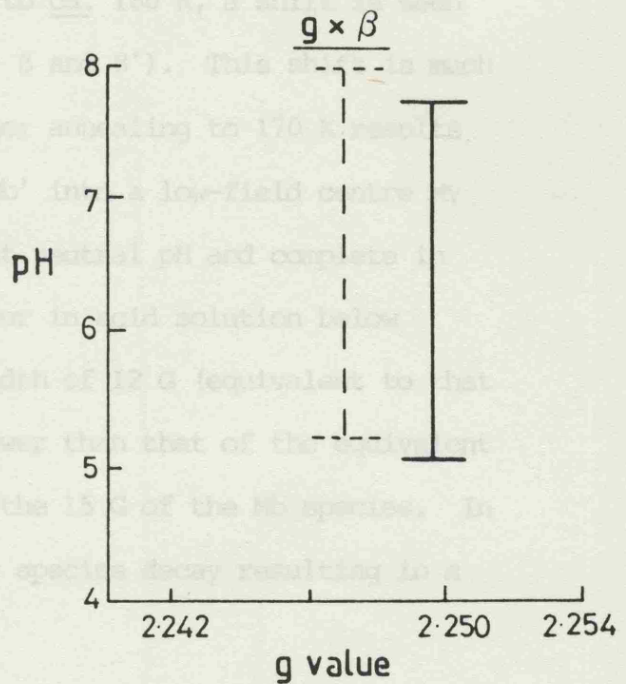
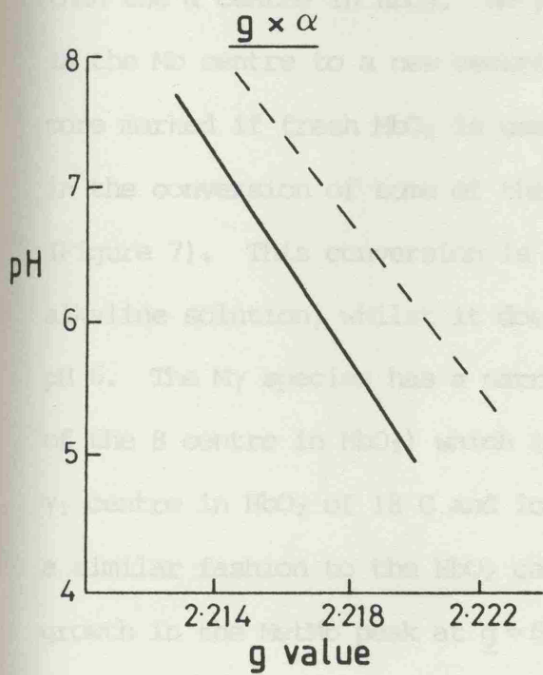
As reported earlier<sup>21</sup> the primary (FeO<sub>2</sub>)<sup>-</sup> centre (Mb) formed in irradiated glasses of oxymyoglobin (MbO<sub>2</sub>) has  $\underline{g}$ -values similar to the  $\alpha$  and  $\beta$  centres in HbO<sub>2</sub>. Its value being very close to that of the  $\alpha$  centre of HbO<sub>2</sub>. The production of a  $\gamma$ -type species (herein labelled M $\gamma$ ), on warming to high temperatures, was also observed. However, there was no mention of any pH dependent changes or other  $\underline{g}$ -value changes. In studies of MbO<sub>2</sub> I used fresh myoglobin (horse heart) as well as commercially available lyophilised myoglobin in frozen aqueous and frozen glassy solutions. The results from the glassy solutions were identical to those from the non-glassy system and the differences between the commercially freeze-dried myoglobin and freshly obtained protein were

FIGURE 5

HbO<sub>2</sub>F in EG/H<sub>2</sub>O glass. Variation of  $\beta$  and  $\alpha$  yields with pH.



a)  $\text{HbO}_2\text{A}$  (dotted lines represent  $\text{HbO}_2\text{F}$ )



b)  $\text{HbO}_2\text{F}$  (dotted lines represent  $\text{HbO}_2\text{A}$ )

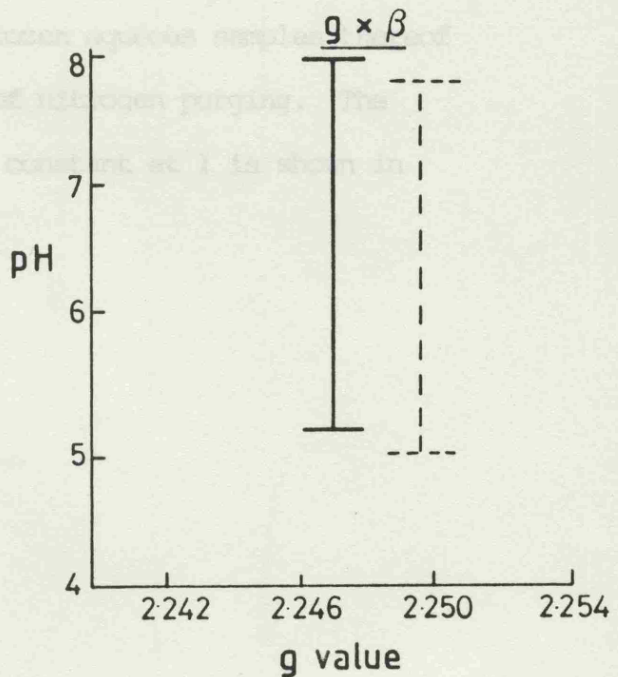
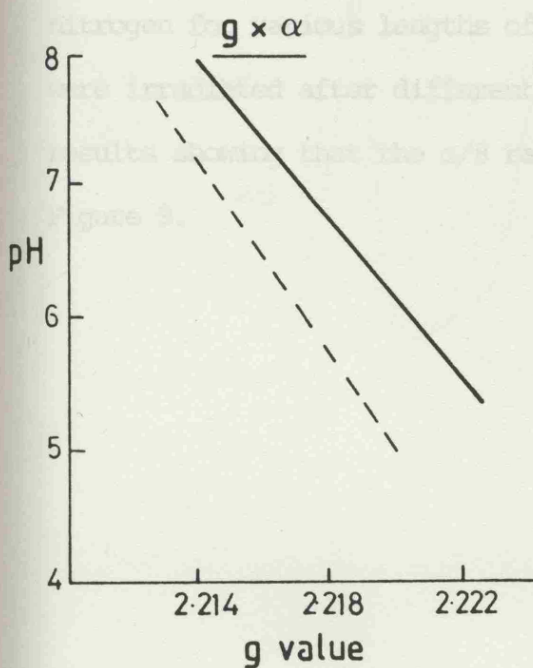


FIGURE 6

Comparison of pH effect on  $g_x$  values for  $\alpha$  and  $\beta$  in  $\text{HbO}_2\text{A}$  and  $\text{HbO}_2\text{F}$ .

only slight.

The  $(\text{FeO}_2)^-$  centre, Mb, is slightly pH sensitive though much less so than the  $\alpha$  centre in  $\text{HbO}_2$ . On annealing to ca. 160 K, a shift is seen in the Mb centre to a new centre Mb' (cf.  $\beta$  and  $\beta'$ ). This shift is much more marked if fresh  $\text{MbO}_2$  is used. Further annealing to 170 K results in the conversion of some of the Mb and Mb' into a low-field centre  $M\gamma$  (Figure 7). This conversion is partial at neutral pH and complete in alkaline solution, whilst it does not occur in acid solution below pH 6. The  $M\gamma$  species has a narrow linewidth of 12 G (equivalent to that of the  $\beta$  centre in  $\text{HbO}_2$ ) which is much lower than that of the equivalent  $\gamma_1$  centre in  $\text{HbO}_2$  of 18 G and lower than the 15 G of the Mb species. In a similar fashion to the  $\text{HbO}_2$  case, these species decay resulting in a growth in the MetMb peak at  $g = 6$

##### 5. Deoxyhaemoglobin A

Degassed samples of HbA were produced by purging with oxygen-free nitrogen for various lengths of time. Frozen aqueous samples thereof were irradiated after different amounts of nitrogen purging. The results showing that the  $\alpha/\beta$  ratio stays constant at 1 is shown in Figure 9.

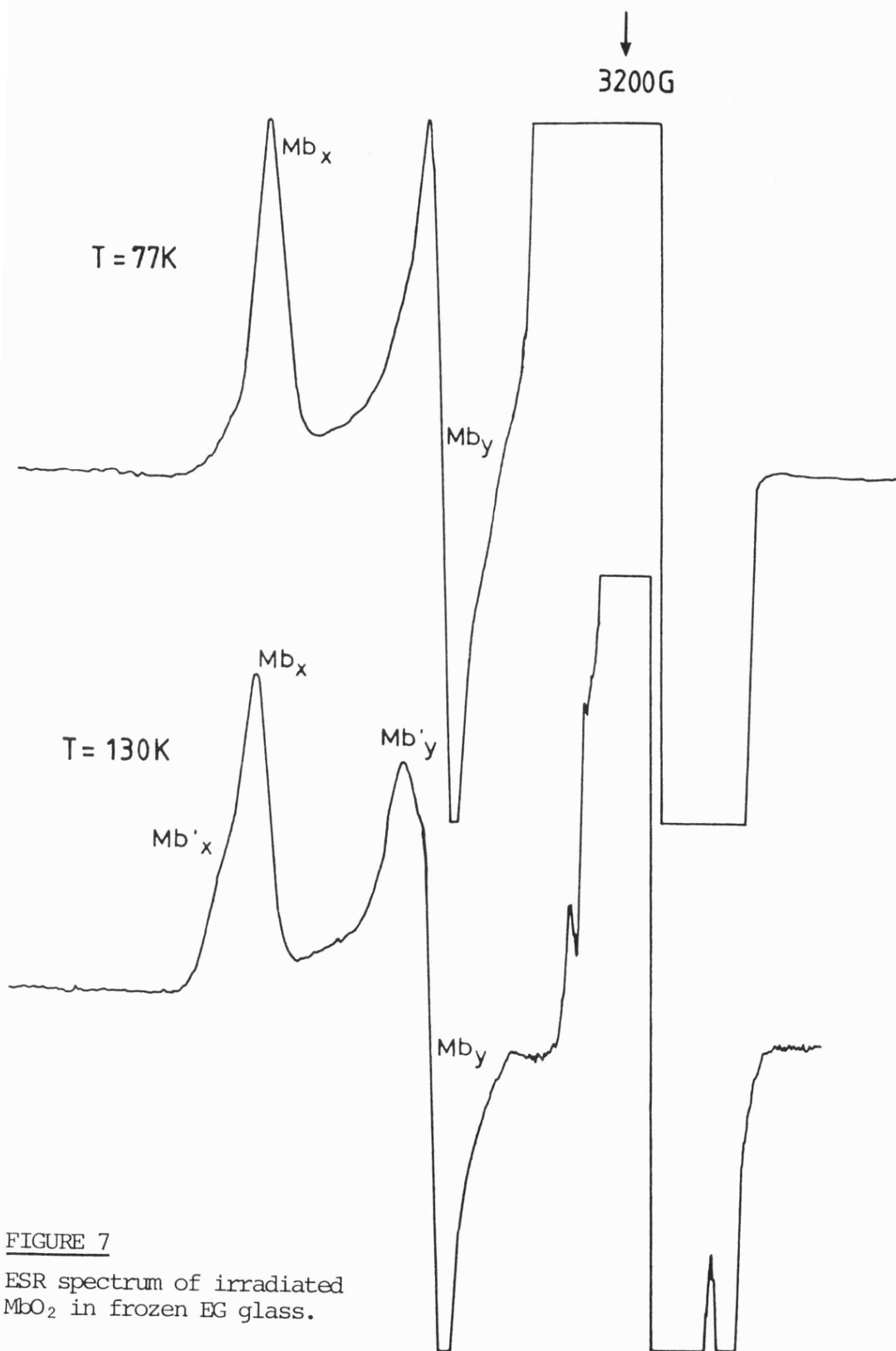


FIGURE 7  
 ESR spectrum of irradiated  
 $MnO_2$  in frozen EG glass.

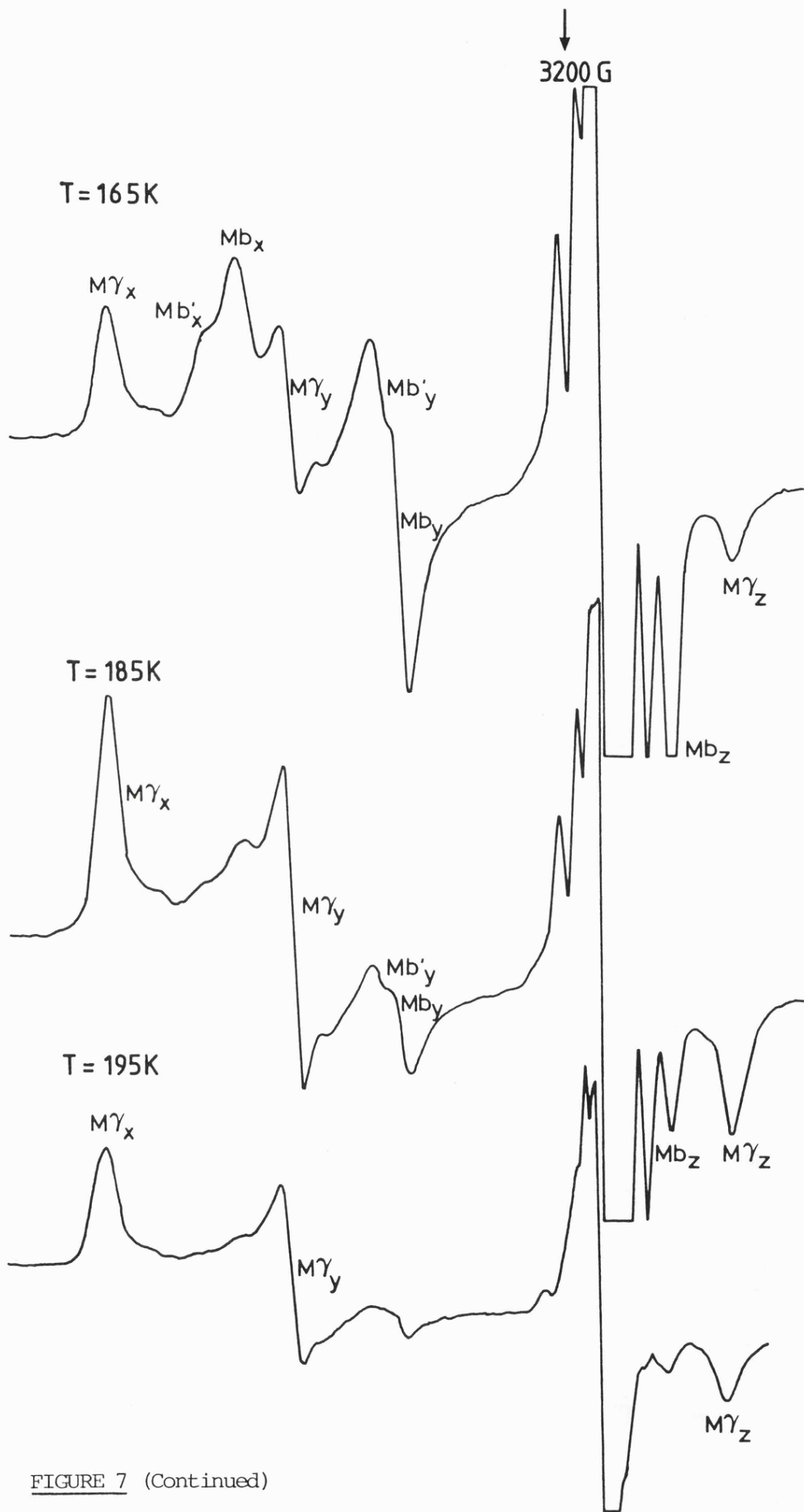


FIGURE 7 (Continued)

FIGURE 8

Effect of various solvents on the  $\beta/\alpha$  ratio.

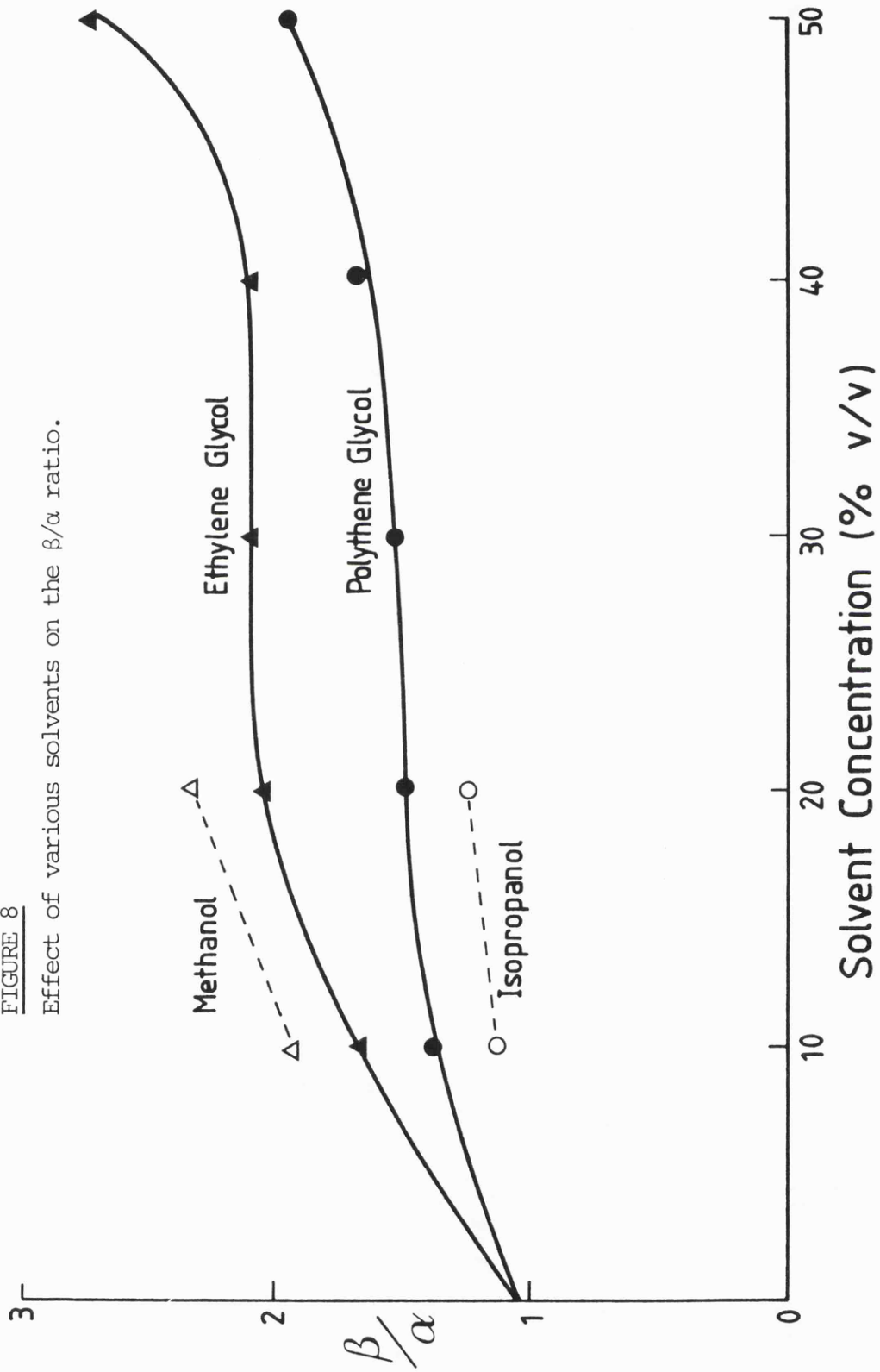
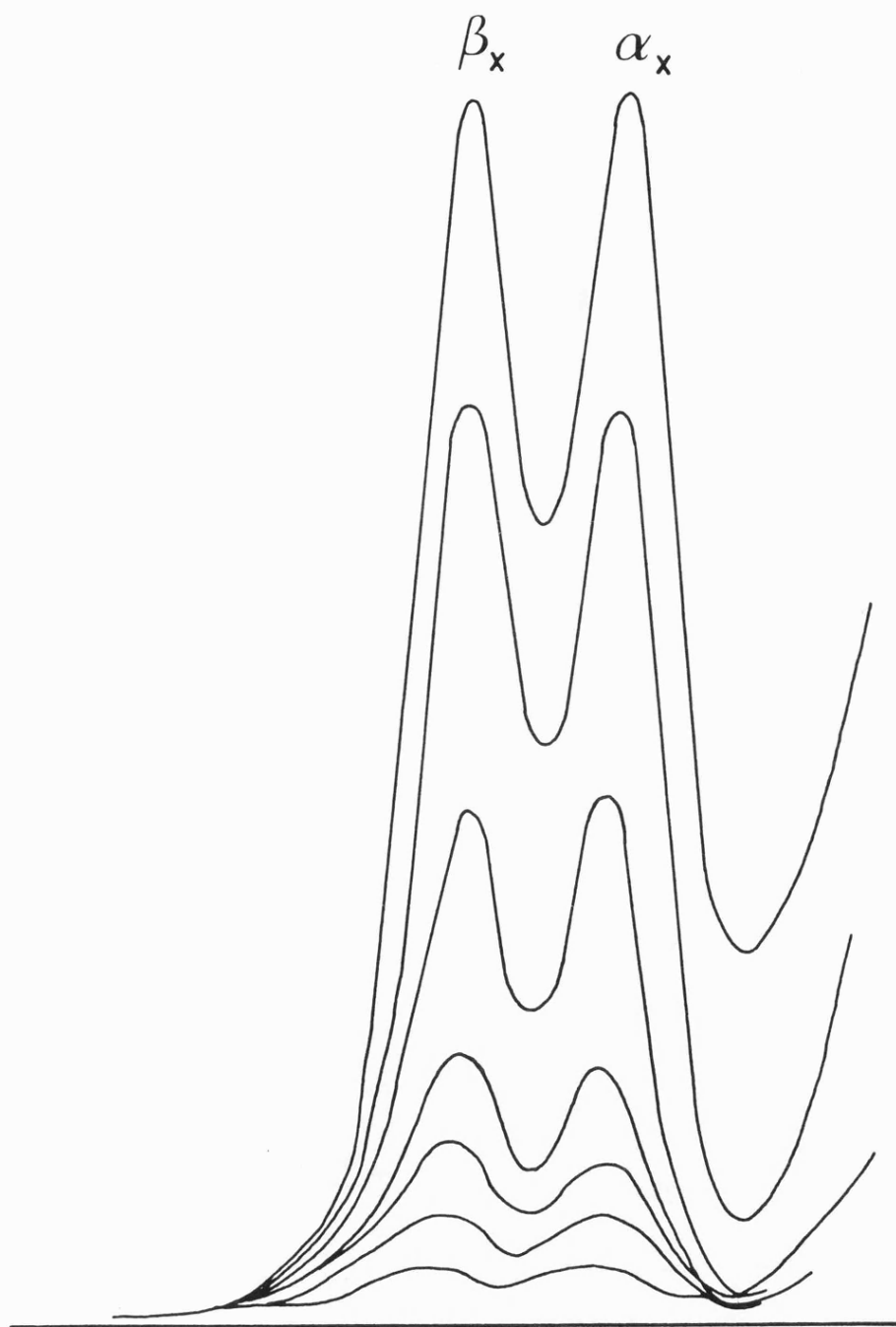


FIGURE 9

Effect of deoxygenation on yields of  $\alpha$  and  $\beta$  species in frozen aqueous solutions of HbO<sub>2</sub>A.



## DISCUSSION

### Solvent effects at 77 K

From the results it is clear that the presence of glassifying agents such as ethylene glycol markedly influence the outcome of the results in the case of haemoglobins A and F but not myoglobin.

In the glassy state the yields of the  $\alpha$  and  $\beta$  centres are no longer equivalent except at very low pH's. The  $\beta$  yield becomes pH dependent to the point where the  $\beta/\alpha$  ratio reaches just over 3:1 in alkaline glasses. This effect is likely to be caused by conformational changes induced in the  $\beta$  chains by the glassy state. This results in the increased channelling and capture of electrons at the  $\text{FeO}_2$  moiety with increasing pH. Isotopic substitution with  $\text{D}_2\text{O}$  and  $\text{d}_6$  deuterated EG did not affect the results other than to shift the corresponding graphs by approximately 0.2-0.4 of a pH/pD unit (Figures 3a and 3b). This is in line with the relationship  $\text{pH} = \text{pD} + 0.4$ .<sup>92</sup>

### g-Values at 77 K

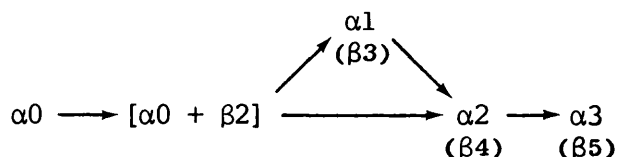
The  $g$ -values of the two chains were deduced from separated chain experiments<sup>21,85</sup> and the fact that they are the primary centres was verified by irradiating samples between 4 K and 77 K.<sup>85</sup> The fact that the  $g$ -values of the centres are different reflects differences in the configuration of the haem pockets as sensed by ENDOR<sup>85</sup> and also may reflect the strength of the hydrogen bond to the distal histidine which would appear to be stronger in the case of the  $\beta$  subunit. Unlike the  $\beta$  subunit, the  $g$ -value of the  $\alpha$  chain is strongly influenced by pH (Figure 6), shifting downfield as the pH decreases. This could be caused by an increase in strength of the distal histidine hydrogen bond on going to acid solution.

### Anneal products

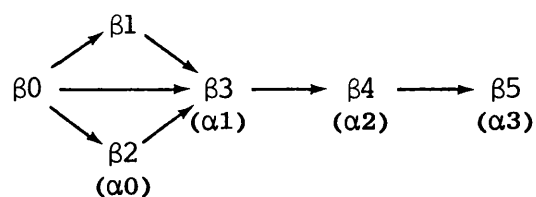
The decay products discovered on anneal of neutral and alkaline pH

samples are common both to frozen aqueous and glassy solutions. Of the array of decay pathways, it is the first reaction, that of growth of the  $\alpha$  centre at the expense of  $\beta$ , that is hardest to rationalise. It seems beyond possibility that the electron in the  $(\text{FeO}_2)^-$  centres in the  $\beta$  chain could be encouraged to leave and channel all the way through the globin path to reach the conjugate  $\alpha$   $\text{FeO}_2$  centre. What must therefore be the case is that the first decay product from the  $\beta$  unit fortuitously has a  $g$ -value that directly overlaps that of the  $\alpha$  unit, giving rise to the mistaken impression that the  $\beta$   $(\text{FeO}_2)^-$  unit converts directly into the  $\alpha$   $(\text{FeO}_2)^-$  unit. For clarification of the origin (be it  $\alpha$  or  $\beta$ ) of the decay centres, I have included the following scheme which illustrates the decay pattern, on anneal, by chain type:-

$\alpha$  chain:



$\beta$  chain:



Nomenclature

$\alpha$ = $\alpha_0$ and $[\alpha_0 + \beta_2]$	$\delta$ = $\alpha_1 \beta_3$
$\beta$ = $\beta_0$	$\gamma_1$ = $\alpha_2 \beta_4$
$\beta'$ = $\beta_1$	$\gamma_1'$ = $\alpha_3 \beta_5$

Conjugate chain decay products are listed below in brackets in instances where two chain decay products have the same  $g$ -values.

Acid pH and solvent effects above 77 K

Unlike the case for neutral and alkaline samples the high temperature

decay pathway differs significantly in the case of frozen glassy solutions of  $\text{HbO}_2$  in acid pH, whilst the temperature decay pathways remain the same over the whole pH range for frozen aqueous  $\text{HbO}_2$  solutions. Here again we are confronted with a fundamental difference brought about by conformational changes induced in the units by the glassy structure of the solvent. The result being the preferential formation of  $\gamma_2$  as opposed to  $\gamma_1$  and  $\gamma_1'$  (Figure 2).

Symons and Petersen<sup>21</sup> suggested that the outer oxygen of the  $(\text{FeO}_2)^-$  centres is hydrogen bonded to the  $\text{N}_\epsilon$  of the distal histidine in the  $\alpha$  and  $\beta$  chains in  $\text{HbO}_2$ . They went on to suggest that the  $\Delta g$  shift associated with the transition of the  $\alpha$  and  $\beta$  centres into  $\gamma$ -type centres, in irradiated  $\text{HbO}_2$ , resulted from the transfer of this proton from the nitrogen to the outer oxygen of the  $\text{FeO}_2$  unit. Subsequent loss of the  $\text{HO}_2^-$  ligand results in loss of  $\gamma$  signal with growth in the free  $\text{Fe}^{\text{III}}$  high-spin signal at  $g=6$ .

In the low pH situation the new species  $\gamma_2$  is formed preferentially to the  $\gamma_1\gamma_1'$  species. The appearance of  $\gamma_2$  is not found until around the pH 6.5 mark, increasing in yield as the pH lowers. As the  $\text{pK}_a$  of the distal histidine is in the 6.5 region, I suggest that the proton linked to the  $\text{N}_\delta$  of the distal histidine, below pH 6.5, is able to also transfer to the  $\text{FeO}_2^-$  unit along with  $\text{N}_\epsilon$  proton. Thus producing  $\text{FeO}_2\text{H}_2^+$  which undergoes rapid loss of  $\text{H}_2\text{O}_2$  to produce the  $\text{Fe}^{\text{III}}$  low-spin species  $\gamma_2$ , which subsequently reverts to the more stable high-spin  $\text{Fe}^{\text{III}}$  on increasing the temperature.

In the higher pH situation only one proton is readily available and hence the ligand is  $\text{HO}_2^-$ . As  $\text{HO}_2^-$  is a much less labile ligand than  $\text{H}_2\text{O}_2$  the iron centre cannot lose its ligand at temperatures that will stabilise the low-spin ferric species.

Support for the hypothesis that the  $\text{FeO}_2$  units are hydrogen bonded in the  $\alpha$  and  $\beta$  chains as well as in  $\text{MbO}_2$  is available from ENDOR, ESR and XRD studies. Kappl *et al.*,<sup>85</sup> using  $^1\text{H}$  ENDOR, showed that there is an exchangeable proton coupling in the  $\alpha$  and  $\beta$  subunits as well as in  $\text{MbO}_2$ . Phillips showed, from an XRD study of  $\text{MbO}_2$ ,<sup>11</sup> that the positioning of the oxygen ligand was ideal for hydrogen bonding to the  $\text{N}_\epsilon\text{H}$  of the distal histidine. My work on the ESR of Hb Glycera (which has a distal leucine instead of histidine), in the next chapter, shows that the  $g$ -value of the  $(\text{FeO}_2)^-$  unit produced at 77 K is significantly upfield from those in the  $\alpha$ ,  $\beta$  and  $\text{MbO}_2$  chains. The fact that the  $g$ -value is close to free-spin shows that there is little spin-density on the iron, i.e. the unit is similar to free superoxide. Any proton interaction would involve more spin-density on the iron and, therefore, a greater  $\Delta g$  as found for the  $\alpha$  and  $\beta$  units in  $\text{HbO}_2$  and the Mb unit in  $\text{MbO}_2$ .

The next stage in the mechanism, proton transfer and subsequent ligand loss, finds support from ENDOR and ESR data. Kappl *et al.*<sup>85</sup> discovered that the exchangeable proton coupling from the  $\text{N}_\epsilon\text{H}$  of the distal histidine is lost on annealing up to 190 K in the  $\alpha$ ,  $\beta$  and  $\text{MbO}_2$  units, implying that proton transfer had taken place. Using isotopic ligand substitution with gaseous  $^{17}\text{O}$ , they were able to see satellite hyperfine coupling in the ESR of  $\text{Hb}^{17}\text{O}_2$  and  $\text{Mb}^{17}\text{O}_2$  at 77 K. As with the ENDOR case for the exchangeable proton they found that all satellite coupling had disappeared on annealing to 190 K.

#### HbO<sub>2</sub>F

Results show that the  $\beta/\alpha$  ratio at 77 K is lower than for  $\text{HbO}_2\text{A}$  at neutral pH. Variation of pH shows that  $\beta/\alpha$  ratio actually falls below zero at pH 6.0. The  $\beta$  centre yield is reduced compared to that in  $\text{HbO}_2\text{A}$ , presumably as a result of the differences between the  $\beta$  chain in

HbF and HbA. The other significant difference between HbO<sub>2</sub>F and HbO<sub>2</sub>A is the  $g_x$ -values of both the  $\alpha$  and  $\beta$  species. The  $g_x$  value of the  $\beta$  chain of HbO<sub>2</sub>F (Figure 6) is 0.0025 upfield from that of HbO<sub>2</sub>A, again presumably as a result of structural differences in the globin chain, whilst the  $\alpha$  peak of HbO<sub>2</sub>F is downfield of the  $\alpha$  peak in HbO<sub>2</sub>A by the same amount. This small shift in  $g_x$   $\alpha$  may be as a result of small differences at the haem centre, affecting the hydrogen bond strength, or as a result of conformational changes elsewhere in the chain. Nonetheless, the  $\alpha$  chain peak in HbO<sub>2</sub>F parallels the  $g$ -value variation with pH seen in HbO<sub>2</sub>A.

### MbO<sub>2</sub>

Unlike HbO<sub>2</sub>, MbO<sub>2</sub> is unaffected by the use of glass-forming solvents. The (FeO<sub>2</sub>)<sup>-</sup> centre is pH dependent to a small degree. Curiously enough, the  $g$ -value shift found in MbO<sub>2</sub> is opposite in direction to that found in the case of the  $\alpha$  centre in HbO<sub>2</sub>, decreasing in  $g$ -value on decrease of pH, i.e. more spin onto oxygen on reduction in pH. On anneal of glassy solutions, a conjugate  $\gamma$ -type species, M $\gamma$ , is formed which, interestingly, has a much reduced linewidth, cf.  $\gamma_1$  or  $\gamma_2$  in HbO<sub>2</sub>, which is probably due to the fact that only one centre constitutes the species unlike the  $\alpha_2\beta_4$  or  $\alpha_3\beta_5$  situation with  $\gamma_1$  and  $\gamma_1'$  in HbO<sub>2</sub>. This M $\gamma$  species increases in yield at neutral pH and above. The likely reason for this being that ligand loss is too rapid after proton transfer in acidic solution, where additional protons may be available from water molecules in the haem pocket. Clearly the low-spin Fe<sup>III</sup> form is not stabilised in MbO<sub>2</sub>, with rapid formation of the high-spin MetMb occurring.

### Conclusion

This study, along with supporting ENDOR evidence, confirms the suggested mechanism<sup>21</sup> of proton transfer and subsequent ligand loss as

the likely mechanism for autoxidation in irradiated MbO<sub>2</sub> and HbO<sub>2</sub>. This serves as an analogous model for the autoxidation mechanism in undamaged HbO<sub>2</sub> and MbO<sub>2</sub>.

The study also highlights the strong effect that glass-forming solvents have on the relative yields of the (FeO<sub>2</sub>)<sup>-</sup> centres which is particularly interesting in view of the fact that ENDOR results show that the haem conformation is not affected by addition of glass-forming agents.<sup>85</sup> The sensitivity of the ESR technique both to changes at the haem itself and to more distant conformational changes is reflected by the myriad of very subtle changes that occur in the yield and g-values of the different species in HbO<sub>2</sub>A and MbO<sub>2</sub>. However, to get a complete picture of the system, it is necessary to study single crystals as well as frozen solutions using ESR as well as the complimentary ENDOR technique.

## REFERENCES FOR CHAPTER 2

1. Pauling, L., Stanford Med. Bull., 1948, 6, 215.
2. Pauling, L., Hemoglobin, 57 (Butterworths Sci. Publ. London 1949).
3. Pauling, L., Coryell, C.D., Proc. Natl. Acad. Sci. U.S.A., 1936, 22, 210.
4. Weiss, J.J., Nature, 1964, 202, 83.
5. Cerdonio, M., Congiu-Castellano, A., Mogno, F., Pispisa, B., Romani, G.L., Vitale, S., Proc. Natl. Acad. Sci. U.S.A., 1977, 74, 398.
6. Pauling, L., Proc. Natl. Acad. Sci. U.S.A., 1977, 74, 2612.
7. Cerdonio, M., Congiu-Castellano, A., Calabrese, L., Morante, S., Pispisa, B., Vitale, S., Proc. Natl. Acad. Sci. U.S.A., 1978, 75, 4916.
8. Herman, Z.A., Loew, G.H., J.A.C.S., 1980, 102, 1815.
9. Makinen, M.W. in Biochemical and Clinical Aspects of Oxygen (ed. W.S. Caughey) 1979, Academic Press, New York, p.143.
10. Goddard, W.A. III, Olafson, B.D. in Biochemical and Clinical Aspects of Oxygen (ed. W.S. Caughey) 1979, Academic Press, New York, p.87.
11. Phillips, S.E.V., J. Mol. Biol., 1980, 142, 531.
12. Shaanan, B., Nature, 1982, 296, 683.
13. Misra, H.P., Fridovich, I., J. Biol. Chem., 1972, 247, 6960.
14. Koster, A.S., J. Chem. Phys., 1975, 63, 3284.
15. Barlow, C.H., Maxwell, J.C., Wallace, W.J., Caughey, W.S., Biochem. Biophys. Res. Commun., 1973, 55, 91.
16. Basolo, F., Hoffman, B.M., Ibers, J.A., Acc. Chem. Res., 1975, 8, 384.
17. Lang, G., Marshall, W., Proc. Phys. Soc. Lond., 1966, 87, 3.
18. Bennett, J.E., Gibson, J.F., Ingram, D.J.E., Proc. Chem. Soc. (London), 1957, A240, 67.
19. Dickinson, L.C., Symons, M.C.R., Chem. Soc. Rev., 1983, 12, 387.
20. Hoffman, B.M., Petering, D.H., Proc. Natl. Acad. Sci. U.S.A., 1970, 67, 637.
21. Symons, M.C.R., Petersen, R.L., Proc. Roy. Soc. Lond. B., 1978, 201, 285.
22. Rhein, H., Ristau, O., Scheler, W., FEBS Lett., 1972, 24, 24.
23. Maxwell, J.C., Caughey, W.S., Biochemistry, 1976, 15, 388.
24. Perutz, M.F., Kilmartin, J.V., Nagai, K., Szabo, A., Simon, S.R., Biochemistry, 1976, 15, 378.
25. Szabo, A., Baron, L.D., J.A.C.S., 1975, 97, 660.
26. Trittelvitz, E., Gersonde, K., Winterhalter, K.H., Eur. J. Biochem., 1975, 51, 33.

27. Twilfer, H., Gersonde, K., Z. Naturforsch. C: Biosci., 1976, 31C, 664.
28. Henry, Y., Banerjee, R., J. Mol. Biol., 1973, 73, 469.
29. Nagai, K., Hori, H., Yoshida, S., Sakamoto, H., Morimoto, H., Biochim. Biophys. Acta, 1978, 532, 17.
30. Szabo, A., Perutz, M.F., Biochemistry, 1976, 15, 4427.
31. Banerjee, R., Stetzkowski, F., Henry, Y., J. Mol. Biol., 1973, 73, 455.
32. Chien, J.C.W., Dickinson, L.C., J. Biol. Chem., 1977, 252, 1331.
33. Nagai, K., Hori, H., Morimoto, H., Hayashi, A., Taketa, F., Biochemistry, 1979, 18, 1304.
34. Höhn, M., Hüttermann, J., Chien, J.C.W., Dickinson, L.C., J.A.C.S., 1983, 105, 109.
35. Höhn, M., (1982) Doctoral dissertation, University of Regensburg.
36. Dickinson, L.C., Chien, J.C.W., J.A.C.S., 1971, 93, 5036.
37. Dickinson, L.C., Chien, J.C.W., Biochem. Biophys. Res. Commun., 1974, 59, 1292.
38. Hori, H., Ikeda-Saito, M., Yonetani, T., J. Biol. Chem., 1981, 256, 7849.
39. Chien, J.C.W., J. Chem. Phys., 1969, 51, 4220.
40. Doetschman, D., Utterback, S.G., J.A.C.S., 1981, 103, 2847.
41. Deatherage, J.F., Moffat, K., J. Mol. Biol., 1979, 134, 401.
42. Shiga, T., Hwang, K-J., Tyuma, I., Biochemistry, 1969, 8, 378.
43. Morse, R.H., Chan, S.I., J. Biol. Chem., 1980, 255, 7876.
44. Dickinson, L.C., Chien, J.C.W., Proc. Natl. Acad. Sci. U.S.A., 1972, 69, 2783.
45. Dickinson, L.C., Chien, J.C.W., Proc. Natl. Acad. Sci. U.S.A., 1980, 77, 1235.
46. Hori, H., Ikeda-Saito, M., Yonetani, T., Nature, 1980, 288, 501.
47. Hori, H., Ikeda-Saito, M., Yonetani, T., J. Biol. Chem., 1982, 257, 3636.
48. Petsko, G.A., Rose, D., Tsernoglou, D., Ikeda-Saito, M., Yonetani, T., in Frontiers of Biological Energetics (eds. Dutton, P.L., Scarapa, A., Leigh, J.S.), Academic Press, New York, 1978, pp.1011-16.
49. Gupta, R.J., Mildvan, A.S., Yonetani, T., Srivastava, T.S., Biochem. Biophys. Res. Commun., 1975, 67, 1005.
50. Yonetani, T., Yamamoto, H., Iizuka, T., J. Biol. Chem., 1974, 249, 2168.
51. Ikeda-Saito, M., Iizuka, T., Yamamoto, H., Kayne, F.J., Yonetani, T., J. Biol. Chem., 1977, 252, 4882.
52. Höhn, M., Hüttermann, J., J. Biol. Chem., 1982, 257, 10554.
53. Symons, M.C.R., Chem. Commun., 1975, 357.

54. Symons, M.C.R., Petersen, R.L., Biochim. Biophys. Acta, 1978, 535, 241.
55. Nietsche, W., Diplom-Arbeit, Regensburg, 1982.
56. Fermi, G., J. Mol. Biol., 1975, 97, 237.
57. Jaffe, E.R., in The Red Blood Cell (eds. Bishop, C., Surgenor, D.M.), 1964, Academic Press, New York, p.397.
58. Ranney, H.M., Nagel, R.L., Udem, L., in Genetical, Functional and Physical Studies of Hemoglobins (eds. Arends, T., Bernski, G., Nagel, R.L.), S. Karger, 1971, Basel, p.143.
59. Nagel, R.L., Ranney, H.M., Seminars in Haematology, 1973, X, 269.
60. Cohen, J.A., Caughey, W.S., Biochemistry, 1968, 7, 636.
61. Wever, R., Oudega, B., Van Gelder, B.F., Biochim. Biophys. Acta, 1973, 302, 475.
62. Brunori, M., Falcioni, G., Fioretti, E., Giardino, B., Rotillo, G., Eur. J. Biochem., 1975, 53, 99.
63. Carrell, R.W., Winterbourn, C.C., Rachmilowitz, E.A., Br. J. Haematol., 1975, 30, 259.
64. Gotoh, T., Shikima, K., J. Biochem. (Tokyo), 1976, 80, 397.
65. Wallace, W.J., Maxwell, J.C., Caughey, W.S., FEBS Lett., 1974, 43, 33.
66. Wallace, W.J., Caughey, W.S., Biochem. Biophys. Res. Commun., 1974, 57, 1104.
67. Wallace, W.J., Caughey, W.S., Biochem. Biophys. Res. Commun., 1975, 62, 561.
68. Cohen, G., Hochstein, P., Biochemistry, 1964, 3, 895.
69. Asakura, T., Lau, P.W., Proc. Natl. Acad. Sci. U.S.A., 1978, 75, 5462.
70. Asakura, T., Lau, P.W., J. Biol. Chem., 1980, 255, 1617.
71. Ogata, R.T., MacConnell, H.M., Cold Spring Harbor Symp. Quant. Biol., 1971, 36, 325.
72. Ogata, R.T., MacConnell, H.M., Biochemistry, 1972, 11, 4792.
73. Johnson, M.E., Ho. C., Biochemistry, 1974, 13, 3652.
74. Ikeda-Saito, M., Inubushi, T., McDonald, G.G., Yonetani, T., J. Biol. Chem., 1978, 253, 7134.
75. Huang, T., Redfield, A.G., J. Biol. Chem., 1976, 251, 7114.
76. Lindstrom, T.R., Ho. C., Proc. Natl. Acad. Sci. U.S.A., 1972, 69, 1707.
77. Huestis, W.H., Raftery, M.A., Biochem. Biophys. Res. Commun., 1972, 49, 1358.
78. Edelstein, S.J., Ann. Rev. Biochem., 1975, 44, 209.
79. Makino, N., Sugita, Y., J. Biol. Chem., 1978, 253, 1174.
80. Nagai, K., J. Mol. Biol., 1977, 111, 41.

81. Nasuda-Kouyama, A., Tachibana, A., Wada, A., J. Mol. Biol., 1983, 164, 451.
82. Rossi Fanelli, A., Antonini, E., Caputo, A., J. Biol. Chem., 1961, 236, 391.
83. Yamazaki, I., Yokota, K., Shikama, K., J. Biol. Chem., 1964, 239, 4151.
84. Brivati, J.A., Symons, M.C.R., Tinling, D.J.A., Wardale, H.W., Williams, D.O., Trans. Faraday Soc., 1967, 63, 2112.
85. Kappl, R., Höhn, M., Nietsche, W., Hüttermann, J., Bartlett, N., Symons, M.C.R., Biochem. Biophys. Acta, 1985, 827, 327.
86. Haire, R.N., Hedlund, B.E., Biochemistry, 1983, 22, 327.
87. Schroeder, W.A., Shelton, J.R., Shelton, J.B., Cormick, J., Jones, R.T., Biochemistry, 1963, 2, 992.
88. Tyuma, I., Shimizu, K., Arch. Biochem. Biophys., 1969, 129, 404.
89. Tyuma, I., Shimizu, K., Fed. Proc. Fed. Amer. Soc. Exp. Biol., 1970, 29, 1112.
90. Frier, J.A., Perutz, M.F., J. Mol. Biol., 1977, 112, 97.
91. Symons, M.C.R., Petersen, R.L., Biochem. Biophys. Acta, 1978, 537, 70.
92. Long, P., Glasoe, J., J. Phys. Chem., 1960, 64, 188.



# CHAPTER 3

**Electron Addition to the (FeO<sub>2</sub>) Unit  
of Oxyhaemoglobin Glycera**

## INTRODUCTION

The coelomic cells of the polychaete annelid *Glycera dibranchiata* contain two types of haemoglobin, one a high molecular weight 'polymeric' portion, the other a low molecular weight 'monomeric' portion. The latter exhibits minor electrophoretic heterogeneity<sup>1-4</sup> whilst the polymeric fraction appears to be a heterogeneous mixture of several polypeptide chains previously described as a dimer with a tendency towards aggregation<sup>1</sup> or an oligomer of molecular weight greater than 100,000.<sup>2,5</sup> More recently,<sup>4</sup> it has been reported that the polymeric fraction appears to have a quaternary structure that is heterogeneous in nature and constituted mainly of monomeric sub-units with a small fraction of dimers in a non-covalently linked state of aggregation. Additional non-covalent sub-unit aggregation of this quaternary structure is clearly evident on storage or age of the sample.

Both the monomer<sup>4,6-11</sup> and the polymer<sup>4,7,8</sup> have higher oxygen affinities than human haemoglobin,<sup>12</sup> but lower than that of myoglobin.<sup>13</sup> The monomeric fraction has a hyperbolic oxygen uptake curve and no alkaline Bohr effect<sup>4,7,8,10</sup> whilst a positive alkaline Bohr effect has been observed for the polymer.<sup>4,7,8,10</sup>

The major monomeric component has been sequenced<sup>14</sup> and its three-dimensional structure at 2.5 Å resolution has been deduced.<sup>15</sup> This shows that the tertiary structure closely corresponds to that of myoglobin. The principal differences being the absence of the D helix (as in the α chains of vertebrate haemoglobins) and the replacement of the distal histidine by leucine. Of the seven "invariant" residues found in vertebrate haemoglobins, only three are present in this molecule; Glycine (B6), Phenylalanine (CD1) and Histidine (F8). It contains 147 amino acid residues, 23% of which are identical with those in sperm

whale myoglobin and 79% of which make up the seven helical segments which are disposed in the familiar "myoglobin fold".

The absence of a distal histidine in this molecule was the reason for this study. In the initial studies of electron addition to oxyhaemoglobin and oxymyoglobin<sup>17-19</sup> giving  $(\text{FeO}_2)^-$  units, Symons and Petersen postulated the formation of a hydrogen bond between the outer oxygen of the  $(\text{FeO}_2)^-$  unit and the NH group of the distal histidine.

Consequently, the idea was to use haemoglobin *Glycera* to determine the validity of this postulate. Recent work by Phillips and Schoenborn<sup>20</sup> on neutron diffraction of oxymyoglobin indicating the existence of this hydrogen bond supports this postulate. Furthermore, Ikeda-Saito et al.<sup>16</sup> discovered reversible pH dependent changes as well as a deuterium substitution effect in their spectra of oxycobalt-myoglobin. These effects were not present in their study of oxyhaemoglobin *Glycera*, the reason being the absence of hydrogen bonding to the oxygen ligand.

#### EXPERIMENTAL PROCEDURE

100 worms were purchased from Maine Bait Co., Newcastle, ME, USA. The blood was extracted by incising the coelomic cavity, the blood being drained into a beaker standing in an ice bath. The blood was then filtered through glass wool to remove debris, diluted 4-fold with a 1.1% NaCl solution and centrifuged at 6,000 r.p.m. for 15 minutes at 4°C. After centrifugation the supernatant was removed and discarded, this process being repeated a further four times.

An equal volume of distilled water was added to the red cell 'pellet' to dissolve it, the resulting solution being sonicated for 10 s (setting 10  $\mu\text{m}$ ) at 4°C for cell lysis. Cell debris was removed by centrifugation at 18,000 r.p.m. at 4°C for 1 hour, the pellet being discarded. The

monomeric and polymeric species were separated on a 2 × 35 cm Sephadex G-100 (10-40  $\mu$ s coarse grade) column equilibrated with 0.5 M  $\text{KH}_2\text{PO}_4$ / $\text{K}_2\text{HPO}_4$  mixed buffer at pH 6.8. The haemolysate solution was always resolved into two clearly separate peaks, that of the polymer being eluted first.

The efficiency of separation was checked by measuring the protein absorption at 280 nm of the various fractions collected. The visible absorption spectrum was checked after each column separation as a test for intactness of structure. The band maxima<sup>5</sup> occur very close to those of oxyhaemoglobin<sup>21</sup> and oxymyoglobin.<sup>21</sup>

Separations were pooled and concentrated in an Amicon ultrafiltration cell using a YM50 filter under nitrogen pressure, the visible spectrum being re-checked after concentration.

The aqueous samples used for radiolysis were mixed in a 1:1 ratio (v/v) with ethylene glycol, as a glass former. For the acid and alkaline pH runs the haemolysate was dialysed for 24 hours at 4°C against mixed phosphate buffers at pH 5.8 and 8.1 respectively.

The samples were prepared for irradiation by pipetting drops of solution into liquid nitrogen to form solid beads which were then irradiated in small glass bottles at 77 K in a  $^{60}\text{Co}$   $\gamma$ -cell for 2 hours at a dose rate of 0.96 Mrad/hr.

The X-band spectra were recorded on a Varian E-109 spectrometer at 77 K in a glass Dewar flask. Samples were annealed either by using the Varian V6040 variable temperature system or, alternatively, by warming the samples in the Dewar flask, without liquid nitrogen, simultaneously monitoring the spectrum until a change occurs at which point the sample is quickly recooled to 77 K. g-Values were calculated using an HP 5246 C frequency counter in conjunction with a Bruker B-H1ZE field calibrant.

## RESULTS AND DISCUSSION

Figure 1 displays the high and low temperature species formed in the monomer on exposure to  $\gamma$ -radiation. The 77 K spectrum indicates the formation of a completely novel  $(\text{FeO}_2)^-$  unit. As before<sup>17-19</sup>  $g_x$  and  $g_y$  features are evident at low fields whilst the  $g_z$  is hidden under the strong central features arising from globin and solvent radicals. Trends in the  $g$ -values for the various centres found previously<sup>17-19</sup> as well as a range of low spin Fe(III) complexes are shown in Figure 2, the  $g$ -values being listed in Table 1. The shifts from the free spin value (2.0023) of the low temperature monomeric species are much smaller than any of the shifts previously assigned to  $(\text{FeO}_2)^-$  units.

Assuming that  $g$ -value convergence is caused by a shift of spin-density from iron to oxygen, it follows that the low temperature species, G, has a high spin-density on oxygen. Alternatively, the decrease in  $g$ -value could be caused not by transfer of spin-density onto oxygen, but by a significant change in ligand bonding causing increased splitting between the semi-occupied molecular orbital and the filled levels coupled by the magnetic field. However, if, as seems most likely, the only change is the presence or absence of hydrogen bonds, there seems no reason for changes in ligand bonding. The presence of a hydrogen bond is likely to induce a drift of negative charge-density onto oxygen, and hence of spin-density onto iron. This means that the ligand becomes increasingly like  $\text{O}_2^{2-}$  as proton transfer increases until full transfer to give  $\text{HO}_2^-$  is achieved, forcing the unpaired electron even more onto the iron atom.

If this postulate is accepted it would appear that the species labelled  $\alpha$  and  $\beta$  in irradiated human oxyhaemoglobin and the species Mb in irradiated oxymyoglobin are already strongly hydrogen-bonded to the

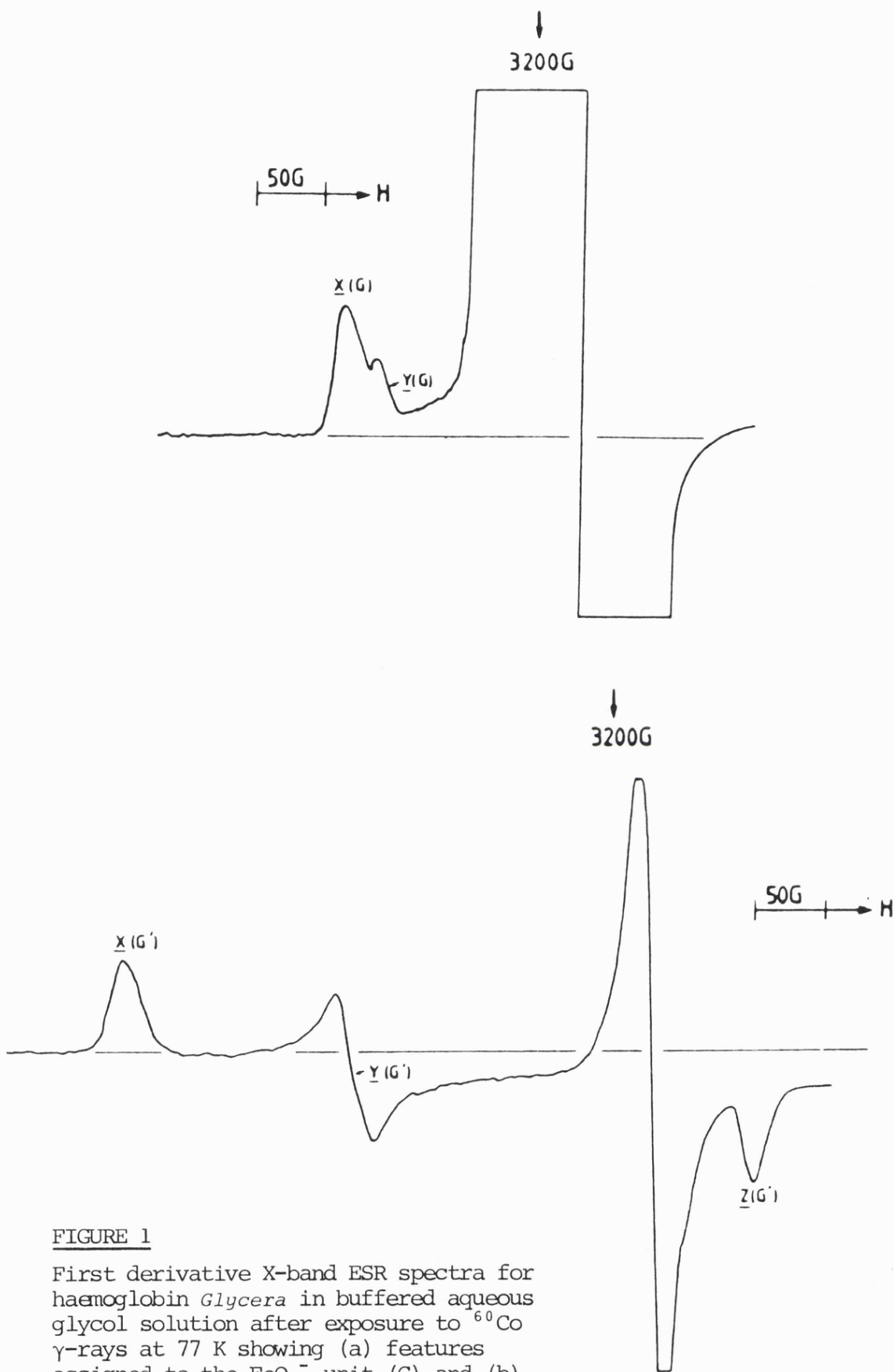


**FIGURE 1**

First derivative X-band ESR spectra for haemoglobin *Glycera* in buffered aqueous glycol solution after exposure to  $^{60}\text{Co}$   $\gamma$ -rays at 77 K showing (a) features assigned to the  $\text{FeO}_2^-$  unit (G) and (b) after annealing to 160 K showing features assigned to  $\text{FeO}_2^-$ ----HOH units (G').

FIGURE 2

Trends in the three g-values for a range of low-spin Fe(III) complexes together with those for centres formed by electron addition to FeO<sub>2</sub> in various porphyrin systems. The key is given in Table 1. F.S., free spin.

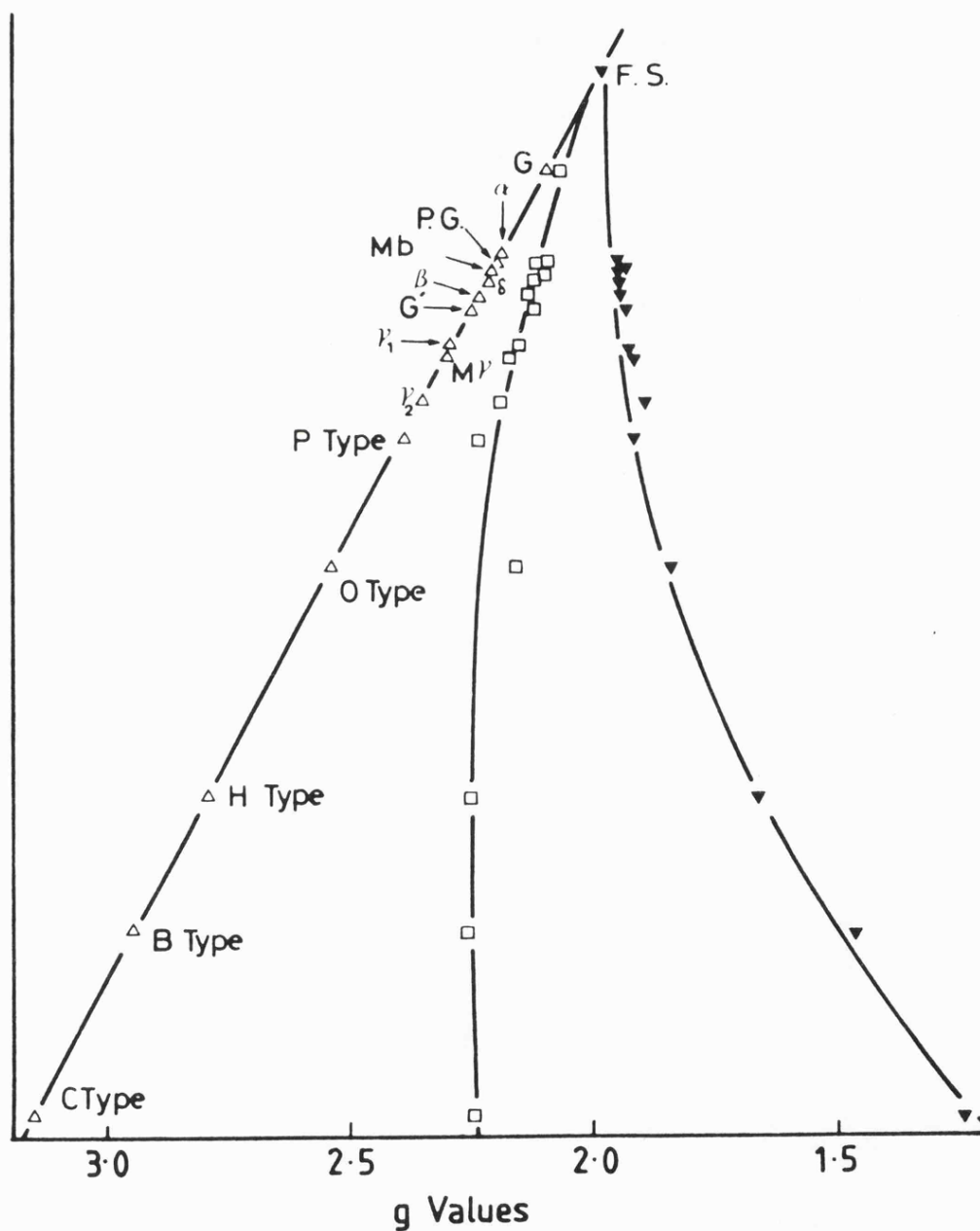


TABLE 1

ESR Parameters for Low-Spin Fe(III) Centres including those formed by Electron Addition to FeO<sub>2</sub> Porphyrin Units

Type	$\underline{g}_x$	$\underline{g}_y$	$\underline{g}_z$
O <sup>a</sup>	2.55	2.17	1.85
H <sup>a</sup>	2.80	2.26	1.67
C <sup>a</sup>	3.15	2.25	1.25
B <sup>a</sup>	2.95	2.26	1.47
P <sup>a</sup>	2.41	2.25	1.93
G <sup>b</sup>	2.113	2.091	-
G' <sup>b</sup>	2.263	2.141	1.957
PG <sup>b</sup>	2.216	2.125	1.956
Mb <sup>c</sup>	2.221	2.119	1.959
My <sup>c</sup>	2.319	2.186	1.936
$\alpha$ <sup>d</sup>	2.215	2.120	1.965
$\beta$ <sup>d</sup>	2.250	2.146	1.965
$\delta$ <sup>d</sup>	2.231	2.132	1.965
$\gamma_1$ <sup>d</sup>	2.307	2.177	1.946
$\gamma_2$ <sup>d</sup>	2.365	2.208	1.909

<sup>a</sup> Ref. 22; the centres O, H, C, B and P are typical of low-spin Fe(III) complexes.

<sup>b</sup> Present work. Centre G is the primary electron addition centre, G' is the centre formed from G on annealing and centre PG is the (FeO<sub>2</sub>)<sup>-</sup> centre formed in the polymeric fractions of haemoglobin *Glycera*.

<sup>c</sup> Mb and My are centres formed by electron addition to the Fe-O<sub>2</sub> unit in myoglobin (Ref. 15).

<sup>d</sup>  $\alpha$ ,  $\beta$ ,  $\delta$ ,  $\gamma_1$  and  $\gamma_2$  are centres formed by electron addition to the Fe-O<sub>2</sub> units in haemoglobin (Ref. 15).

NH groups of the distal histidines whilst the primary monomeric unit, G, is not. This is in good accord with the results of Phillips and Schoenborn<sup>22</sup> which show the presence of incipient hydrogen-bonding in crystals of oxymyoglobin.

However, on annealing, the primary  $(\text{FeO}_2)^-$  *Glycer*a unit converts into a unit (G') (Figure 1b) almost indistinguishable from the  $(\text{FeO}_2)^-$  units found in human haemoglobin and myoglobin. The above postulate would require this new centre, G', to be hydrogen-bonded. In the haem pocket, on the distal side, there are no sources of proton donors, the near neighbour amino acids being Phe-45 (CD1), Leu-58 (E7) and Val-62 (E11). The answer is possibly provided by the presence of water in the haem pockets which can move on annealing to solvate the negative oxygen ligand. That this new centre, G', nevertheless differs from human haemoglobin and myoglobin primary centres is shown by the fact that on further annealing G' did not undergo a change to give a  $\gamma$ -type centre, in contrast with the normal primary centres. The formation of a  $\gamma$ -type species is due to proton transfer from the distal histidine to form  $\text{HO}_2^-$  as the ligand (see Chapter 2). I therefore suggest that in the monomeric *Glycer*a component this process does not occur due to the weak proton-donating power of the water molecule.

As I explained in Chapter 2, the previous sequence postulated<sup>17</sup> for the oxidation of irradiated oxyhaemoglobin and oxymyoglobin to the Met forms incorrectly assumed that the primary centres were not hydrogen-bonded. This conclusion is drawn from this work on the monomeric fraction of haemoglobin *Glycer*a where the primary centre is the non-hydrogen-bonded  $(\text{FeO}_2)^-$  unit G, the secondary centre, G', being the hydrogen-bonded species  $\text{FeO}_2^- \text{---} \text{HOH}$ .

## The Polymer Centre

$\gamma$ -Radiolysis of the polymeric fraction of oxyhaemoglobin *Glycera* produces a centre, PG, whose features are akin to the primary centres formed in human haemoglobin and myoglobin. This indicates that there is a major difference in the FeO<sub>2</sub> unit or its environment for the polymer centre compared with the monomer centre. Interpreted in terms of the above theory, this means that the oxygen is hydrogen-bonded to some proton donor even at 77 K which, like the monomer unit, doesn't undergo proton transfer to a  $\gamma$ -type species on annealing. At the moment, there is insufficient evidence to determine the nature of the proton donor.

### REFERENCES FOR CHAPTER 3

1. Seamonds, B., Forster, R.E., Gottlieb, A.J., J. Biol. Chem., 1971, 246, 1700.
2. Vinogradov, S.N., Machlik, C.A., Chao, L.L., J. Biol. Chem., 1970, 245, 6533.
3. Sima, P.D., Doctoral dissertation, 1979, University of Nebraska.
4. Harrington, J.P., Suareg, G., Borgese, T.A., Nagel, R.L., J. Biol. Chem., 1978, 253, 6820.
5. Seamonds, B., Forster, R.E., George, P., J. Biol. Chem., 1971, 246, 5391.
6. Hoffman, R.J., Mangum, C.P., Comp. Biochem. Physiol., 1970, 36, 211.
7. Vinogradov, S.N., Mizukami, H., Biochim. Biophys. Acta, 1972, 285, 314.
8. Seamonds, B., Forster, R.E., Am. J. Physiol., 1972, 223, 734.
9. Seamonds, B., McCray, J.A., Parkhurst, L.J., Smith, P.D., J. Biol. Chem., 1976, 251, 2579.
10. Weber, R.E., Sullivan, B., Bonaventura, J., Bonaventura, C., Comp. Biochem. Physiol., 1977, 58B, 183.
11. Parkhurst, L.J., Sima, P., Goss, D.J., Biochem., 1980, 19, 2688.
12. Antonini, E., Wyman, J., Brunori, M., Bucci, E., Fronticelli, C., Rossi-Fanelli, A., in Structure and Activity of Enzymes, Symposium No. 1, (Goodwin, T.W., Harris, J.I., Hartley, B.S., eds.), Federation European Biochemists Society, p.143, Academic Press, New York.
13. Rossi-Fanelli, A., Antonini, E., Arch. Bioch., 1958, 77, 478.
14. Imamura, T., Baldwin, T.O., Riggs, A., J. Biol. Chem., 1972, 247, 2785.
15. Padlan, E.A., Love, W.E., J. Biol. Chem., 1974, 249, 4067.
16. Ikeda-Saito, M., Iizuka, T., Yamamoto, H., Kayne, F.J., Yonetani, T., J. Biol. Chem., 1977, 252, 4882.
17. Symons, M.C.R., Petersen, R.L., Proc. R. Soc. Lond., 1978, B201, 285.
18. Symons, M.C.R., Petersen, R.L., Biochim. Biophys. Acta, 1978, 537, 70.
19. Symons, M.C.R., Petersen, R.L., Biochim. Biophys. Acta, 1978, 535, 241.
20. Phillips, S.V., Schoenborn, B.P., Nature, 1981, 292, 81.
21. Brill, A.S., Williams, R.J.P., Biochem. J., 1961, 78, 246.
22. Blumberg, P.M., Peisach, J. (1971) in Probes of Structure and Function of Macromolecules and Membranes, Vol. II (Chance, B., Yonetani, T., and Mildvan, A.S. eds.), p.222, Academic Press, New York.



# CHAPTER 4

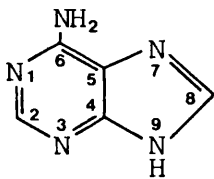
**ESR of  $\gamma$ -irradiated DNA and Constituents**

## A. THE STRUCTURE AND FUNCTION OF DNA

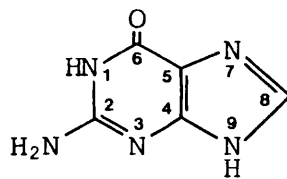
Deoxyribonucleic acid (DNA) is the nucleic acid which houses the genetic information of the cell. This fundamental cell constituent, which serves to direct protein synthesis, is located in the nucleus. Ribonucleic acid (RNA), the second member of the nucleic acid group, is responsible (in its messenger form) for the translation of the genetic information from the cell nucleus to the ribosomes (the site of protein synthesis) in the cytoplasm. The basic structure of these nucleic acids is very similar. They are unbranched polymeric molecules constructed from a basic building block, called the nucleotide, which consists of a nitrogenous purine or pyrimidine base, a five carbon (deoxy) ribose sugar and a phosphate group. Each nucleotide contains one of four different nitrogenous bases (two purine and two pyrimidine) three of which - adenine, guanine and cytosine are the same in both DNA and RNA whilst the fourth is thymine in DNA and uracil in RNA as shown below in Figure 1.

FIGURE 1

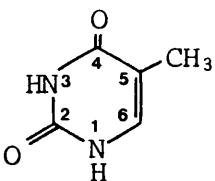
The Common Nucleic Acid Constituent Bases



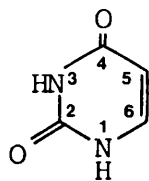
ADENINE



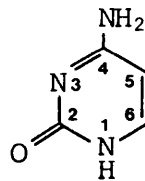
GUANINE



THYMINE



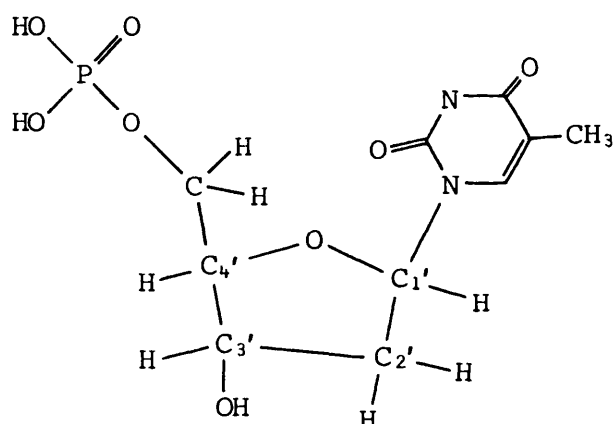
URACIL



CYTOSINE

A further basic difference between RNA and DNA is in the sugar moiety. Both nucleic acids have ribose sugars in the D configuration. However, they differ in that DNA has no hydroxyl group on the second carbon of the sugar ring and hence is termed "deoxyribo" as opposed to "ribo" in RNA. The nucleotide unit is made up by joining the C1' of the sugar to the N1 or N9 of the base (pyrimidine or purine respectively) via a glycosidic linkage. The phosphate group is linked to the sugar either at C3' or at C5' depending on whether it is a 5'-dNMP or 3'-dNMP (deoxy-nucleoside monophosphate). Figure 2 below shows the 5' nucleotide of thymine.

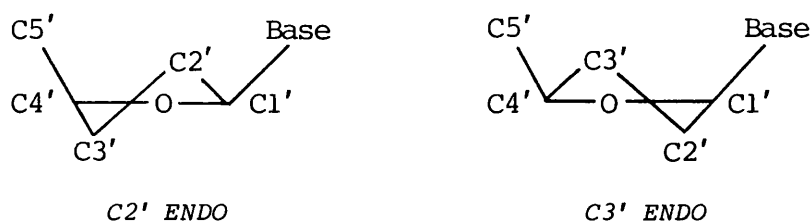
FIGURE 2    5'-dTMP



In DNA and RNA the nucleotides are linked together through 5'- and 3'-sugar-phosphate bonds forming the polynucleotide chain with a phosphodiester backbone.<sup>1</sup> Unlike the nucleic acid bases, the ring atoms of the sugars do not lie in a common plane. X-ray crystallographic studies<sup>1,2</sup> and NMR solution studies<sup>3</sup> reveal the rings to be puckered. The particular conformation of the sugar ring can be defined in terms of the displacement of the carbon atoms, C2' and C3', from the plane defined by the atoms C1', C4' and O, as shown in Figure 3.

Puckering of the ring displaces C2' and C3' above or below this plane.

FIGURE 3



If the major displacement of an atom is toward the same side as the C5' carbon atom, the conformation is designated *endo*. Displacement towards the opposite side is designated *exo*. For instance, in a C2' *endo* conformation the C2' carbon is displaced  $\sim 0.5 \text{ \AA}$  from the ring plane on the same side as C5', correspondingly the C3' carbon is displaced  $\sim 0.1 \text{ \AA}$  to the opposite side. This puckering of the sugar ring defines the stereochemistry of double stranded polynucleotides. Double stranded DNA duplexes are characterised by both the C2' *endo* and C3' *endo* conformations while in RNA duplexes only C3' *endo* configurations occur.

The tertiary structure of duplex DNA consists of two interconnected helical polynucleotide strands running in opposite directions, one strand in the 5'  $\rightarrow$  3' direction, the other in the 3'  $\rightarrow$  5'. The polynucleotide strand comprises of a phosphodiester backbone chain with pyrimidine and purine bases jutting out at right angles towards the opposing strand. The two strands are connected by hydrogen bonds between the bases of each strand. The resultant configuration is that of a double stranded right-handed helix (Figure 4). This structure was first proposed by Watson and Crick<sup>4</sup> in 1953 based on X-ray diffraction analysis of DNA crystals. They concluded that the distance between base pairs was  $3.4 \text{ \AA}$  and that the repeat distance of the helix was  $34 \text{ \AA}$  (as the structure has one narrow and one broad groove called the minor and the major groove respectively).

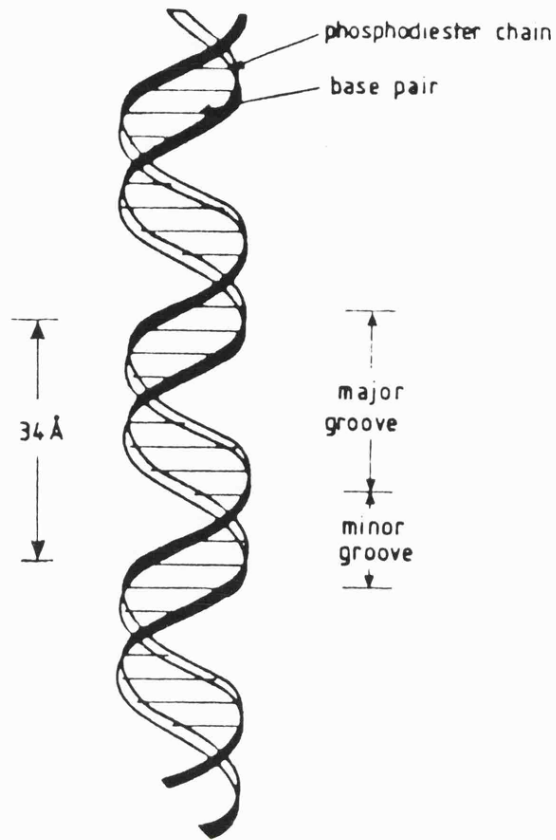
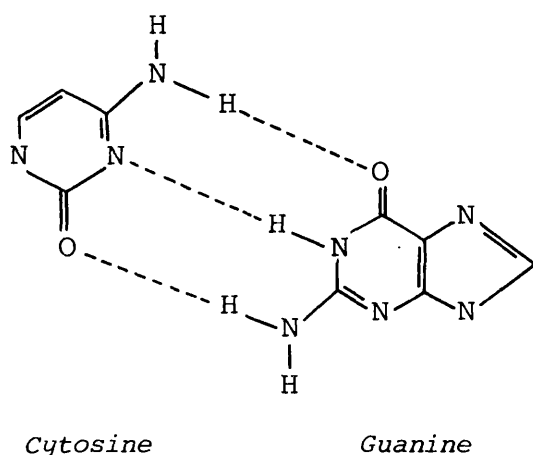
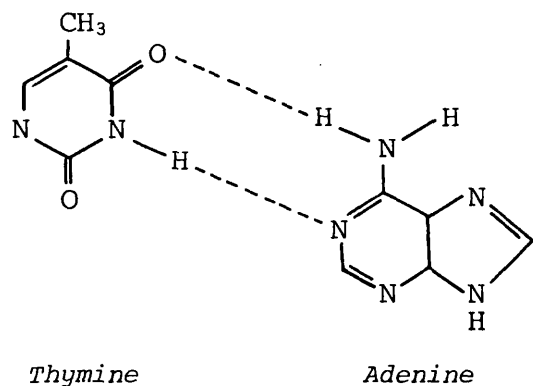


FIGURE 4 The Double Helix

The geometry of the structure only permits base pairing between purine and pyrimidine bases as a pair of pyrimidines could not bridge the gap between the chains and a pair of purines would be too large for the gap. The chemistry of the bases is such that adenine forms two hydrogen bonds with thymine and guanine forms three hydrogen bonds with cytosine as shown in Figure 5.

The hydrogen bonding between the bases is the primary stabilising factor in the double helical structure. However, there is further stability lent to this configuration by the overlapping  $\pi$  orbitals of the purine and pyrimidine bases as they "stack" on top of each other in the helix. This latter phenomenon results in the depression of the UV absorption of the bases in duplex DNA. Hence a measure of the intactness



**FIGURE 5** The Watson-Crick base pairing scheme

of the DNA structure can be obtained from the UV absorption spectrum. Another factor contributing to the stability of the helix is the ionic strength. High concentrations of positive ions have a stabilising effect on the structure by reducing the electrostatic repulsion between the phosphate groups in the phosphodiester chains.

DNA is stabilised in the cell nucleus by positively charged proteins known as histones. The cell nucleus houses the chromatin comprising of tightly folded DNA-histone (nucleohistone) fibres. Various authors have postulated the existence of a nucleohistone repeat unit called a nucleosome.<sup>5,6</sup> Olins<sup>7</sup> saw chains of particles in electron micrographs of chromatin and later Kornberg<sup>8,9</sup> identified, using X-ray diffraction, regular repeat structures along the chromatin fibre. The nucleosome

consists of an octamer of histones surrounded and contained by 200 base pairs of helical DNA. The octamer comprises two tetramers made up from four of the five histones:  $(H2A)_2$ ,  $(H2B)_2$ ,  $(H3)_2$  and  $(H4)_2$ . Of the 200 base pairs, only 140 are tightly linked to the octamer. The other 60 are termed linker DNA and function to join the nucleosome particles together. Evidence from digestive and sedimentation studies<sup>10</sup> indicates that the fifth histone, H1, is associated with the linker DNA and is involved in holding together the nucleosome particles.

#### B. ESR OF $\gamma$ -IRRADIATED DNA AND CONSTITUENTS

The second half of this thesis is concerned with the effect of gamma irradiation on DNA. High energy radiation is known to produce damage, mutations or death to the cells of living organisms. The cause of changes in cell behaviour results from the alteration or failure of one or more important functions or processes in the cell. Alteration to the structure and thereby function of the nucleic acid DNA, which is fundamental to the cell's metabolism, is thought to result in cell death, carcinogenesis and mutagenesis. In nucleic acids, energetic radiation initially produces electronic excitations and ionisations. Both of these processes lead to the formation of stable new species most commonly via radical intermediates. Consequently, ESR can be used to follow and analyse the intermediate species and thereby identify the mechanism of damage in the molecule.

The aim of this work was to study the effect of incorporating metal additives into the DNA solutions and determine whether this altered the mechanism and/or the extent of radiation damage to the DNA. Such effects could be relevant to cancer therapy. In the first DNA Chapter, I shall briefly describe the structure and function of DNA and then review the

literature on ESR of nucleic acid bases, nucleotides and DNA. The following Chapter contains the results and discussion of the DNA metal additive ESR study.

Much of the early work in this area centred around studies of bases, nucleosides and nucleotides. Samples were irradiated (both at 77 K and 300 K) either as single crystals, dry polycrystalline powders, alkaline glasses or in aqueous solution. Broadly speaking the low temperature events involve ion formation via electron ejection and subsequent capture. Whilst at higher temperatures the ion radicals become neutralised by reaction with hydrogen and hydroxyl ions and eventually decay into more stable paramagnetic species.

### B.1 Guanine Compounds

The low temperature species are not easy to identify as they both give rise to overlapping singlets. Gregoli et al.,<sup>11</sup> in a study of frozen aqueous dGMP solutions, identified the species as the base cation ( $G^+$ ) and anion ( $G^-$ ). They used electron scavengers to selectively produce the cation which had a width of 23 G with some unresolved fine structure. Previously, Sevilla and Mohan<sup>12</sup> and Sevilla<sup>13</sup> had produced a cation from dGMP with a 14 G linewidth. The discrepancy between the two widths most probably arises from the fact that the latter cation was produced in fully deuterated glassy matrices. At higher temperatures Gregoli et al. showed that  $G^+$  converted into the OH adduct (GOH) in alkaline pH but not at neutral pH (unless electron scavengers were present). They assigned the doublet spectrum of 33 G splitting to an OH addition radical at C8.

The  $G^-$  singlet, of linewidth 8 G according to Gregoli et al., was in good agreement with previous work which also attributed a narrow singlet to  $G^-$ .<sup>14</sup> At higher temperatures Gregoli et al. showed that  $G^-$

converted into the H adduct (GH) which has been identified as the C8 adduct by other workers.<sup>15-17</sup> The spectrum consists of a 1:2:1 triplet of around 36 G splitting. The last radical type has been discovered in the sugar moiety of a crystal of 5'-dGMP by Rakvin and Herak.<sup>15</sup> They established that there were two proton splittings giving a quartet spectrum for which they assigned a possible structure to be  $\text{PO}_4\text{C}(5')\dot{\text{H}}\text{C}(4')\text{H}=\text{O}$ , produced by a breakdown of the sugar ring structure after  $\dot{\text{H}}$  abstraction. Gregoli et al. also found a quartet structure (in low yield) in their spectra which they attributed to a H abstraction radical at C5' of the sugar. Notably, this quartet had a larger coupling than in the case of the radical found by Rakvin and Herak.

## B.2 Adenine Compounds

In the main, adenine and derivatives behave in a very similar manner with respect to irradiation as guanine. At low temperatures the cation ( $\text{A}^+$ ) and anion ( $\text{A}^-$ ) species have been identified in alkaline glasses by Sevilla and coworkers.<sup>12,18,19</sup> Both consist of unresolved singlets which are broader in width and poorer in resolution than in the case of  $\text{G}^+$  and  $\text{G}^-$ . As with the guanine derivatives the anion is shown to protonate at high temperatures<sup>21</sup> to produce the H adduct (AH) which is a triplet of 40 G splitting. In most cases (cf. GH), this is a C8H adduct, although C2H adducts have also been reported.<sup>20-26</sup> Schmidt and Borg<sup>27</sup> showed that N7 is the preferred site of attack using adenine derivatives deuterated at C8. Westhof et al.<sup>28</sup> showed that the C8H adduct is converted into the C2H adduct by irradiation with light and went on to show that the C2H adduct needs a specific environment to be stabilised.

The cation was inferred (as the cation and anion spectra were not separated due to the broadness of the poorly-resolved singlets), by

Gregoli et al.<sup>20</sup> to convert into the C8OH adduct which has a characteristic slightly anisotropic doublet spectrum of 29 G splitting (much like that of GOH).

Single crystal studies of deoxyadenosine<sup>29-31</sup> show the presence of a sugar radical thought to result from hydrogen atom abstraction from the C5' of the sugar. Gregoli et al.<sup>20</sup> discovered a quartet structure in dAMP (of the same splitting as the one found in dGMP) which they attributed to the C5' abstraction radical in the sugar.

### B.3 Cytosine Compounds

The anionic and cationic species have been identified at low temperatures in single crystals,<sup>32-35</sup> polycrystalline powders<sup>36</sup> and alkaline glasses.<sup>18,37,38</sup> Spin-density distribution has been calculated by Baudet et al.<sup>39</sup> showing, in line with experimental data, that the maximum spin-density of the anion resides on C6 whilst the main density is evenly distributed over C5 and N3 in the cation. A third radical, found at low temperatures in cytosine, has been identified as resulting from hydrogen abstraction from N1.<sup>33</sup>

Irradiation at higher temperatures leads to the production of hydrogen addition radicals.<sup>33-35,40-43</sup> Flossmann et al.<sup>33</sup> have analysed the different hydrogen adducts and identified them as adducts at C5 and C6 (a further adduct at O2 is found if doses >10 MRad are used). Both radicals are 1:1:2:2:1:1 sextets with A(H)C6 = 18 G, A(H<sub>2</sub>)C5 = 37 G for C5H and A(H)C5 = 17 G, A(H<sub>2</sub>)C6 = 50 G for C6H. The main radical formed is C5H but this can be converted into C6H by irradiation with light of wavelength >400 nm.<sup>44</sup> Flossmann et al.<sup>33</sup> confirmed the assignment of the radicals by studying single crystals of cytosine-D<sub>2</sub>O. They also note that C6H adducts are formed via an anion intermediate whilst C5H radicals are formed by direct addition of  $\dot{\text{H}}$  to the neutral molecule. Protonation

of anions in N1 substituted cytosine derivatives to give C6H adducts does not take place to any significant degree<sup>45,46,26</sup> as C6H radicals are only stabilised in an anionic environment.<sup>33</sup> However, Gregoli et al.<sup>45</sup> showed that protonation can be induced by illumination with white light to give the C6H adduct.

In nucleoside and nucleotide derivatives four different radicals have been reported that are located in the sugar moiety. Bernhard et al.<sup>47</sup> reported the existence of a C5' hydrogen abstraction radical in 3'-CMP at 77 K. This radical reorients and deprotonates on warming to room temperature. Above room temperature this radical converts into an allylic radical, denoted 3 $\alpha$ H, by radical rearrangement, ring opening, breakage of the phosphodiester bond and finally base elimination.<sup>48</sup> In 5'-dCMP, at 77 K, Krilov and Herak reported the existence of a C5' hydrogen abstraction radical<sup>49</sup> which also, subsequently, converted to a 3 $\alpha$ H type radical<sup>50</sup> at room temperature agreeing with the results of Fouse et al.<sup>51</sup> This 3 $\alpha$ H allylic radical has been also characterised in cytidine by Hampton and Alexander<sup>52</sup> and was shown by Alexander and Allison<sup>53</sup> to decay into a species with a doublet spectrum. The last type of sugar radical seen in cytosine derivatives arises from hydrogen abstraction from C1' of the sugar moiety. Herak, Krilov and McDowell assigned a radical with two equivalent  $\beta$ -proton splittings to the  $\dot{C}_1'$  radical in 5'-dCMP,<sup>50</sup> whilst Bernhard and Snipes assigned a radical with a doublet resonance to the  $\dot{C}_1'$  in 3'-CMP.<sup>54</sup>

#### B.4 Thymine Compounds

Box and Budzinski, in studies of irradiated thymidine at 4 K, discovered an alkoxy radical, produced by hydrogen abstraction from the hydroxyl group in thymidine, as well as the radical anion (T<sup>-</sup>).<sup>59</sup> This alkoxy radical is characterised by a highly anisotropic g-value and

a hyperfine splitting from the two C5'  $\beta$ -protons. Various other workers have identified the anion<sup>18,26,37,46,57-60</sup> as well as the cation<sup>38,55-57</sup> at 77 K.

The anion has been shown to readily protonate, on warming to higher temperatures, by a variety of workers.<sup>12,18,26,46,57,58,60-67</sup> The hydrogen adduct (TH) has a very characteristic octet spectrum which results from hyperfine splitting from three equivalent  $\beta$ -protons of the methyl group and two nearly equivalent protons of the methylene group. The maximum spin-density is at C5, as calculated by Pullman and Mantione.<sup>68</sup> Confirmation of the protonation site was obtained using a single crystal grown in a D<sub>2</sub>O medium by Herak.<sup>64</sup>

The fate of the cation is less certain as two decay products have been found. Single crystal studies of thymine<sup>62</sup> and thymidine,<sup>69</sup> at room temperature, show the presence of a species identified as resulting from hydrogen abstraction from the methyl group (TCH<sub>2</sub>). The spin-density is delocalised over C6, C5 and the carbon of the methylene group, coupling to the two equivalent  $\alpha$ -protons of the methylene group and the  $\alpha$ -proton of C6. This radical has been shown to be the decay product of the thymine cation, in dry polycrystalline powders by Hartig and Dertinger<sup>57</sup> and in 8M NaOH glasses by Sevilla and Englehardt.<sup>70</sup>

However, Sevilla and Englehardt found that cations of thymine nucleosides/tides tended to decay by reacting with hydroxyl ions to form the C6OH adduct (TOH) in 8M NaOH glasses. Whilst in NaClO<sub>4</sub> glasses these N1 substituted thymines decayed either into TOH or into TCH<sub>2</sub>. Gregoli *et al.*,<sup>60</sup> in a study of dTMP, obtained the TCH<sub>2</sub> spectrum in good yield (using electron scavengers) at low temperatures (135 K). This radical, on heating, appeared to convert into the TOH radical. As this would be highly unlikely chemically, the effect is possibly caused by slower

growth of the TOH radical from decay of residual cation hidden beneath the TCH<sub>2</sub> spectrum. There has been some question over the identification of the TOH species caused by the temperature and matrix dependence of the C6 proton splitting.<sup>71</sup> This has been analysed by Sevilla and Englehardt<sup>70</sup> who have conclusively proven that the quintet arises from the TOH species. In conclusion, it would appear that the mechanism of decay of the cation proceeds via the deprotonation route in single crystals, where no source of hydroxyl ions is available. In aqueous solutions, where hydroxyl ions are available, the decay can proceed both by deprotonation and by hydroxyl ion addition at C6.

#### B.5 DNA

The first reports of radiation damage in DNA all showed that a single broad absorption was produced.<sup>72-77</sup> Later a number of workers concluded that at least one of the radicals produced by irradiating DNA has its unpaired electron on the thymine base.<sup>78-85</sup> This radical was identified<sup>78,80,83,84,86,87</sup> as the TH radical with its characteristic octet spectrum. As with the thymine base, nucleoside and nucleotide, the precursor of TH was shown to be the thymine anion.<sup>88-90</sup>

Apart from the thymine anion the 77 K spectrum of irradiated DNA is also made up of the guanine cation. Gräslund et al. analysed the two radicals formed at 77 K in DNA in 1971. Using oriented DNA samples they derived the coupling constants and allocated the anion spectrum to cytosine or thymine and the cation to guanine or cytosine.<sup>91</sup> Confirming their early results, the same workers analysed fully deuterated oriented samples and successfully compared their experimental spectra with computed simulations based on the parameters from<sup>91</sup> with couplings altered from hydrogen to deuterium where appropriate.<sup>92</sup> In mind of the quantitative conversion of the anion to the TH radical,<sup>90</sup> Gräslund et

al.<sup>91</sup> suggested that the anion in DNA must be thymine rather than cytosine. Furthermore, they suggested that the cation is guanine as the observed partial deuterium exchange of a carbon bound hydrogen<sup>91</sup> is most likely that of an exchange in a purine.<sup>93,94</sup> This assignment is supported by theoretical data on spin-density calculations.<sup>39</sup> Since then, Sevilla et al.<sup>19</sup> have produced a cation in the dinucleoside phosphate GpG which is identical to the cation they produced in DNA. They also showed that computer simulated spectra, based on the data of Gräslund et al. for the guanine cation, closely match the cation spectra they produced experimentally. More recently, Gregoli et al.<sup>89</sup> have studied  $\gamma$ -irradiated frozen aqueous solutions of DNA. They also produced the  $G^+$  and  $T^-$  species at low temperatures. For analysis and spectral reconstruction purposes they selectively produced the guanine cation in DNA using the method of Sevilla et al.<sup>19</sup> of UV photolysis. As this was done in aqueous solution the singlet produced was broader than in the case of Sevilla et al. which was produced in deuterated solution. The spectral parameters did, however, agree with those of the cation produced by Gräslund et al. in non-deuterated solutions.<sup>92</sup>

On annealing the DNA Gregoli et al. confirmed that the thymine anion protonated whilst the guanine cation signal slowly decayed into a diamagnetic species. They also observed a strong oxygen mediated effect at higher temperatures consisting of the replacement of TH radicals by peroxy radicals ( $RO_2$ ) in oxygenated solutions. Such an effect is explained by the attack of oxygen on thymine radicals (either  $T^-$  or TH) to give the  $O_2$  adduct. By spectral reconstruction, using the four radical patterns found in DNA ( $T^-$ , TH,  $G^+$ ,  $RO_2$ ), they showed that the  $[G^+]$ , in deoxygenated solution, is approximately equal to that in oxygenated solution suggesting that the  $RO_2$  radical arises only from

oxygen addition to thymine, not guanine base radicals. This formation of a peroxy radical in DNA is in accord with the oxygen fixation hypothesis<sup>97,98</sup> used to explain oxygen's significant radiosensitizing effect on DNA. The theory suggests that this irreversible formation of a peroxy radical, which leads to cell damage, competes with the reaction in which hydrogen atoms are donated by SH-containing compounds, endogenous to the cell, to repair the DNA by radical termination.

The fact that  $\gamma$ -irradiation of DNA, at low temperatures, selectively produces a guanine cation and a thymine anion is not as surprising as it might seem initially, in light of earlier studies on irradiation of dinucleotides<sup>18,19</sup> and co-stacking complexes of nucleotides.<sup>45,66</sup> Sevilla *et al.*<sup>18</sup> investigated electron transfer reactions within various dinucleoside phosphate anions showing that in purine/pyrimidine complexes electrons are transferred to pyrimidines with thymine being slightly more electronegative than cytosine and adenine slightly more than guanine. This observed order of electron affinities in stacked dinucleoside phosphates agrees with theoretical calculations of electron affinity of the DNA bases themselves.<sup>95,96</sup> The conjugate study on hole transfers<sup>19</sup> within various dinucleoside phosphates showed that guanine had the highest affinity for electron-loss centres or positive holes, in agreement with the order of electron affinities.<sup>18</sup> This work was backed up by studies of  $\gamma$ -irradiated co-stacked dAMP.dTMP complexes by Gregoli *et al.*,<sup>66</sup> who showed that electrons were preferentially located on thymine whilst holes were preferentially located on adenine. Later, Gregoli *et al.*<sup>45</sup> studied various  $\gamma$ -irradiated co-stacked complexes of DNA nucleotides and concluded that positive charges migrated towards guanine whilst negative charges migrated towards cytosine (rather than thymine). These studies do indeed show that charge migration can take

place in stacked bases to give guanine cations and either thymine or cytosine anions. Thus, in DNA, long distance charge migration reactions proceeding as a result of stacked bases competes with local recombination reactions. The fact that only thymine anions were seen in frozen aqueous solutions of  $\gamma$ -irradiated DNA suggests that the stacking conformation in the nucleic acid raises the electron affinity of thymine over cytosine.

The results of my own studies of  $\gamma$ -irradiated frozen aqueous DNA solutions are in agreement with those of Gräslund et al.,<sup>91,92</sup> Sevilla et al.<sup>19</sup> and Gregoli et al.,<sup>89</sup> whereby thymine anions and guanine cations are produced at low temperatures. On annealing deoxygenated DNA samples the thymine anions protonate to form the octet spectrum whilst guanine cations decay into diamagnetic species. In oxygenated solutions, on annealing, the thymine radicals ( $T^-$  and TH) react with oxygen to form peroxy radicals. However, my results of studying  $\gamma$ -irradiated dry DNA samples show a novel result in that, on anneal to room temperature, the octet spectrum of TH is lost and there remains a sextet spectrum of 19 G splitting (Figure 6a,b which conforms to the C5H spectrum [ $A(H_2)C5 = 37 G$ ,  $A(H)C6 = 18 G$ ] as identified by Flossmann et al.<sup>33</sup> C5H is formed by reaction with a hydrogen atom<sup>33</sup> rather than by protonation of an anion. Hence it is most unlikely that a cytosine anion was formed in this case, rather that the base reacted with a free hydrogen atom possibly released from the sugar moiety.

In these DNA studies there has been no trace of the existence of any sugar (or phosphate) radicals which is surprising considering that strand breakage would proceed by rupture of the sugar phosphate bond and also considering that sugar radicals were identified in dAMP, dCMP and dGMP. Possible reasons for this are that the stability of sugar radicals, once

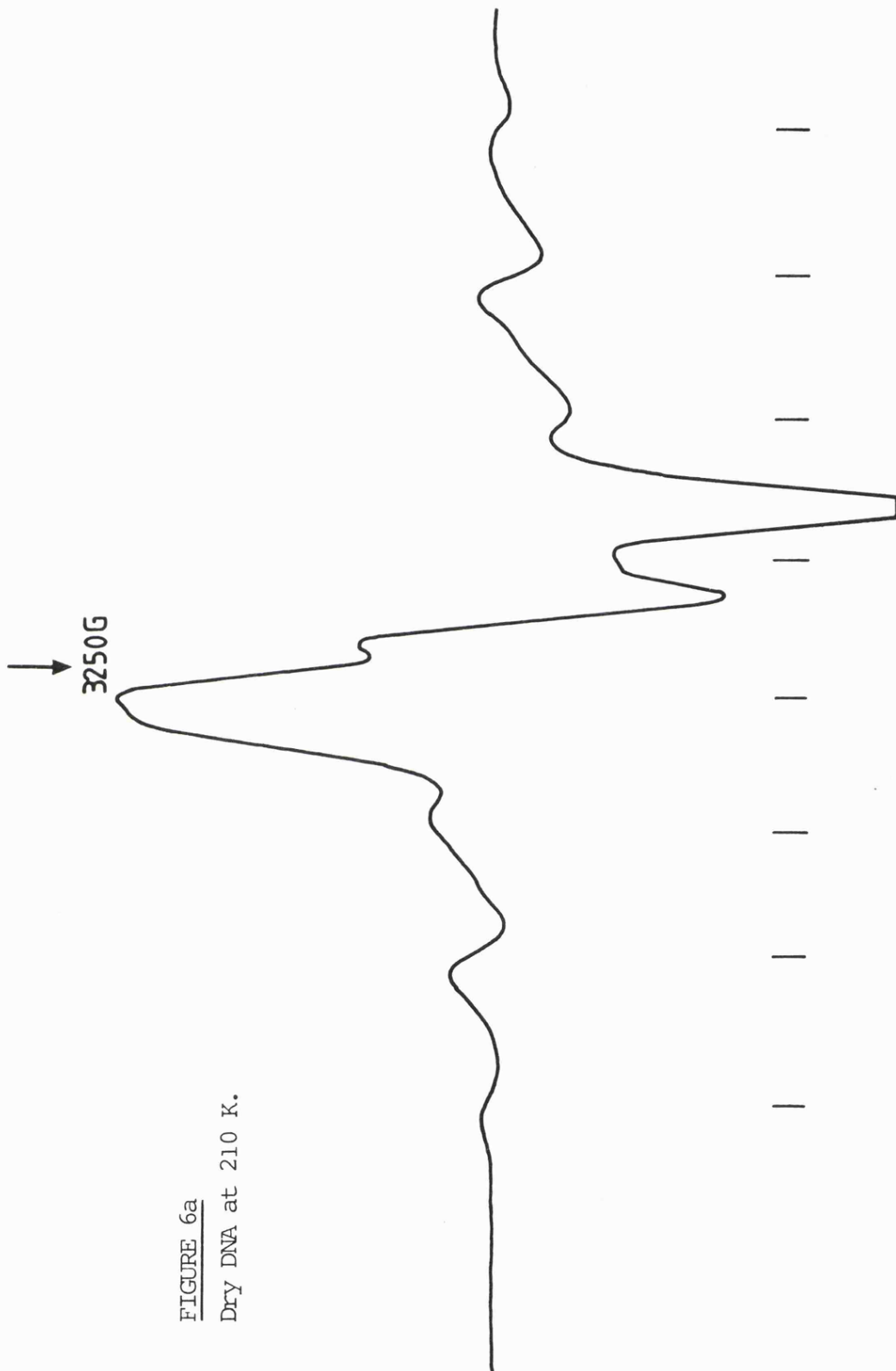
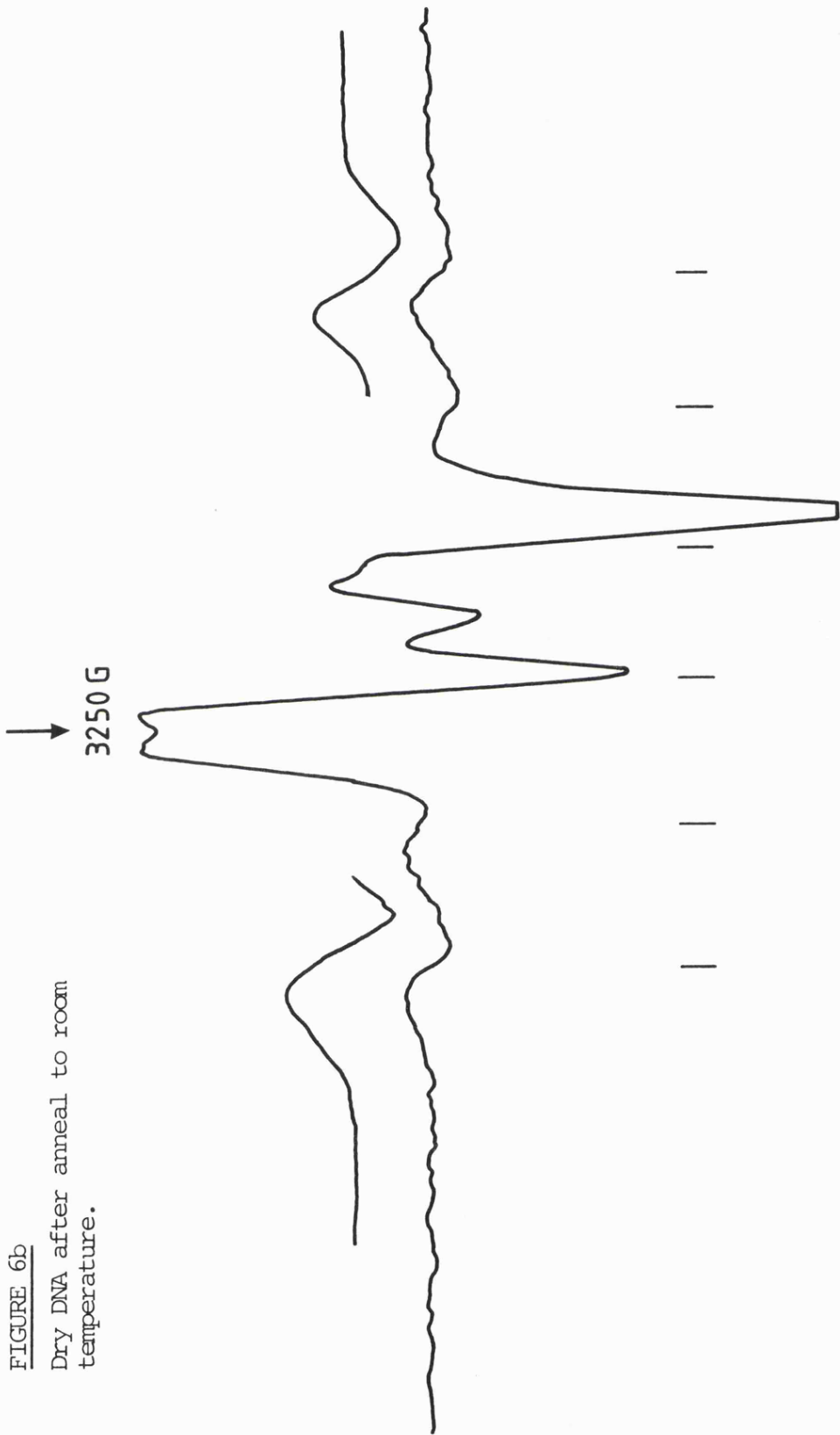


FIGURE 6a  
Dry DNA at 210 K.

FIGURE 6b

Dry DNA after anneal to room temperature.



formed at higher temperatures, is very short lived such that they are not detected by ESR. Furthermore, the signals are likely to be centred close to free spin, thus are unlikely to be readily detectable unless in significant quantities, not least if broad line widths are involved in the spectra. An ENDOR study of oriented DNA might shed light onto this problem.

Sugar radicals are, however, well known in room temperature pulse radiolysis studies of dilute aqueous DNA solutions. Schulte-Frohlinde<sup>99</sup> and Von Sonntag et al.<sup>100</sup> have shown that hydroxyl radicals abstract hydrogen atoms from the deoxyribose unit with resultant  $\beta$ -elimination of the phosphodiester group and chain breakage. In these studies radiation damage is mainly indirect and the primary damage is confined to the solvent water. This results in the production of solvated electrons, hydrogen atoms and hydroxyl radicals which then attack the DNA. However, this situation does not approximate the in vivo conditions where the local hydration degree of DNA is very low due to the tightly folded nucleohistone fibres in chromatin.<sup>101</sup> Furthermore, the water molecules interacting with the DNA (hydration water) possess a highly ordered ice-like structure and are strongly immobilised by electrostatic interactions with the polar groups of DNA.<sup>102</sup> Consequently, it is much more likely that frozen aqueous solutions of DNA (where phase separation occurs preventing indirect attack<sup>89</sup>) approximate the in vivo conditions.

#### REFERENCES FOR CHAPTER 4

1. Voet, D., Rich, A., Prog. Nucl. Acid Res. Mol. Biol., 1970, 10, 183.
2. Arnott, S., Dover, S.D., Wonacott, A.J., Acta Cryst., 1969, B25, 2192.
3. Jardetsky, C.D., JACS, 1961, 83, 2919.
4. Watson, J.D., Crick, F.H., Nature, 1953, 171, 964.
5. Kornberg, A., Ann. Rev. Biochem., 1977, 46, 931.
6. Thomas, P., M.T.P. Int. Rev. Sci., (eds. Kornberg, A., Phillips, P.), 1977.
7. Olins, R., Olins, P., Science, 1974, 183, 330.
8. Kornberg, A., Science, 1974, 184, 868.
9. Kornberg, A., Ann. Rev. Biochem., 1977, 46, 931.
10. Noll, D., Kornberg, A., J. Mol. Biol., 1977, 109, 393.
11. Gregoli, S., Olast, M., Bertinchamps, A.J., Rad. Res., 1977, 72, 201.
12. Sevilla, M.D., Mohan, P.A., Int. J. Rad. Biol., 1974, 25, 635.
13. Sevilla, M.D., in Excited States in Organic and Biochemistry, (eds. Pullman, B., Goldblum, N.), Reidel, Holland, 1978.
14. Pullman, B., in Molecular Biophysics, (eds. Pullman, B., Weissbluth, M.), Academic Press, N.Y., 1965, pp.170-3.
15. Rakvin, B., Herak, J.N., Rad. Res., 1981, 88, 240.
16. Alexander, C., Gordy, W., PNAC, 1967, 58, 1279.
17. Dertinger, H., Z. Naturforsch., 1967, 22b, 1261.
18. Sevilla, M.D., Failor, R., Clark, C., Holroyd, R.A., Pettei, M., J. Phys. Chem., 1976, 80, 353.
19. Sevilla, M.D., D'Arcy, J.B., Morehouse, K.M., Englehardt, M.L., Photochem. Photobiol., 1978, 29, 37.
20. Gregoli, S., Olast, M., Bertinchamps, A.J., Rad. Res., 1974, 60, 388.
21. Hüttermann, J., J. Mag. Res., 1975, 17, 66.
22. Lichter, J.D., Gordy, W., PNAC, 1968, 60, 450.
23. La Croix, M., Depireux, J., Van de Vorst, A., PNAC, 1967, 58, 399.
24. Müller, A., Hüttermann, J., in The Purines Theory and Experiment, (eds. Bergmann, E.D., Pullman, B.), Israel Academy of Sciences and Humanities, Jerusalem, 1972.
25. Hüttermann, J., Z. Naturforsch., 1969, 246, 1648.
26. Lion, Y., Van der Vorst, A., Int. J. Rad. Biol., 1971, 3, 513.
27. Schmidt, J., Borg, D.C., Rad. Res., 1971, 46, 36.
28. Westhof, E., Flossmann, W., Zehner, H.E., Müller, A., Faraday Disc. Chem. Soc., 1977, 63, 248.

29. Lichter, J.L., Gordy, W., PNAC, 1968, 60, 450.
30. Alexander, C., Franklin, C.E., J. Chem. Phys., 1971, 54, 1909.
31. Combs, L.L., Holloman, M., Young, J., Rad. Res., 1973, 58, 8.
32. Herak, J.N., Galogaza, V., J. Chem. Phys., 1969, 50, 3101.
33. Flossmann, W., Westhof, E., Müller, A., Int. J. Rad. Biol., 1976, 30, 301.
34. Westhof, E., Flossmann, W., Müller, A., Int. J. Rad. Biol., 1975, 28, 427.
35. Close, D.M., Bernhard, W.A., J. Chem. Phys., 1979, 70, 210.
36. Westhof, E., Int. J. Rad. Biol., 1973, 23, 389.
37. Sevilla, M.D., Van Paemel, C., Photochem. Photobiol., 1972, 15, 407.
38. Sevilla, M.D., Suryanarayana, D., Morehouse, K.M., J. Phys. Chem., 1981, 85, 1027.
39. Baudet, J., Berthier, G., Pullman, B., C.R. Acad. Sci., 1962, 264, 762.
40. Herak, J.N., Galogaza, V., Dulcic, A., Mol. Phys., 1969, 17, 555.
41. Cook, J.B., Elliott, J.P., Wyard, S.J., Mol. Phys., 1967, 13, 49.
42. Westhof, E., Hüttermann, J., Int. J. Rad. Biol., 1963, 24, 627.
43. Rustgi, E., Box, H., J. Chem. Phys., 1974, 60, 3343.
44. Flossmann, W., Westhof, E., Müller, A., J. Chem. Phys., 1976, 64, 1688.
45. Gregoli, S., Olast, M., Bertinchamps, A.J., Rad. Res., 1979, 77, 417.
46. Holroyd, R.A., Glass, J.W., Int. J. Rad. Biol., 1968, 14, 445.
47. Bernhard, W., Close, D.M., Mercer, K.R., Corelli, J.C., Rad. Res., 1976, 66, 19.
48. Bernhard, W., Hüttermann, J., Müller, A., Close, D.M., Fouse, G.W., Rad. Res., 1976, 68, 390.
49. Krilov, D., Herak, J.N., Biochim. Biophys. Acta, 1974, 366, 396.
50. Herak, J.N., Krilov, D., McDowell, C.A., J. Mag. Res., 1976, 23, 1.
51. Fouse, G.W., Close, D.M., Bernhard, W.A., Bull. Amer. Phys. Soc., 1976, 21, 256.
52. Hampton, D.A., Alexander, C., J. Chem. Phys., 1973, 58, 4891.
53. Alexander, C., Allison, D.L., J. Mag. Res., 1974, 14, 366.
54. Bernhard, W., Snipes, W., J. Chem. Phys., 1967, 46, 2848.
55. Sevilla, M.D., J. Phys. Chem., 1976, 80, 1898.
56. Dulcic, A., Herak, J.N., J. Chem. Phys., 1971, 57, 2537.
57. Hartig, G., Dertinger, H., Int. J. Rad. Biol., 1971, 20, 577.
58. Srinivasan, V.T., Singh, B.B., Gopal-Ayengar, A.R., Int. J. Rad. Biol., 1970, 17, 577.

59. Box, H.C., Budzinski, E.E., J. Chem. Phys., 1975, 62, 197.
60. Gregoli, S., Olast, M., Bertinchamps, A.J., Rad. Res., 1976, 65, 202.
61. Snipes, W., Henriksen, T., Int. J. Rad. Biol., 1970, 17, 367.
62. Hüttermann, J., Int. J. Rad. Biol., 1971, 17, 249.
63. Pruden, B.L., Snipes, W., Gordy, W., PNAC, 1965, 53, 917.
64. Herak, J.N., J. Chem. Phys., 1970, 52, 6440.
65. Gordy, W., Pruden, B.L., Snipes, W., PNAC, 1965, 53, 751.
66. Gregoli, S., Olast, M., Bertinchamps, A.J., Rad. Res., 1977, 70, 255.
67. Sevilla, M.D., J. Phys. Chem., 1970, 74, 3366.
68. Pullmann, B., Mantione, M.J., Biochim. Biophys. Acta, 1964, 91, 387.
69. Herak, J.N., McDowell, C.A., J. Mag. Res., 1974, 16, 434.
70. Sevilla, M.D., Englehardt, M.L., Faraday Disc. Chem. Soc., 1977, 63, 255.
71. Kaalhus, O., Johansen, S.A., Ann. N.Y. Acad. Sci., 1973, 222, 432.
72. Boag, J.W., Müller, A., Nature (London), 1959, 183, 831.
73. Gordy, W., Rad. Res., 1959, 1, 491.
74. Shen-Pei-Gen, Blumenfeld, L.A., Kalmanson, A.E., Pasynski, A.G., Biofizika, 1959, 4, 263.
75. Shields, A., Gordy, W., PNAC, 1959, 45, 269.
76. Alexander, P., Lett, L.T., Ormerod, M.G., Biochim. Biophys. Acta, 1961, 51, 207.
77. Van de Vorst, A., Villée, F., C.R. Acad. Sci., 1964, 259, 928.
78. Ehrenberg, A., Ehrenberg, L., Löfroth, G., Nature (London), 1963, 200, 376.
79. Eisinger, J., Shulman, R.G., PNAC, 1963, 50, 694.
80. Salovey, R., Shulman, R.G., Walsh, W.M., J. Chem. Phys., 1963, 39, 839.
81. Lett, L.T., Parkins, G., Alexander, P., Ormerod, M.G., Nature (London), 1964, 203, 593.
82. Pershan, P.S., Shulman, R.G., Wyluda, B.J., Eisinger, J., Physics, 1964, 1, 163.
83. Ormerod, M.G., Int. J. Rad. Biol., 1965, 9, 291.
84. Pershan, P.S., Shulman, R.G., Wyluda, B.J., Eisinger, J., Science, 1965, 148, 378.
85. Zimmer, K.G., Müller, A., Curr. Top. Rad. Res., (eds. Ebert, M., Howard, A.), North Holland Publishing Co., Amsterdam, 1965.
86. Cook, J.B., Wyard, S.J., Int. J. Rad. Biol., 1966, 11, 357.
87. Holmes, D.E., Weiss, J.J., Int. J. Rad. Biol., 1968, 14, 187.
88. Lenherr, A.D., Ormerod, M.G., Biochim. Biophys. Acta, 1968, 166, 298.

89. Gregoli, S., Olast, M., Bertinchamps, A.J., Rad. Res., 1982, 89, 238.
90. Gräslund, A., Ehrenberg, A., Rupprecht, A., Tjülldin, B., Ström, G., Rad. Res., 1975, 61, 488.
91. Gräslund, A., Ehrenberg, A., Rupprecht, A., Ström, G., Biochim. Biophys. Acta, 1971, 254, 172.
92. Gräslund, A., Ehrenberg, A., Rupprecht, A., Ström, G., Cresp, H., Int. J. Rad. Biol., 1975, 28, 313.
93. Shelton, K.R., Clark, J.M., B.B. Res. Commun., 1968, 33, 850.
94. Shelton, K.R., Clark, J.M., Biochem., 1967, 6, 2735.
95. Bodor, N., Dewar, M.J.S., Harget, A.J., JACS, 1970, 92, 2929.
96. Berthod, H., Gressner-Prettre, C., Pullman, A., Theor. Chim. Acta, 1966, 5, 53.
97. Alexander, P., Charlesby, A., in Radiobiology Symposium (eds. Bacq, Z.M., Alexander, P.), Butterworths, London, 1954, pp.49-59.
98. Alper, T., Howard-Flanders, P., Nature, 1956, 178, 987.
99. Schulte-Frohlinde, D., Proc. 6th. Cong. Rad. Res., (eds. Okada, S., Imamura, M., Terasima, T., Yamaguchi, H.), Tappan Printing Co., Tokyo, 1979, pp.408-422.
100. Von Sonntag, C., Hagen, U., Schön-Bopp, S., Schulte-Frohlinde, D., Adv. Rad. Biol., 1981, 9, 109.
101. Bram, S., Kouprach, S., Baudy, P., in Cold Spring Harbour Symposia : Chromatin, Cold Spring Harbour Laboratory, N.Y., 1978.
102. Bloomfield, V., Crothers, D., Tinoco, I., in Physical Chemistry of Nucleic Acids, Harper & Row, N.Y., 1974.



# CHAPTER 5

**Modification of  $\gamma$ -induced DNA Damage  
in the Presence of Additives**

## INTRODUCTION

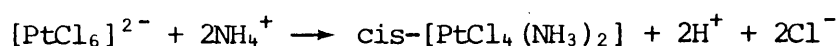
In the preceding Chapter the radiolysis of DNA was discussed. The anomalous situation whereby radicals associated with the cleavage of the phospho-diester backbone of DNA were undetected was also discussed. In an effort to gain further insight into the mechanistic pathways of irradiated DNA, I studied the effect of radiation on frozen aqueous solutions of DNA containing transition metal complexes and a positive hole scavenger. The rationale behind this study was to try and alter the mechanism of radiation damage, with a view either to sensitize further DNA to radiation or to protect the DNA from damage. Clearly agents that could sensitize or desensitize DNA to radiation would be very important in cancer therapy.

The predominantly favoured binding site of metal cations to DNA is the phosphate group. The positive charge of the metal neutralises the charge repulsion between neighbouring nucleotides. This increases the stability of the helix and is reflected by an increase in the melting temperature,  $T_m$ , of the DNA. In the case of the alkaline earth metals, this is the exclusive binding mode. Alternatively, metal complexes can bind directly to the bases or they can stack between the hydrogen bonded base pairs. This latter mode is called intercalation and only occurs in complexes containing aromatic rings whose  $\pi$  orbitals overlap with the  $\pi$  orbitals of the base pairs. Intercalation of complexes increases stacking interactions, lowers overall energy and, consequently, stabilises the helix.

The strength of metal binding to the phosphate groups varies according to the size and charge of the metal ion as well as to the degree of polarization. On moving across and down the Periodic Table, phosphate binding gives way to binding to the bases as the metals become 'softer'.<sup>1</sup>

For instance, there is a 40% higher association constant for  $Mn^{2+}$  over  $Mg^{2+}$  for 5'-dGMP<sup>2</sup> and no interactions between the phosphate moiety and the methyl mercuric ion were detected by Raman Difference Spectroscopy.<sup>3</sup> The binding of metals directly to the bases disrupts the base pair hydrogen bonding and destabilises the helix which is again reflected by a decrease in  $T_m$ . Due to the predominance of base binding of soft transition metals, I studied the effect of the presence of cis-[Pt(NH<sub>3</sub>)<sub>2</sub>(Cl)<sub>2</sub>],<sup>†</sup> HgCl<sub>2</sub> and CuCl<sub>2</sub> on the radiolysis of DNA. The binding of these complexes to DNA has been studied,<sup>4-34</sup> particularly that of cis Pt.

Cis Pt is a powerful anti-cancer drug particularly effective against testicular, ovarian, bladder, head and neck cancers. Its effectivity as an anti-cancer drug was discovered, somewhat fortuitously, by B. Rosenberg in the middle 60's. Rosenberg and his coworkers were investigating the effects of an electric field on growth processes in bacteria when they found that cell division, but not growth, was inhibited.<sup>35</sup> This effect was discovered to be caused by the dissolution of a small amount of platinum from the platinum electrodes. Subsequently, Rosenberg et al. noted that solutions containing [PtCl<sub>6</sub>]<sup>2-</sup> produced this effect if left for two or three days. Spectroscopic studies established that the neutral species cis-[Pt(NH<sub>3</sub>)<sub>2</sub>Cl<sub>4</sub>] was responsible, being formed after 2-3 days by the photochemical reaction:<sup>36</sup>



The trans isomer was tested and found to be biologically inactive. At the same time, the four coordinate cis Pt complex was tested and found to be active. Inhibition of cell division without effect on cell growth suggested that cis Pt might have useful anti-tumour properties. This

<sup>†</sup> Herein denoted cis Pt.

was supported by the fact that other anti-tumour agents (alkylating agents, Actinomycin D, etc.), also caused elongation and lysis in lysogenic bacteria. Cis-[PtCl<sub>4</sub>(NH<sub>3</sub>)<sub>2</sub>], cis-[Pt(NH<sub>3</sub>)<sub>2</sub>Cl<sub>2</sub>], Pt(en)Cl<sub>4</sub>, Pt(en)Cl<sub>2</sub> were initially tested against Sarcoma 180 in the ICR strain of mice and were found to be effective in inhibiting tumour growth.<sup>37</sup> Cis Pt was the most effective of the four and is now used in the clinical treatment of various cancers.<sup>38</sup> The fact that the trans isomer is inactive suggests that the molecular stereochemistry of cis Pt is responsible for its cytotoxicity. The biological target appears to be DNA. Evidence pointing to this conclusion can be summarised as follows:-

a) Cis Pt can induce filamentous growth in cultured E. coli bacteria.

This suggests that cell division is inhibited without markedly influencing cell growth.<sup>35,36</sup>

b) Cis Pt induces lysis in lysogenic bacteria. This phenomenon, indicative of a reaction with DNA, is used in preliminary screenings for anti-tumour activity of platinum compounds.<sup>39-42</sup> Reslova was able to show that a good correlation existed between the anti-tumour activity of platinum compounds and their ability to induce the production of phage in lysogenic E. coli cells.<sup>41</sup>

c) Several studies have shown that platinum compounds are mutagenic in a number of procaryotic and eucaryotic cell systems.<sup>42-52</sup> In all cases, the cis derivatives were much more mutagenic than the corresponding trans isomers. Mutation studies using the Ames assay have shown that both base pair substitution mutations and frameshift mutations occur after treatment of salmonella typhimurium cells with cis Pt. Other platinum compounds (both anti-tumour active and inactive) also cause mutations as judged by the Ames test. However, the types and amounts differ widely for the various platinum

compounds.<sup>50,51</sup>

d) A number of studies have shown that cis Pt and some analogues selectively inhibit DNA synthesis, rather than RNA or protein synthesis.<sup>53-55</sup> This may be related to the number of platinum atoms bound per DNA, RNA or protein molecule. At a cis Pt concentration which reduces the survival of HeLa cells to 37%, several platinum atoms are bound per DNA molecule, while only a small portion of the RNA and protein molecules contain a Pt atom. This is not primarily the result of selective binding to DNA, but is mainly due to the high molecular weight of DNA molecules. To obtain the same cytotoxic effect about five times as much trans Pt has to be bound to DNA as cis Pt.<sup>55-57</sup>

The specific sensitivity of tumour cells to platinum compounds may be due either to the fact that they divide more rapidly than normal cells or that the repair processes in tumour cells are less efficient at removing damage caused by cis Pt.

Binding of cis Pt and other Pt compounds strongly perturbs the DNA structure even at low binding levels. This is reflected by a decrease in  $T_m$ <sup>58,59</sup> in solution viscosity,<sup>60,61</sup> unwinding and shortening of DNA,<sup>62,28</sup> changes in the electrophoretic mobilities of closed circular DNA's<sup>63</sup> and changes in UV and CD spectra.<sup>60,64,65</sup> UV studies have confirmed that cis Pt binds to the DNA bases.<sup>66</sup> It also became evident that the hydrolysed form is the reactive entity.<sup>64,67</sup> Water is an excellent leaving group and hence can be easily substituted on nucleophilic attack by the electron-rich atoms of the heterocyclic bases. In vivo, the hydrolysis reaction should take place primarily after the drug has diffused across the cell membrane since the  $[Cl^-]$  is much lower in the cell than in the plasma. This is backed up by studies showing

that complexes with poor leaving groups are inactive and those with very labile ligands are too highly toxic.<sup>68</sup>

Possible binding sites are indicated by sites of protonation on the pyrimidine and purine bases. The softness of the base, the pH, and the degree of solvation are the prime factors governing the binding of heavy metals to the base substituents. Because of this range of variables, conflicting experimental results have been obtained from NMR, Raman, electronic and X-ray diffraction studies.<sup>69,70,71</sup>

A summary of pK values and protonation site assignments is listed in Table 1:-

Compound	Ionization Site	pK <sub>a</sub>
Adenine	HN-1 <sup>+</sup> / HN-9	3.5 - 4.2 / 10
Guanosine	HN-7 <sup>+</sup> / HN-1	1.9 - 2.1 / 9.0 - 9.2
Uracil	HN-1 / HN-3	9.2 - 9.5
Cytosine	HN-3 <sup>+</sup>	4.0 - 4.2

Guanine and its derivatives have N-7 as the predominant site of protonation. <sup>15</sup>N-NMR<sup>72</sup> studies support this assignment and reveal N3 as a further site in guanosine. Neutral guanosine deprotonates at the amidate nitrogen atom N-1 with a pK value of 9.0-9.2.

Adenine and derivatives have N1 as the most basic atom according to XRD studies of adenine HCL,<sup>73</sup> 5'-AMP<sup>74</sup> and 3'-AMP.<sup>75</sup> Proton ionization of neutral adenine is generally thought to be from the N9 position.<sup>76</sup>

Pyrimidines, which are N1 substituted in nucleotides and nucleic acids, have N3 as the most basic nitrogen atom. This is backed up by NMR studies of N<sup>15</sup>-cytosine derivatives.<sup>77</sup>

Sites of metal binding have been found by studies on metal nucleoside and metal nucleotide complexes. These sites correlate with protonation sites and are listed in Table 2.

Compound	Coordination Site	Additional Site
Adenosine	N7	N1
Guanosine	N7	N1,O6
Uridine	N3	O2,O4
Cytidine	N3	N2,O4

NMR,<sup>78-81,25</sup> UV<sup>66</sup> and Raman<sup>25,81</sup> studies of several Pt complexes of nucleosides and nucleotides show that the main binding sites on the bases are N(7) and N(1) for A, N(7) for G and N(3) for C. Crystal structures have been reported for cis-bis-guanosine,<sup>82-4</sup> cis-bis(5'-IMP),<sup>32,85</sup> 9Me-Adenine<sup>86,87</sup> and cis-bis(3'-CMP) Pt(II) complexes. All display N7 binding except the cytosine derivatives which bind at N3. The order of nucleophilicity towards the diaquo or the dichloro complexes has been reported as GMP > AMP » CMP.<sup>25</sup> N1 substituted thymine or uracil derivatives do not react with cis Pt under normal conditions. Binding of cis Pt to two 5'-GMP molecules has been monitored by NMR<sup>88,89</sup> which showed that the first molecule binds faster than the second, the reaction proceeding via the intermediate cis Pt (NH<sub>3</sub>)<sub>2</sub> (5'-GMP) (H<sub>2</sub>O). These N7 bound metal complexes are stabilised by hydrogen bonding to O6. Binding by cis Pt to DNA itself can therefore take place via two coordination sites.

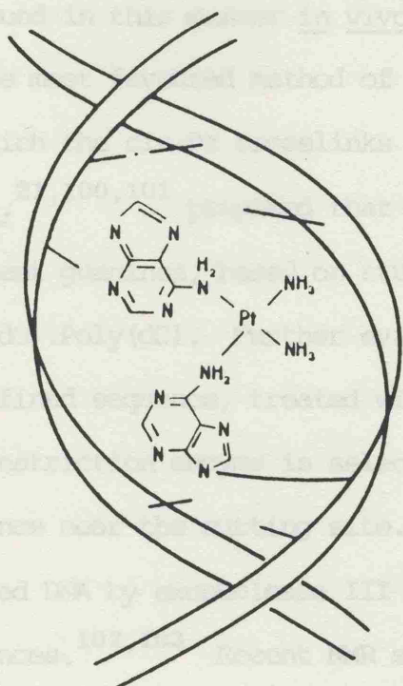
Several bifunctional binding modes for cis Pt have been proposed to explain the specific anti-neoplastic activity of cis Pt compounds. The different binding modes are (i) interstrand crosslinks, (ii) intrastrand crosslinks, (iii) DNA-protein crosslinks and (iv) bifunctional binding to guanine. These are shown in Figure 1.

Interstrand crosslinking has been suggested as it offers an explanation for the prevention of DNA synthesis by cis Pt. Evidence for this type of binding comes from the fact that high molecular weight DNA exists under denaturing conditions in the presence of cis Pt when separation of the two DNA strands should occur.<sup>55,90-95</sup> Although

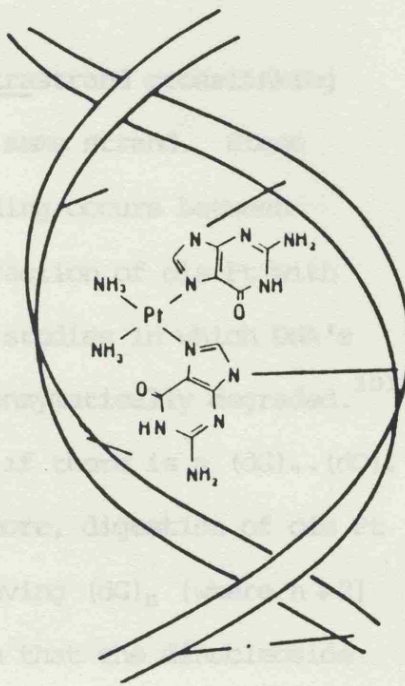
FIGURE 1

Different DNA-cis Pt binding modes.

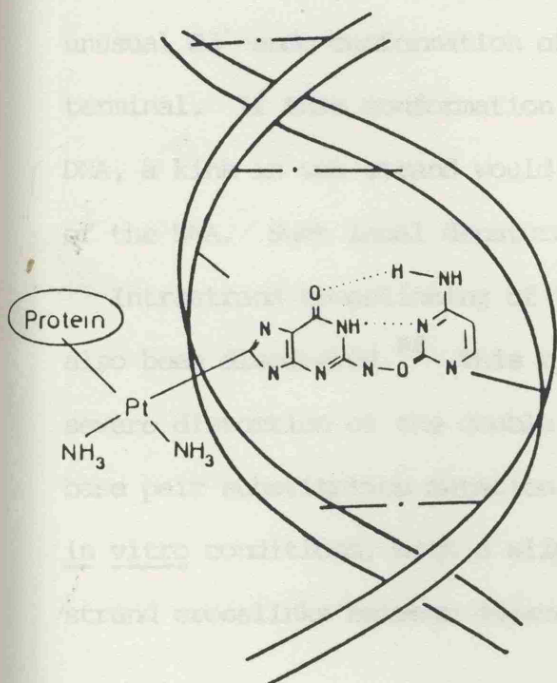
(i) Interstrand Crosslink



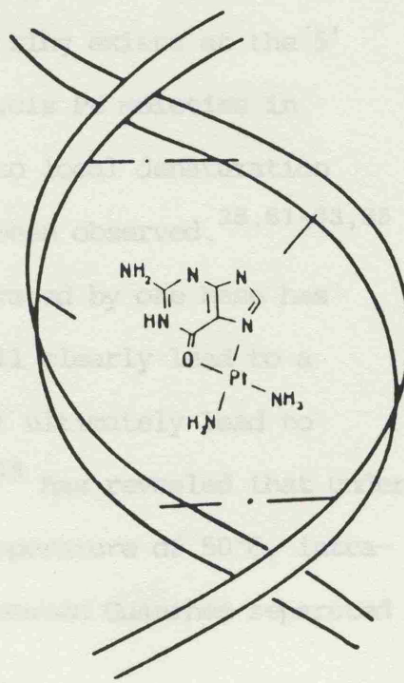
(ii) Intrastrand Crosslink



(iii) DNA-Protein Crosslink



(iv) Bifunctional Binding



Zwelling et al.<sup>96-98</sup> found a correlation between cytotoxicity and interstrand crosslinking, only 1% of the total amount of bound cis Pt is bound in this manner in vivo.<sup>55,94,99</sup>

The most favoured method of binding is by intrastrand crosslinking in which the cis Pt crosslinks two bases of the same strand. Stone et al.<sup>21,100,101</sup> proposed that this type of binding occurs between adjacent guanines, based on studies of the interaction of cis Pt with Poly(dG).Poly(dC). Further evidence comes from studies in which DNA's of defined sequence, treated with cis Pt, were enzymatically degraded.<sup>101-3</sup> The restriction enzyme is selectively inhibited if there is a (dG)<sub>4</sub>.(dC)<sub>4</sub> sequence near the cutting site.<sup>104,105</sup> Furthermore, digestion of cis Pt treated DNA by exonuclease III stops at sites having (dG)<sub>n</sub> [where n ≥ 2] sequences.<sup>102,103</sup> Recent NMR studies have shown that the dinucleoside monophosphates IpI and GpG bind to cis Pt via both their N7 atoms.<sup>106-8</sup> In the case of CpG chelation is effected either via N7 atoms on guanines of two separate dinucleotides<sup>109,110</sup> or via the Cytosine N3 and Guanine N7 atoms of one dinucleotide.<sup>108</sup> A detailed NMR study of the chelate formed upon reaction of d(GpG) with cis Pt<sup>111</sup> suggests that an unusual C3'-endo conformation of the deoxyribose ring exists at the 5' terminal. If this conformation exists in d(GpG).cis Pt moieties in DNA, a kink in one strand would result, leading to local denaturation of the DNA. Such local denaturation has indeed been observed.<sup>28,61-63,65</sup>

Intrastrand crosslinking of two guanines separated by one base has also been discovered.<sup>52</sup> This type of chelate will clearly lead to a severe distortion of the double helix which might ultimately lead to base pair substitution mutation. Further study<sup>112</sup> has revealed that under in vitro conditions, with a slightly elevated temperature of 50°C, intra-strand crosslinks between adjacent Guanines or between Guanines separated

by a third base are equally probable. It is noteworthy that the cis configuration is fundamental for this type of binding.

DNA-protein crosslinking by Pt has been observed by several workers.<sup>95,96,98,113</sup> This type of defect occurs to only a small extent (approximately three times that of interstrand crosslinks).<sup>95-99</sup> In fact, trans Pt forms DNA-protein and protein-protein crosslinks after short incubation times whilst the cis isomer binds primarily to DNA and only forms DNA-protein crosslinks after long incubation times. Histone-histone crosslinks are formed by the trans isomer between histones H3 with H2a and H2b with H4.<sup>113</sup>

Lastly, bidentate chelation to a single Guanine base via N7 and O6 (breaking the O6-NH<sub>2</sub> hydrogen bond) has been postulated.<sup>29,32,62,63,114-116</sup> Evidence for this type of binding has come from photoelectron spectroscopic data<sup>30</sup> which showed the participation of nitrogen and oxygen atoms in these complexes. Also, IR studies<sup>31,119</sup> showed a decrease in the  $\nu_{C=O}$  stretch. Further evidence comes from UV, CD, fluorescence and T<sub>m</sub> data<sup>62</sup> which indicate a modification of the base pair stacking coupled with DNA denaturation resulting from the disruption of the interstrand hydrogen bonds. However, no supporting X-ray crystallographic data exists and certain investigators have rejected this binding mode on geometric grounds.<sup>117-118</sup>

Studies of the interactions of Cu and Hg compounds with DNA are less common as no specific anti-tumour activity has been associated with any complexes of these metals. However, some work has been done on the interaction of these metals with monomeric and polymeric nucleic acid derivatives.

In a similar fashion to cis Pt binding, Cu(II) complexes bind to the N7 atom of N9-substituted purine bases,<sup>120-4</sup> nucleotides<sup>125</sup> and

polymers.<sup>126</sup> Cu(II) binds to Cytosine and its derivatives in a bidentate fashion via N3 and O2<sup>127-130</sup> as in (glygly)(cytidine)Cu II. Cu(II) does not form complexes with N1 substituted thymine derivatives; however, a thymine anion complex has been discovered in which binding is via the N1 position.<sup>131</sup> Spectrophotometric studies of the interaction of poly(A) and poly(C) with Cu<sup>2+</sup> ions showed that the Cu<sup>2+</sup> ions caused a disordering of the polymer structure which was dependent on the [polymer].<sup>133</sup> This effect was interpreted in terms of interstrand crosslinking. Furthermore, the disordering of the polymer by Cu<sup>2+</sup> ions was found to be cooperative which was explained by intramolecular crosslinking. Studies of metal DNA binding have shown that Cu<sup>2+</sup> (like cis Pt) preferentially binds to GC rich regions of DNA.<sup>132</sup>

Unlike Cu and Pt complexes, Hg(II) binds to thymine. Kosturko et al.<sup>134</sup> showed that one Hg ion can link two 1-methylthymine molecules via the N3 positions. Similarly, binding to 1-methylcytosine proceeds via the N3 position with a weak bond to the exocyclic O2 atom.<sup>135</sup> Binding to the purines is via the N7 atoms as was identified by Authier-Martin et al.<sup>136</sup> in HgCl<sub>2</sub> (guanosine). Studies of Hg binding to Poly[d(A-T).d(A-T)] have revealed that Hg crosslinks thymines from neighbouring strands via the N3 position.<sup>137,138</sup> Supporting evidence comes from the fact that there is no pronounced effect in poly(dA.dT). At higher [Hg], binding to the NH<sub>2</sub> group of Adenine takes place.<sup>139-141</sup> Hg has a strong effect on DNA itself, dramatically reducing the solution viscosity<sup>142</sup> despite retaining a high degree of base stacking as monitored by the hyperchromicity. The residual base stacking is maintained by the crosslinking of the strands.

## EXPERIMENTAL

Calf thymus DNA and pyrimidine derivatives were purchased from the Sigma Chemical Company.  $\text{Br}_2$ ,  $\text{NaI}$ ,  $\text{CuCl}_2 \cdot 2\text{H}_2\text{O}$  from BDH,  $\text{CD}_3\text{OD}$  and  $\text{HgCl}_2$  from the Aldrich Chemical Company whilst the cis Pt was donated by Johnson Matthey Ltd.

Brominated thymine was prepared by reaction with bromine water following the procedure of Moore and Anderson.<sup>143</sup> Aqueous DNA solutions were left for 48 hours to dissolve at  $4^\circ\text{C}$  prior to mixing with solutions of the metal salts. The resultant solutions were incubated in an oil bath at  $37^\circ\text{C}$  for 72 hours and were then degassed by purging the solutions with nitrogen in a dry box. Three samples of 30 mM  $\text{NaI}$  and 13 mM cis Pt were made and added to 10, 50 and 100  $\text{mgs ml}^{-1}$  solutions of DNA and  $\text{D}_2\text{O}$  ( $\text{H}_2\text{O}$  also in the case of cis Pt). Six samples of  $\text{CuCl}_2 \cdot 2\text{H}_2\text{O}$  and  $\text{HgCl}_2$ , varying in concentration from 1.6 - 81 mM, were prepared and mixed with 50  $\text{mgs ml}^{-1}$  DNA in  $\text{D}_2\text{O}$  solutions.

Frozen aqueous glasses of cis Pt were prepared for irradiation by dissolving 4  $\text{mgs ml}^{-1}$  cis Pt in a 60/40  $\text{CD}_3\text{OD}/\text{D}_2\text{O}$  solution and then pipetting drops of solution into liquid nitrogen to form solid beads which were subsequently irradiated at 77 K in a  $^{60}\text{Co}$   $\gamma$  cell for 2 hours at a dose rate of  $0.8 \text{ MRad hr}^{-1}$ .

Frozen aqueous solutions of DNA and pyrimidines were prepared for irradiation by cooling Pyrex tubes containing 0.5 ml of the given solution in liquid nitrogen. Extrusion of this frozen solution from the tube produced uniform solid cylinders 2.5 cm long which were subsequently irradiated in bottles in the  $^{60}\text{Co}$   $\gamma$  cell at 77 K for five hours.

X-band ESR spectra were recorded on a Varian E-109 spectrometer at 77 K in a glass finger Dewar. Samples were annealed either by using the

Varian V6040 variable temperature device or by allowing the samples to warm up in the Dewar flask, without liquid nitrogen, whilst continuously monitoring the spectrum. When significant changes occurred, the sample was recooled to 77 K. G-values were calculated using an HP 5246C frequency counter in conjunction with a Bruker B-H12E field calibrant. Spectral computations were performed on a Hewlett-Packard 9835B computer.

## RESULTS AND DISCUSSION

As mentioned at the beginning of the Chapter, certain compounds were added to the DNA samples, prior to irradiation, in order either to sensitize or to protect the DNA. The four compounds dealt with in this Chapter only exhibited protective effects as judged from the ESR spectra.

The question of radiosensitization mechanisms involving an increase in the number of free radicals has been discussed by Adams.<sup>144</sup> He proposed that the frequency of radical ion recombination in DNA was high (i.e.  $G^+ + T^- \rightarrow G + T$ ) and that sensitizing drugs prevented radical recombination by preferentially capturing the electrons. Unfortunately, ESR results indicate that this attractive theory may not be correct since there is no evidence of radical recombination (i.e. loss of radical yield) on storing DNA samples at low temperatures for periods of weeks.<sup>145</sup> As radical recombination does not take place to any significant degree, it should not be possible to increase radical yields by the use of additives.

The four compounds dealt with herein all reduced yields of either  $G^+$  or  $T^-$  or both by preferential hole and/or electron capture. Cis Pt and  $HgCl_2$  induced the formation of a novel radical (or radicals), denoted by the symbol 'X', which grew in on annealing. Figure 2 is a plot of

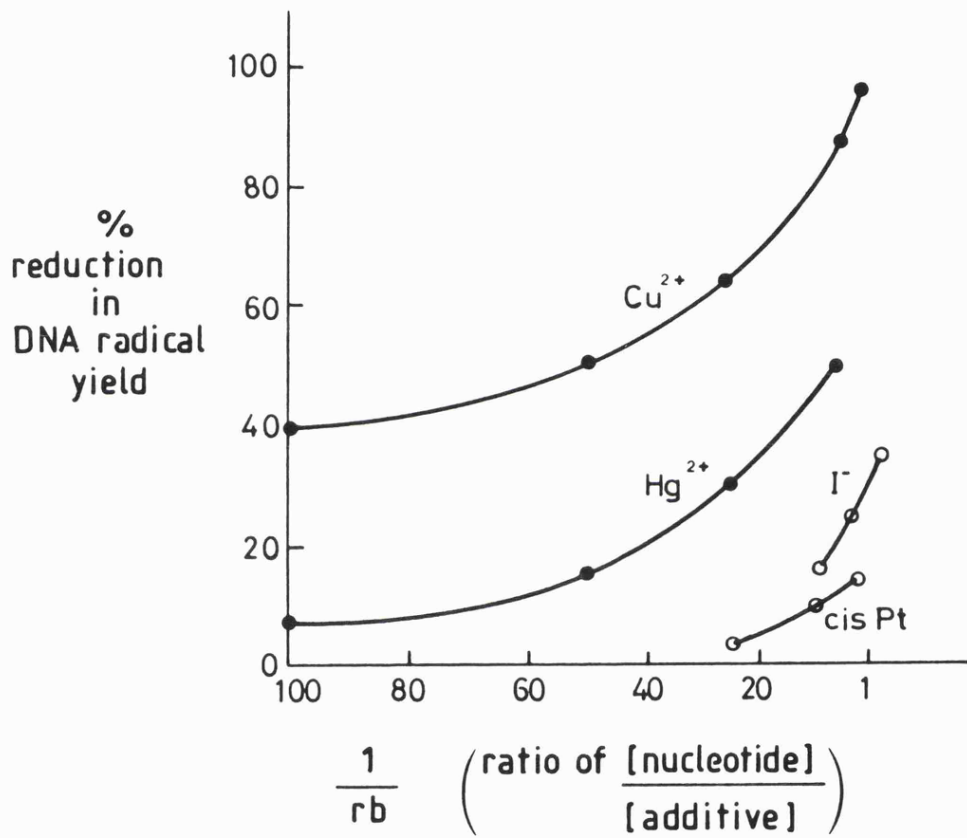


FIGURE 2

Effect of additives on DNA radical yields at 135 K.

the effectiveness of the four additives in reducing radical yields with increasing [additive]. From this graph (Figure 2) it is clear that  $\text{Cu}^{2+}$  is the most effective additive, removing 90% of the DNA radicals at concentrations of 1  $\text{Cu}^{2+}$  to 10 nucleotides. The order is  $\text{Cu}^{2+} > \text{Hg}^{2+} > \text{I}^- > \text{cis Pt}$ .

#### $\text{CuCl}_2 \cdot 2\text{H}_2\text{O}$

Samples with a range of  $r_b$  values were prepared. Before irradiation, the ESR spectra were characteristic of square planar coordinated copper(II). Hyperfine splitting from interaction between the unpaired electron and  $^{63}\text{Cu}$  and  $^{65}\text{Cu}$  nuclei which both have nuclear spins of  $\frac{3}{2}$  gives rise to sets of quartets as shown in Figure 3. The spectrum is anisotropic with  $g_{\parallel} = 2.3$ ,  $A_{\parallel} = 130$  G and  $g_{\perp} = 2.06$ ,  $A_{\perp} < 20$  G.

After irradiation, the  $\text{Cu}^{2+}$  signal decreased in intensity by up to 8% as a result of electron capture, converting the  $\text{Cu}^{2+}$  to  $\text{Cu}^+$ . The reduction of  $\text{Cu}^{2+}$  in a copper-DNA complex has been previously reported in ESR studies.<sup>146</sup> The reduction reaction is in competition with electron capture at thymine and, consequently, there is a reduced yield of thymine anions. By monitoring the DNA spectrum, it is clear that the cupric ion is very effective at scavenging electrons.

The samples studied had the following copper/nucleotide ratios:-

1. 1 : 100
2. 1 : 50
3. 1 : 25
4. 1 : 10
5. 1 : 5

For sample (1) the spectrum at 135 K, at which temperature the  $\dot{\text{O}}\text{H}$  radicals in the ice phase are lost,<sup>147</sup> shows that the yield of DNA radicals is 40% lower and has a modified G:T ratio. Subtraction of this spectrum from the 135 K control spectrum indicates that the  $\text{Cu}^{2+}$ , at this concentration, has mainly reduced the  $\text{T}^-$  signal as expected, but

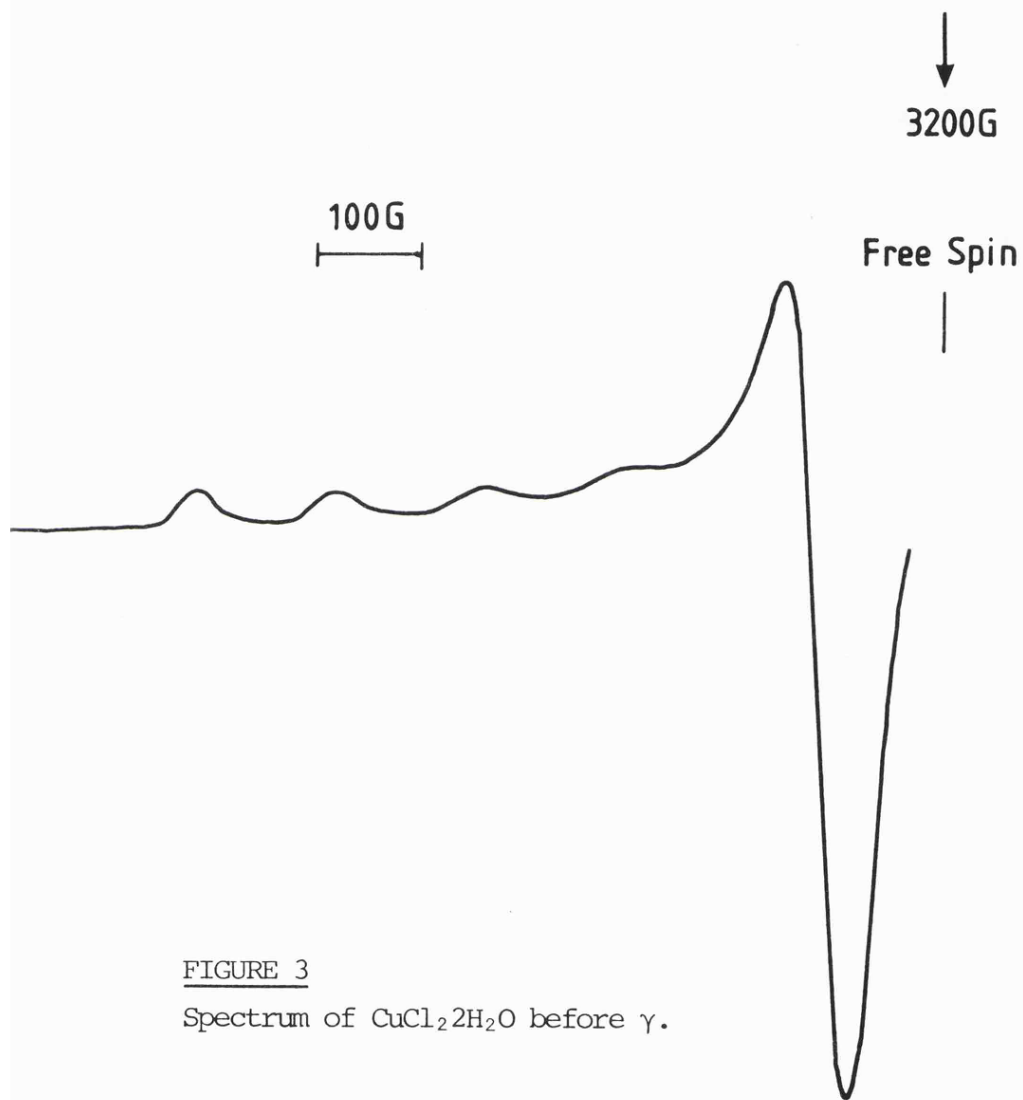


FIGURE 3  
Spectrum of  $\text{CuCl}_2 \cdot 2\text{H}_2\text{O}$  before  $\gamma$ .

may also have reduced the G<sup>+</sup> signal (see Figure 4 and Table 3).

Annealing to 200 K resulted in a complete loss of the anion spectrum leaving a pure G<sup>+</sup> spectrum. This decayed on further warming in the usual manner. This pattern of annealing was repeated for each sample (see Figure 5).

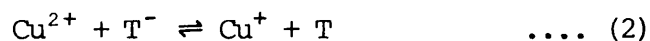
TABLE 3

Effect of Cu<sup>2+</sup> on DNA radical yields at 135 K

1/r <sub>b</sub>	% Total reduction	% G <sup>+</sup> reduction	% T <sup>-</sup> reduction
100	40	20	60
50	50	30	70
25	65	45	85
10	88	75	100
5	98	96	100

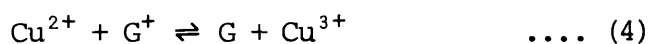
Scheme I gives an explanation for the reduction in the G<sup>+</sup> signal with increasing [Cu<sup>2+</sup>]:-

Scheme I



Reaction (3) is less significant than (1) or (2) but it is noteworthy that this reaction regenerates fresh Cu<sup>2+</sup>, thereby acting catalytically.

Reaction (3) should become increasingly important as the [Cu<sup>2+</sup>] and thereby [Cu<sup>+</sup>] increases with respect to the DNA nucleotides. An alternative explanation for the reduction in G<sup>+</sup> is provided by the following reaction:-



This reaction is less likely since the redox potential for the oxidation of Cu<sup>2+</sup> in most environments is high. Also, the reaction would not be as strongly concentration dependent as (3).

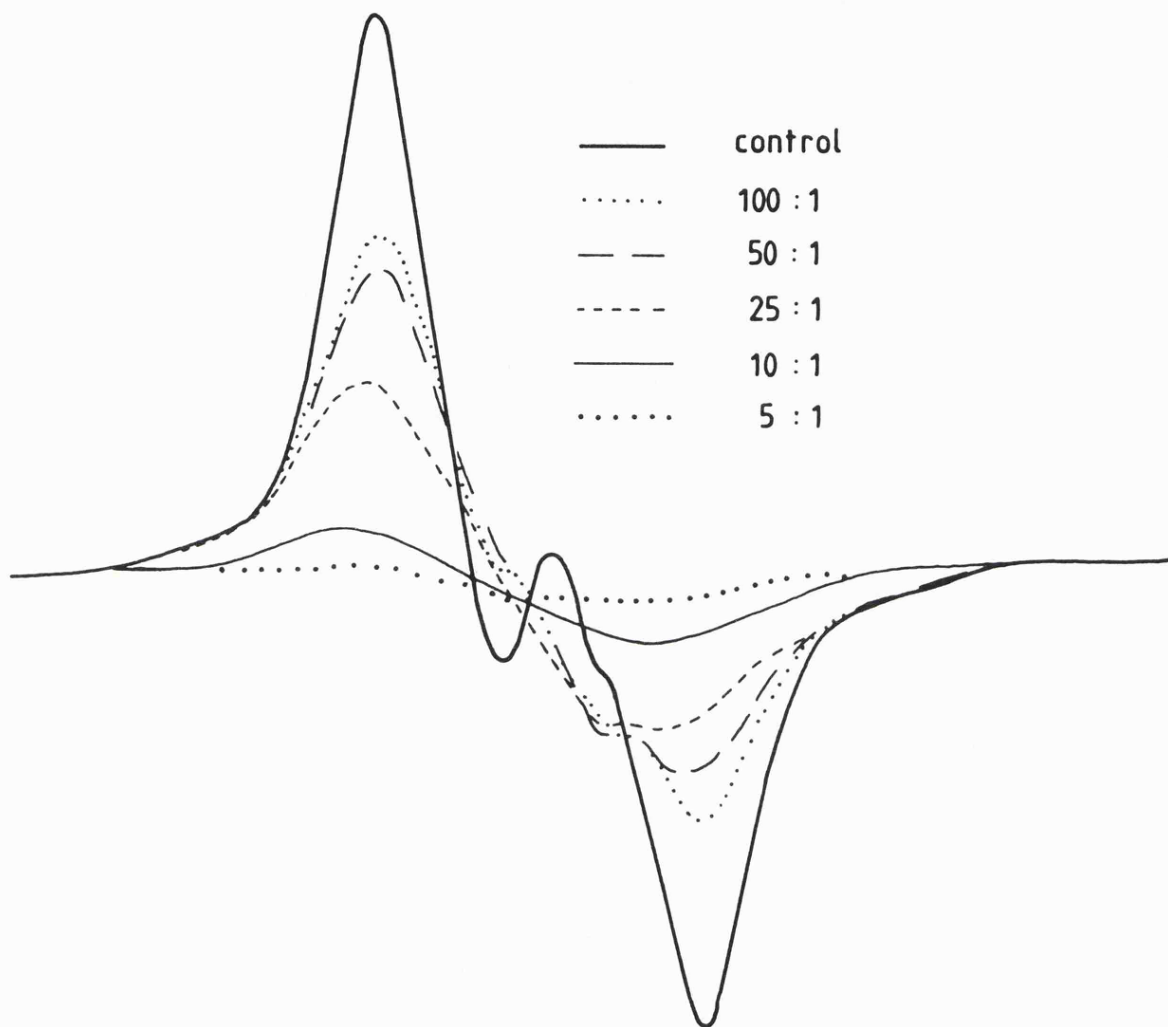
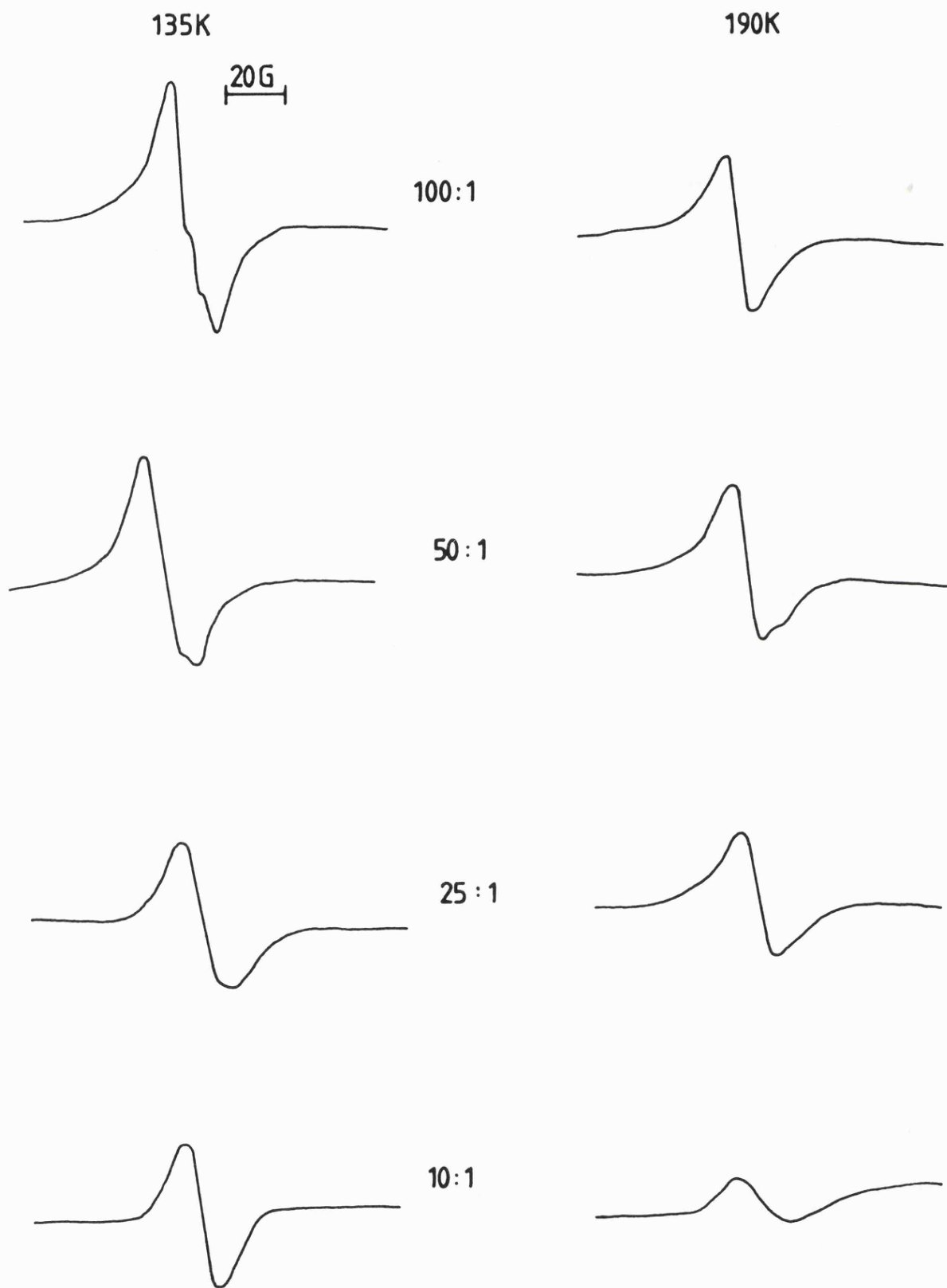


FIGURE 4

Effect of  $\text{Cu}^{2+}$  on DNA radical yield at 135 K.

FIGURE 5

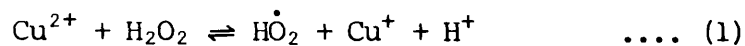
Cu/DNA at various concentrations.



Predictably, the most concentrated samples followed the same trend with increasing reduction in the yield of  $G^+$ . In sample (4), hole and electron scavenging by copper is very efficient, reaching nearly 90% in reduction of DNA radicals at 77 K. The fifth sample was clearly denatured as its consistency was somewhat rubber-like. The ESR spectrum, before exposure, showed that the configuration at the  $Cu^{2+}$  site had altered, presumably as a result of the changed DNA configuration. In this sample, the DNA radical yields were close to zero. The apparent ability of  $Cu^{2+}$  to capture holes from guanine may well be related to the fact that it binds very efficiently to N7 of the guanine moiety in N9 substituted purine bases,<sup>120-4</sup> nucleotides,<sup>125</sup> polymers<sup>126</sup> and has been shown to bind to GC-rich regions of DNA.<sup>132</sup> Indeed, for high concentrations of  $[Cu^{2+}]$  many guanine bases may have copper attached. In that case, even if the 'hole' is retained by  $G^+$ , the overall centre,  $G^+ - Cu^{2+}$  must be either in a triplet or singlet state. The latter would give no ESR signal, hence explaining the "loss" of  $G^+$ . The former might also be difficult to detect because of a large zero-field splitting.

The apparent very strong radio-protecting effect of this copper complex is not borne out in strand-break studies of irradiated plasmid DNA containing cupric chloride.<sup>148</sup> Samples, irradiated at 77 K, are warmed to room temperature and analysed using gel electrophoresis. The results indicate that cupric chloride is a radiosensitizer, causing an increased number of strand-breaks. The reason for this apparently anomalous result probably lies in the ability of  $Cu^{2+}$  to convert  $H_2O_2$  (produced by hydroxyl radical recombination) into hydroxyl radicals which are then able to cause additional strand-breaks by hydrogen abstraction from the sugar moieties. The scheme of reactions is shown in Scheme II.

Scheme II



HgCl<sub>2</sub>

DNA samples with varying [HgCl<sub>2</sub>] were prepared and irradiated. After irradiation, features attributable to Hg<sup>+</sup> ions could be seen in the ESR spectrum. The M<sub>I</sub> = -½ line of the magnetic isotope <sup>199</sup>Hg (which has a nuclear spin of ½) could be seen 2000 G up-field from free spin as well as a signal at g = 1.93 which probably arises from the non-magnetic Hg isotopes.

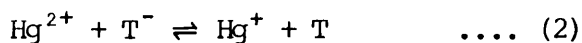
Six samples were studied with the following metal/nucleotides

ratios:-

- 1 : 100
- 1 : 50
- 1 : 25
- 1 : 10
- 1 : 5
- 1 : 2

As can be seen from Figure 2, Hg<sup>2+</sup> is not as effective as Cu<sup>2+</sup> at protecting the DNA bases from radiation damage. Figure 6 shows the effect on the yield of DNA base radicals of increasing [Hg<sup>2+</sup>]. In the case of the first two samples, 1:100 and 1:50, the effect on the radical yield was only slight - a reduction of approximately 10%. Subtractions from the DNA control indicate that the [T<sup>-</sup>] is reduced, presumably due to competitive electron capture by Hg<sup>2+</sup>, as shown in the Scheme below.

Scheme III



Annealing these samples further produced spectra similar to those from

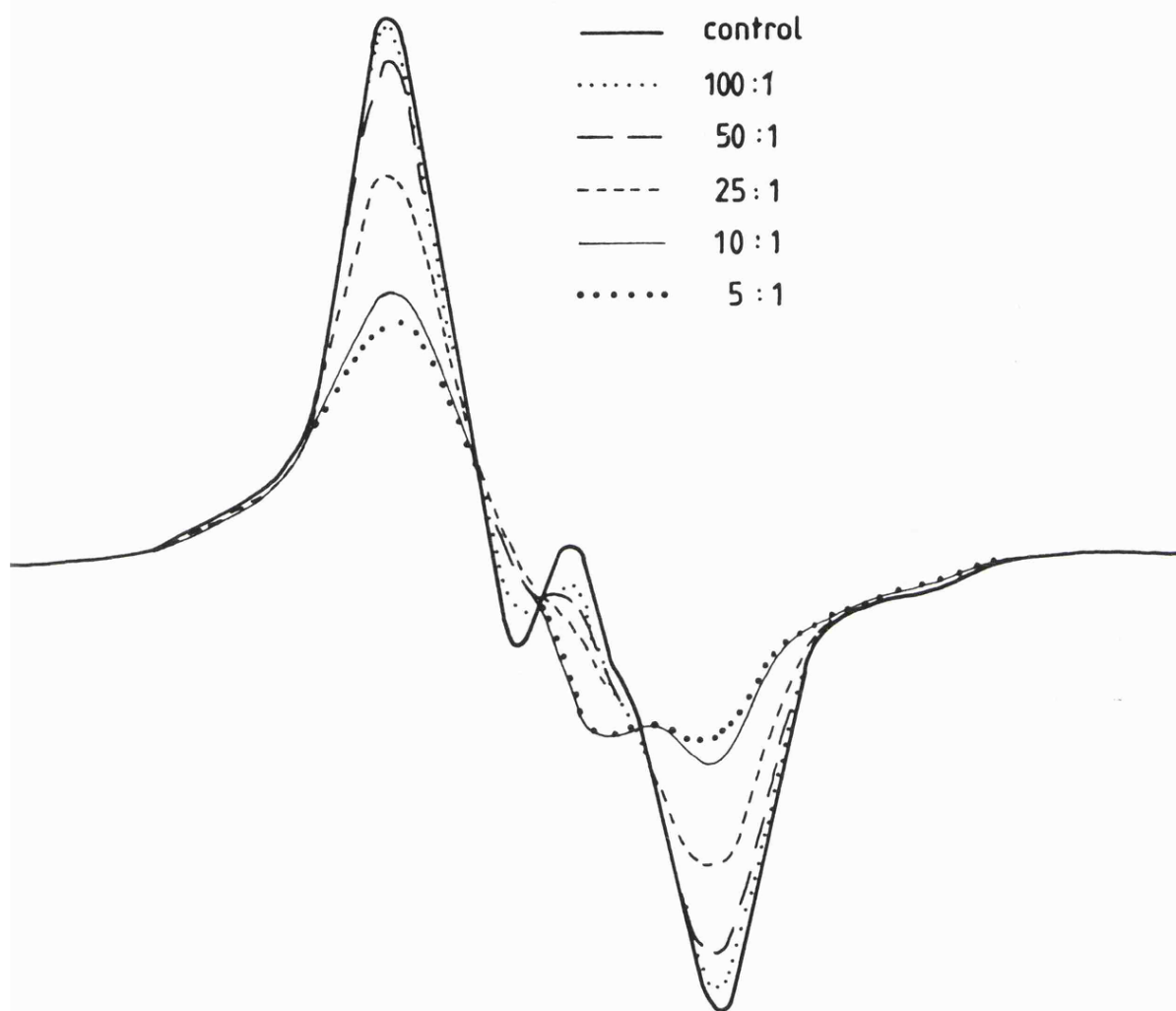


FIGURE 6  
Effect of  $\text{Hg}^{2+}$  on DNA radical yield at 135 K.

native DNA with a 20% smaller contribution from  $T^-$  (Figure 7). Doubling the  $[Hg^{2+}]$  to 1:25 resulted in a significant reduction in radical yield due to loss of  $T^-$ . Annealing this sample to 200 K results in further  $T^-$  loss leaving a spectrum which comprises predominantly of  $G^+$  with a small amount of residual  $T^-$ . Further annealing this sample results in the decay of  $G^+$  as well as decay of residual  $T^-$ .

The next set of samples 1:10, 1:5 and 1:2 can be grouped together as their spectra are very similar, only varying to a small degree in the amount of  $T^-$  present. The 135 K spectra show enhanced electron capture by  $Hg^{2+}$  to the tune of 80-90% as compared to the native DNA spectra without any apparent alteration in  $[G^+]$ . Warming these samples to 200 K results in electron transfer from  $T^-$  to  $Hg^{2+}$ , reflected in a further reduction of  $[T^-]$ . At higher temperatures, 240 K and above,  $G^+$  decays in parallel with the growth of a new radical X which will be discussed more fully later in the Chapter. The spectrum consists of a doublet (almost identical to  $T^-$ ) with a superimposed central singlet plus wing features (these are similar to the outer parallel features in  $G^{+149}$  but are relatively larger).

#### Cis Pt (NH<sub>3</sub>)<sub>2</sub>Cl<sub>2</sub>

Cis Pt is known to bind to the DNA bases and form inter- and intra-strand crosslinks, thereby altering the DNA conformation. Cis Pt was therefore used as an additive in this study as the mechanism of radiation damage might be modified in crosslinked DNA, coupled with the fact that Pt<sup>II</sup> might undergo electron capture and loss reactions in competition with the DNA radicals.

Initially, attempts were made to form the anion and cation radicals of cis Pt in appropriate solvent matrices which promote electron gain and loss reactions. Attempts to form the cation in freon were unsuccessful

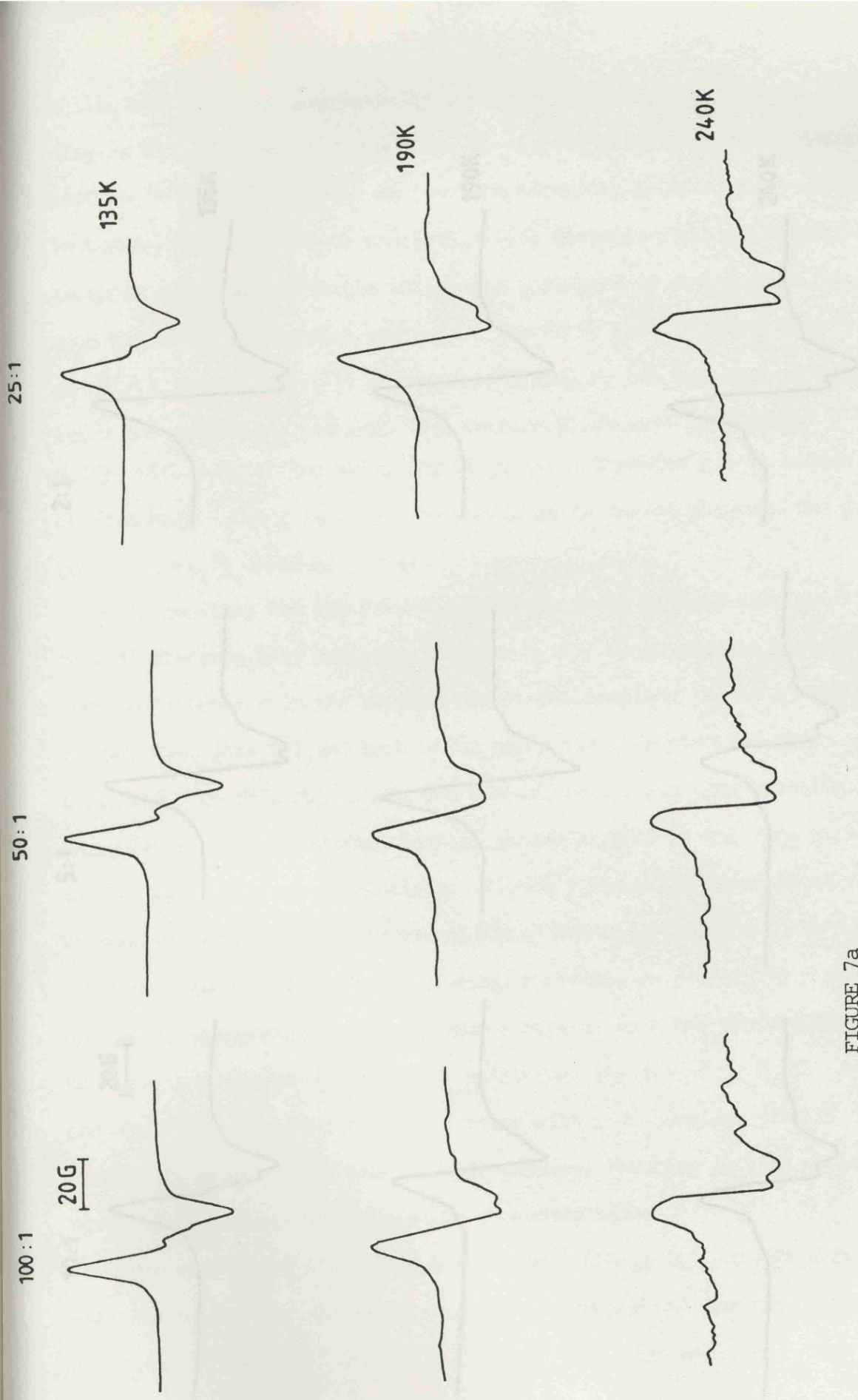


FIGURE 7a  
Hg/DNA at various concentrations.

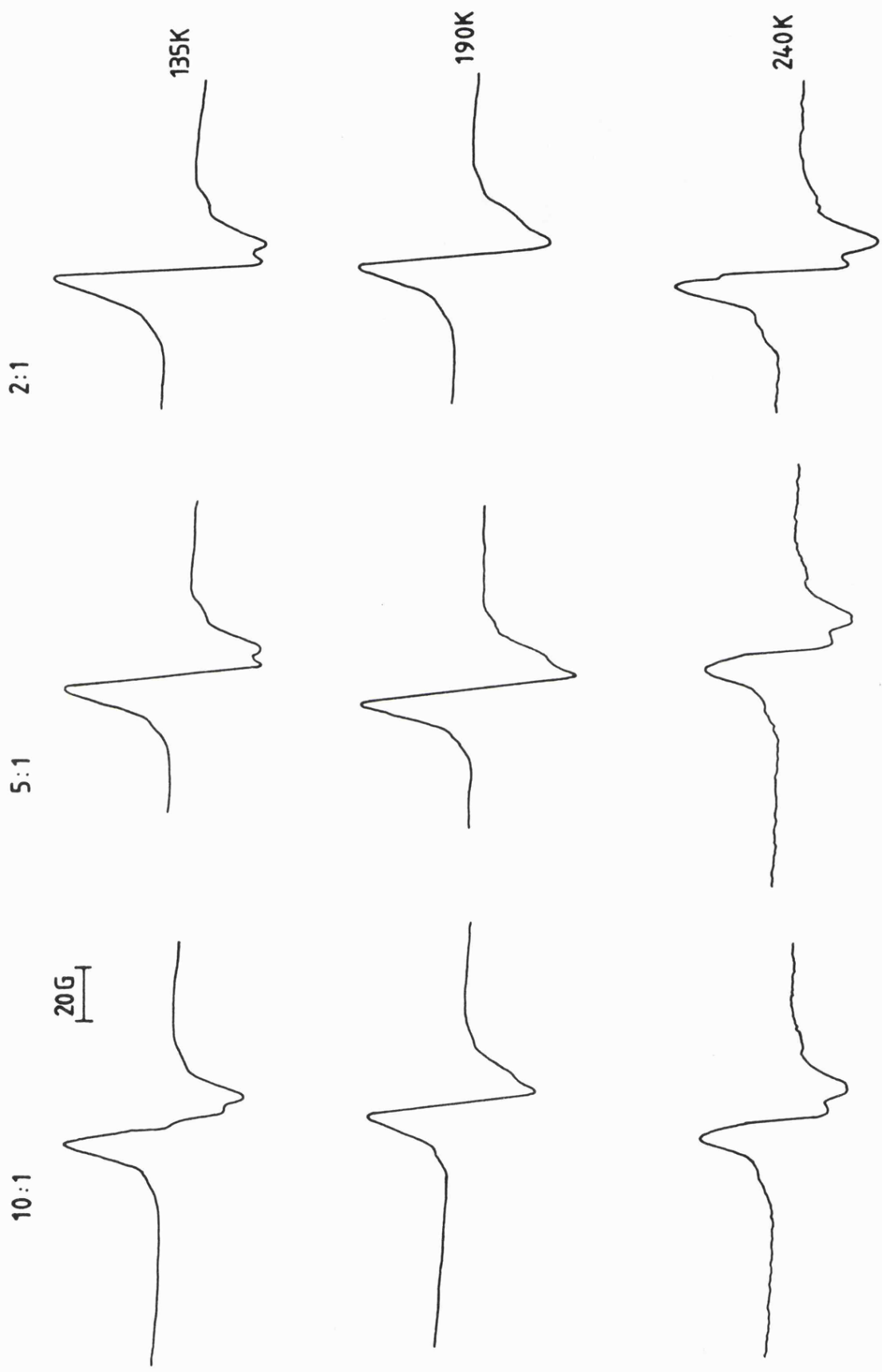


FIGURE 7b  
Hg/DNA at various concentrations.

whilst the anion was successfully generated in a CD<sub>3</sub>OD/D<sub>2</sub>O matrix (Figure 8). The spectrum comprises of signals arising from the magnetic isotope <sup>195</sup>Pt,  $I = \frac{1}{2}$  as well as from the naturally abundant non-magnetic isotopes. The x ( $g_x = 2.6$ ) and y ( $g_y = 2.3$ ) features from the non-magnetic isotopes are clearly visible whilst the z feature is probably at free spin hidden by the solvent radicals. The <sup>195</sup>Pt has  $A_x = 920$  G with  $g_x(+\frac{1}{2}) = 3.22$  whilst  $g_x(-\frac{1}{2})$  is probably hidden by the tail end of the large non-magnetic y feature. The feature at  $g = 2.77$  is probably  $g_y(+\frac{1}{2})$  with a hyperfine splitting of ca. 1000 G making  $g_y(-\frac{1}{2})$  hidden at free spin. The z features are difficult to assign although the small peak at  $g = 1.71$  could be  $g_z(-\frac{1}{2})$ .

On irradiating the cis Pt-DNA complexes, small signals attributable to a  $d^7$  electron loss centre at Pt were seen. These signals were of very low intensity in the studied cis Pt-DNA samples. Hence a sample of very high [cis Pt] was made which had a cis Pt/nucleotide ratio of 1:1. The high [cis Pt] caused the DNA to precipitate from solution. Analysis of these irradiated samples showed signals of the type obtained in the non-precipitated solutions. Figure 9 shows the spectrum of the Pt species obtained from the precipitated DNA-cis Pt sample. The 77 K spectrum consists of a species  $\alpha$  which converts, on anneal, to a new species  $\beta$ , presumably as the Pt centre relaxes to a new conformation. Both species have small satellite splittings [ $A_1(\alpha) = 40$  G,  $A_1(\beta) = 14$  G] and small  $\Delta g$  values which is consistent with a  $d^7$  complex. The  $d^7$  complex is presumably formed by hole capture, reducing  $[G^+]$  which was verified in the cis Pt-DNA spectra discussed below.

Three samples of 10, 50 and 100 mg ml<sup>-1</sup> DNA in D<sub>2</sub>O  $\pm$  cis Pt were examined to monitor the effect of [cis Pt] on the DNA spectra. Samples of 50 and 100 mg ml<sup>-1</sup> DNA in H<sub>2</sub>O  $\pm$  cis Pt were also examined. The

FIGURE 8

Cis Pt anion in  $\text{CD}_3\text{OD}/\text{D}_2\text{O}$  glass.

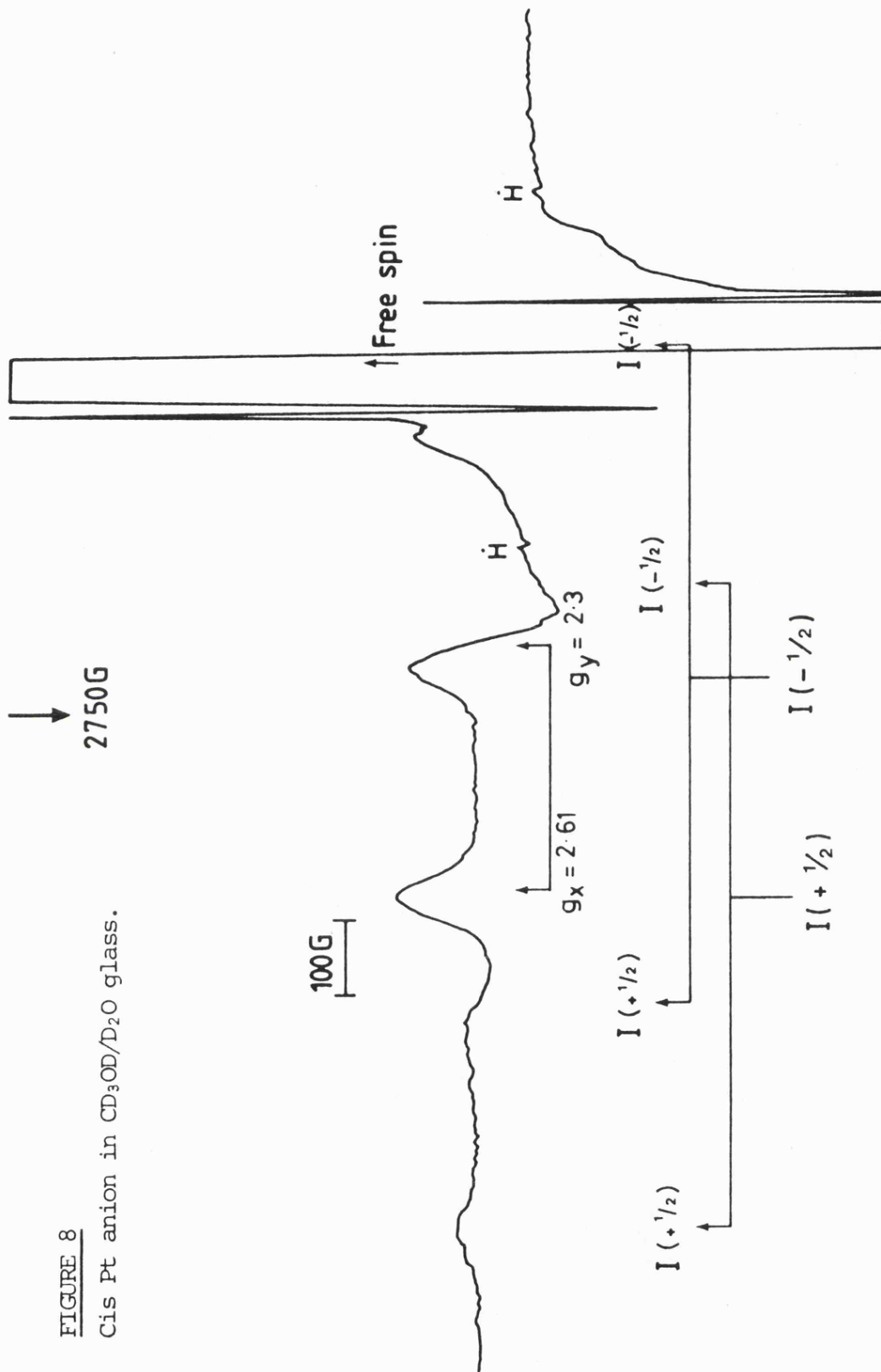
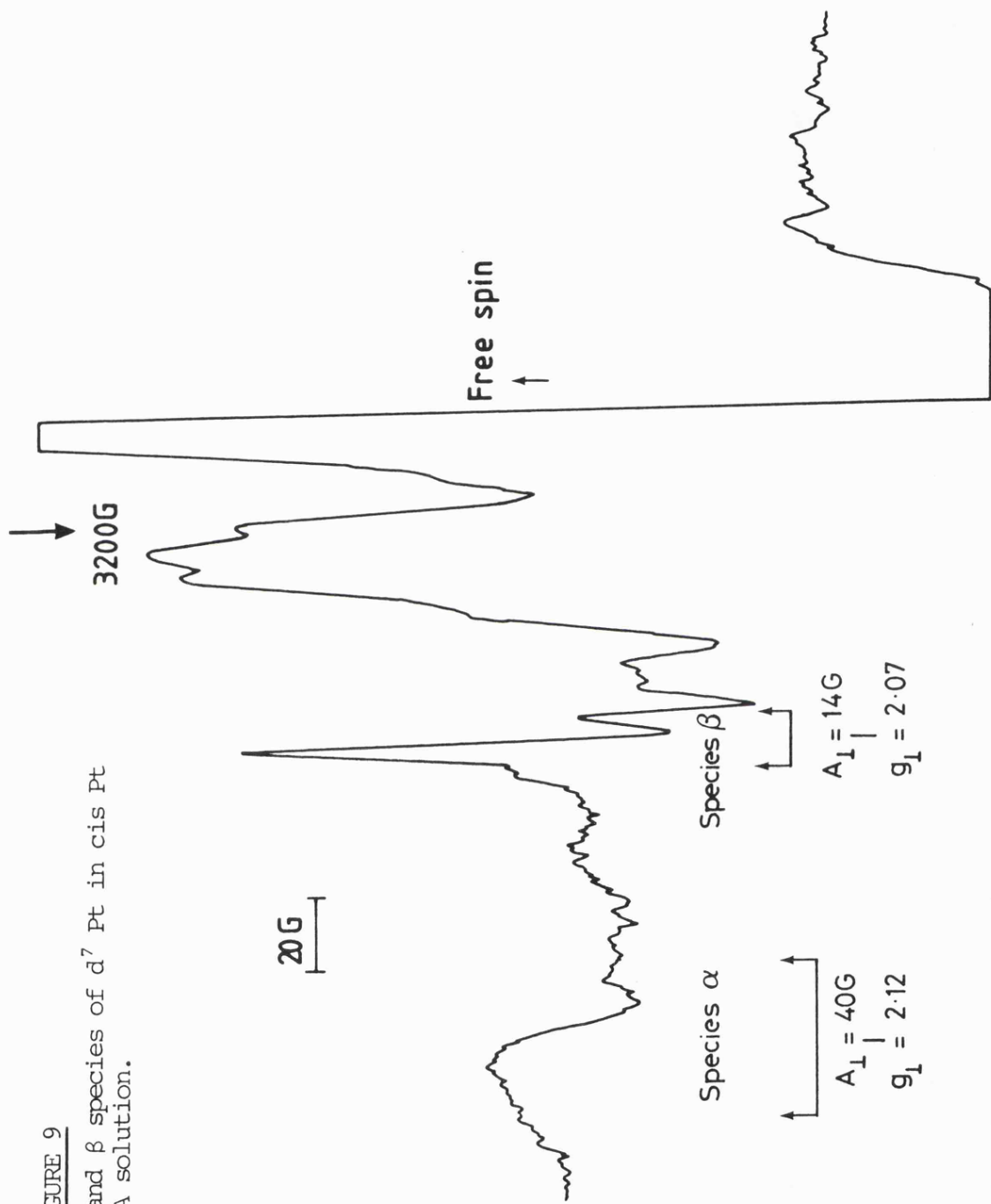


FIGURE 9

$\alpha$  and  $\beta$  species of  $d^7$  Pt in cis Pt DNA solution.



100 mgs ml<sup>-1</sup> samples (with a 25:1 nucleotide/Pt ratio) show a very slight loss of T<sup>-</sup> compared with the control, about 4%, in the 135 K spectra. The cis Pt containing samples annealed in the same way as the control samples until 230 K when a small amount of a new radical appeared. In the case of the 50 mgs ml<sup>-1</sup> samples (with a 12:1 nucleotide/Pt ratio) a 10% total reduction in yield is shown by subtraction, equivalent to a 14% reduction in G<sup>+</sup> and a 6% reduction in T<sup>-</sup>. On warming the samples to 210 K, the spectrum of the new radical again appeared and was sufficiently strong at 230 K to be identified as the radical X (found in the HgCl<sub>2</sub>-DNA spectra) as shown in Figure 10b. The cis Pt containing sample in H<sub>2</sub>O is clearly deficient in TH on comparison with the control. This trend is confirmed in the 10 mgs ml<sup>-1</sup> DNA cis Pt samples (nucleotide/Pt ratio is 4:1). The total yield is reduced by 14% corresponding to a 28% reduction in G<sup>+</sup>. Warming to higher temperatures again resulted in the clear formation of radical X.

The decreased formation of G<sup>+</sup> with increasing [cis Pt] correlates with the increase in size of the d<sup>7</sup> cis Pt signal with increasing [cis Pt], indicating competitive hole capture. The small amount of reduction in T<sup>-</sup> could be due to electron capture at cis Pt to form a d<sup>9</sup> Pt anion. Although no anion spectrum was detected, the reduction in T<sup>-</sup> is only very small and, therefore, the corresponding anion spectrum would only be very low in intensity and probably broad due to its spread of g-values.

### NaI

NaI was used as an additive in these studies as it is known to be a hole scavenger, but not an electron-scavenger,<sup>150</sup> and was thus used to compete with G for hole capture. Any scavenging by I<sup>-</sup> would be of interest as I<sup>-</sup> is the only additive in this study that doesn't bind to DNA.

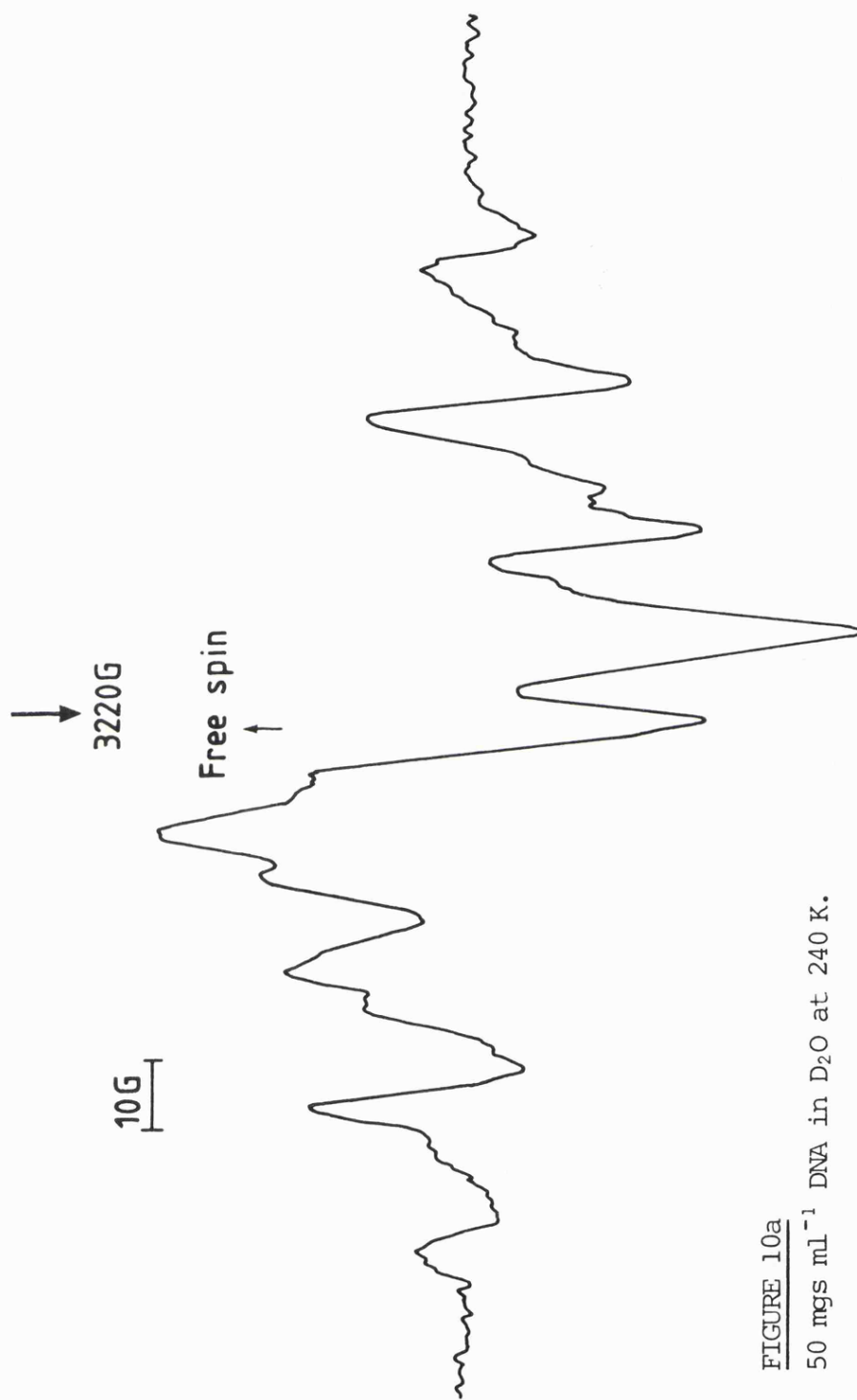


FIGURE 10a  
50 mgs ml<sup>-1</sup> DNA in D<sub>2</sub>O at 240 K.

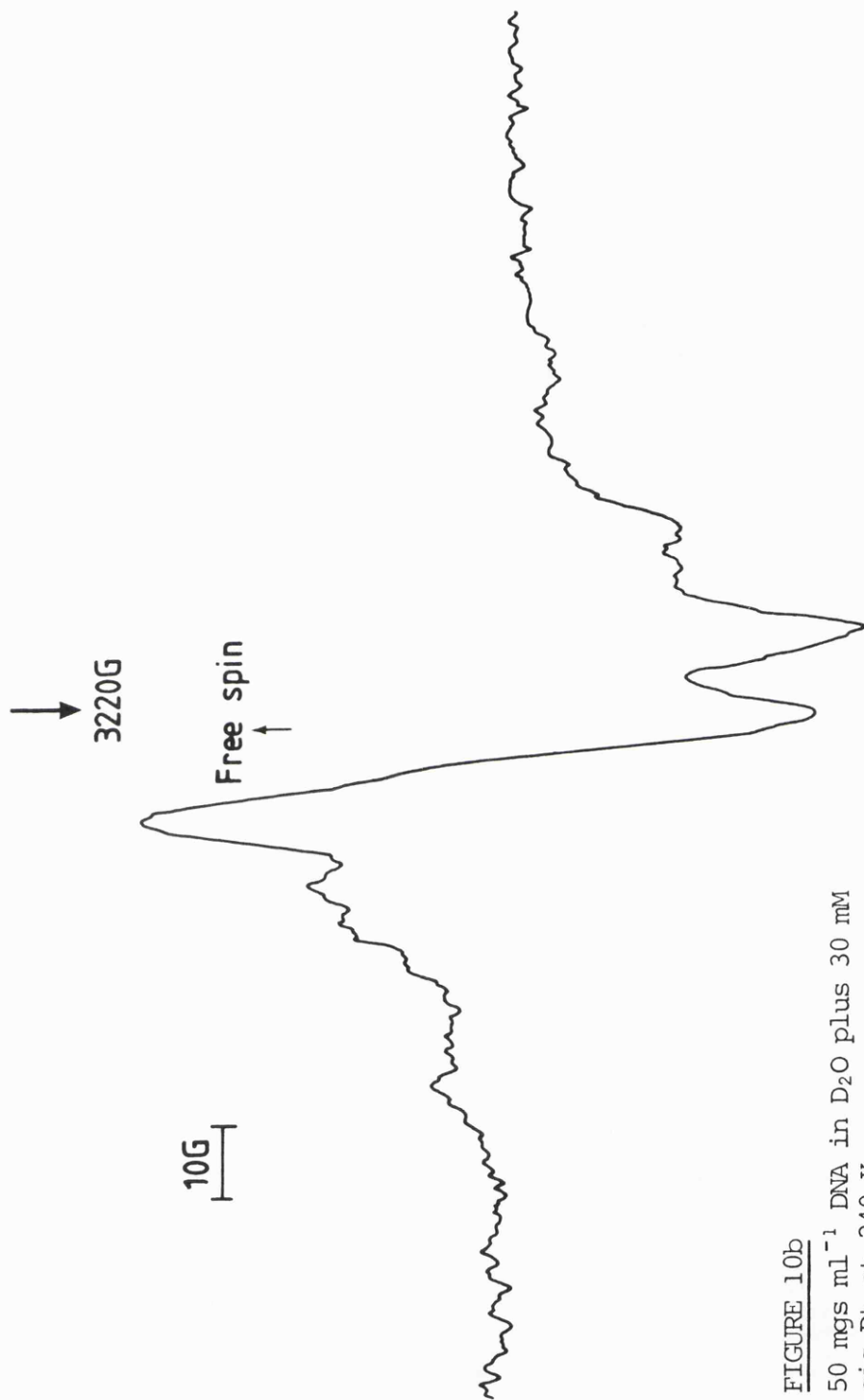


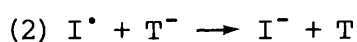
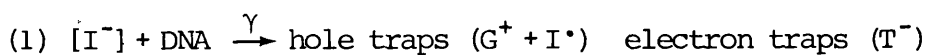
FIGURE 10b  
50 mgs ml<sup>-1</sup> DNA in D<sub>2</sub>O plus 30 mM  
cis Pt at 240 K.

Three experiments were carried out using 100, 50 and 10 mgs ml<sup>-1</sup> DNA in D<sub>2</sub>O solutions with 30 mM I<sup>-</sup> (making the nucleotide/I ratio 10:1, 5:1 and 1:1). In the case of the 100 mgs ml<sup>-1</sup> sample, total radical yield was reduced by 15% and subtractions from the control showed that G<sup>+</sup> yield was reduced by 20% whilst T<sup>-</sup> yield was reduced by 10%. The 50 mgs ml<sup>-1</sup> sample with 30 mM I<sup>-</sup> reduced overall yield by 25%. In terms of G<sup>+</sup> and T<sup>-</sup> subtractions showed a 45% loss of G<sup>+</sup> with only a 5% loss of T<sup>-</sup>. This value is within our experimental error. The 10 mgs ml<sup>-1</sup> sample with added I<sup>-</sup> induced a total yield reduction of 35%, subtractions from the control showed this to consist of a 70% G<sup>+</sup> reduction with no change in the T<sup>-</sup> component yield. The samples did not produce any new radicals on annealing.

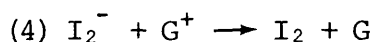
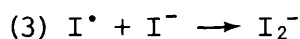
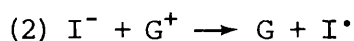
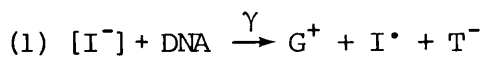
Although the reduction in G<sup>+</sup> yield was expected, the reduction in T<sup>-</sup> (in dilute [I<sup>-</sup>]) was not. To explain these observations the following Scheme is proposed:-

#### Scheme 4

(a) dilute [I<sup>-</sup>]



(b) concentrated [I<sup>-</sup>]



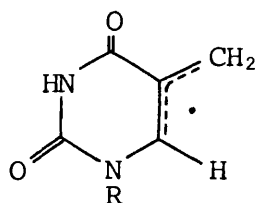
In the dilute [I<sup>-</sup>] case, I<sup>-</sup> captures holes thereby reducing G<sup>+</sup>. The I<sup>•</sup> that is formed might be mobile and hence might undergo electron transfer with T<sup>-</sup> to regenerate I<sup>-</sup> and reduce [T<sup>-</sup>]. This reaction is not likely to occur to any great extent. In the concentrated [I<sup>-</sup>] case, iodine

radicals (produced by hole capture) react with  $I^-$ , as it is present in high concentrations, to produce  $I_2^-$  (a very broad line at  $g = 2.4$ , probably attributable to  $I_2^-$ , was present in spectra of high  $[I^-]$  samples).  $I_2^-$  can go on to react with  $G^+$  thus decreasing its yield. These results show that  $I^-$  competes successfully for the holes in DNA at high  $[I^-]$  showing that additives don't have to be bound to the DNA to scavenge holes or electrons.

### Radical(s) X

As mentioned earlier, novel features, herein assigned to "X", were discovered in the spectra of DNA containing  $HgCl_2$  and cis Pt. This radical (Figure 11) is distinguished by having two outer lines split into doublets of ca. 5 G spacing. The central part of the spectrum consists of a triplet of approximately 7 G splitting.

In order to identify this radical the constituent nucleotide spectra were studied. From these two possible contenders were found. The first is a radical whose spectra is identical to that for X except that it contains a doublet as opposed to a triplet in the centre of the spectrum. The difference could be explained by the fact that the spectrum of X may be composed of two radicals, one of which is a central singlet. This X-like radical is found in spectra of irradiated frozen aqueous solutions of dTMP and it probably arises from the  $-C(5), (CH_2), C(6)H-$  allyl radical which is produced by hydrogen abstraction from the methyl group of the thymine base. The structure is shown below:-



[R = deoxyribose]

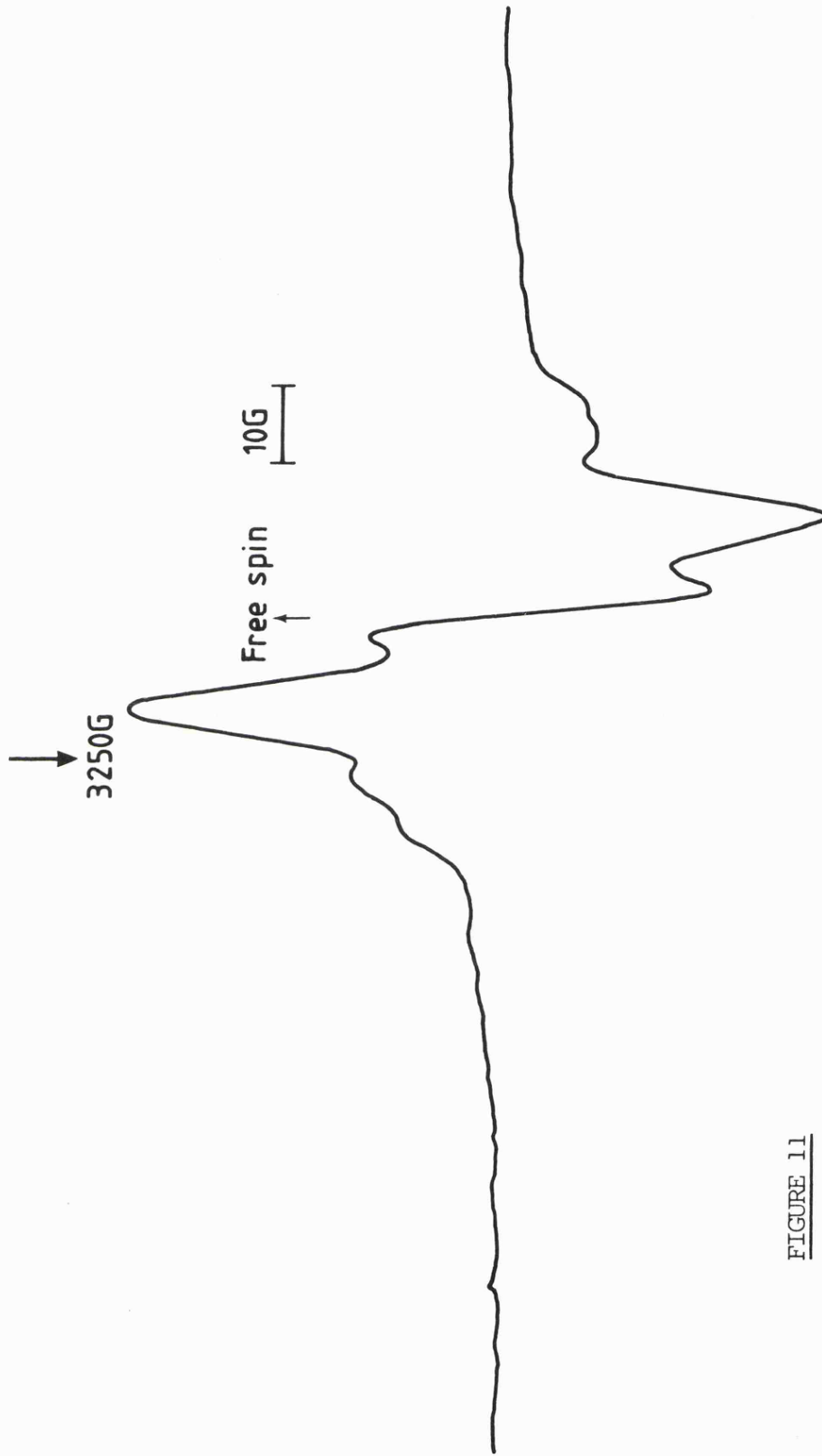


FIGURE 11  
Radical X generated in DNA  $Hg^{2+}$  sample.



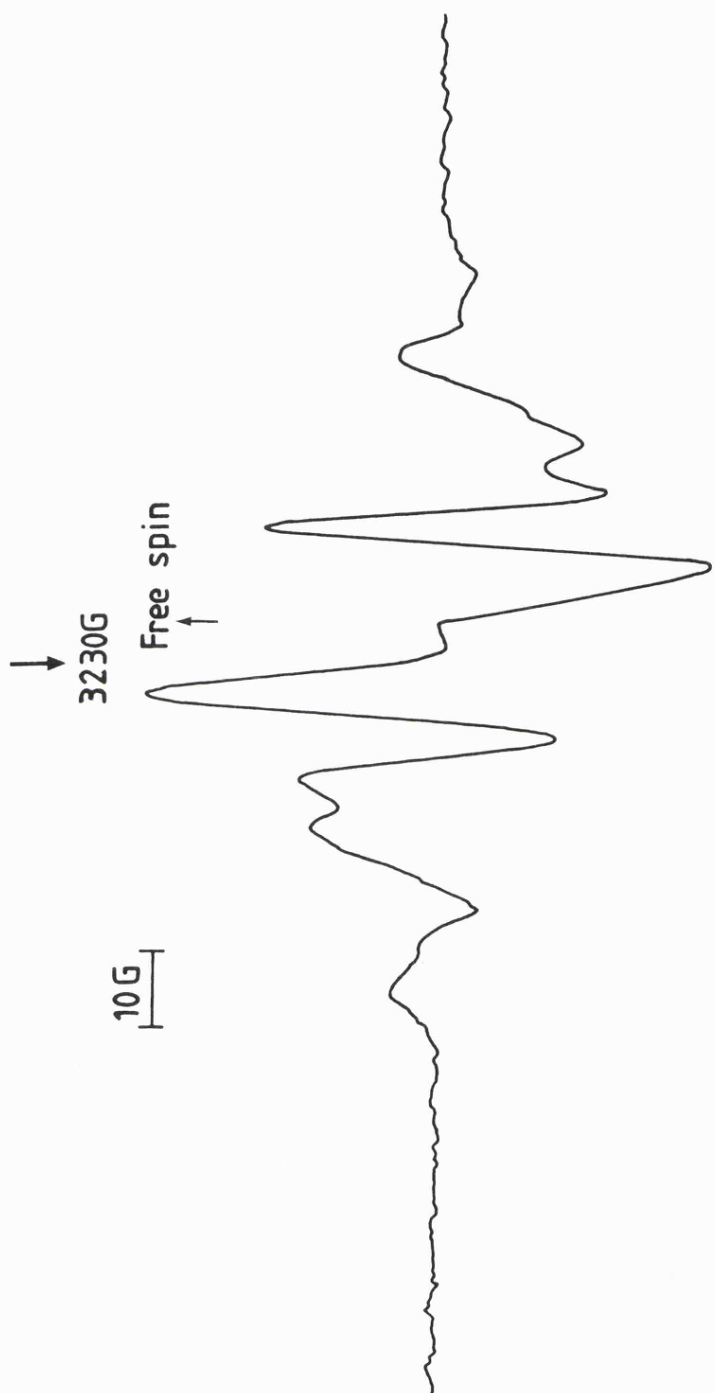


FIGURE 12  
Bromothymine in D<sub>2</sub>O at 190 K.

The spectrum, produced by careful anneal of frozen aqueous solutions, was almost identical to that of species X as it contained a triplet type structure in the centre. In the powder form dCMP exhibited the same pink colour as was seen in the dTMP powders, which is indicative of the characteristic 550 nm absorption of a delocalised allylic type radical.<sup>157</sup> The spectrum is therefore presumably composite containing features from the allyl radical with a central singlet superimposed. Clearly, such a radical could not be produced in the cytosine base (which, after irradiation, formed the C<sub>5</sub>H radical upon anneal) and, therefore, must originate from the sugar moiety. As the spectrum was reproduced in both cytidine and deoxycytidine, the spin-density must be located on the C<sub>4</sub>' or C<sub>5</sub>' side of the ribose ring. Such a radical has been identified in single crystal studies of cytidine,<sup>158</sup> 3'-cytidylic acid<sup>159</sup> and 5'-dCMP.<sup>160</sup> In the crystalline state this radical is stable up to 150°C.<sup>159</sup> The principal values and g-values for this radical in cytidine<sup>150</sup> are listed below in Table 4.

TABLE 4

A ( $\alpha$ H <sub>1</sub> )	A ( $\alpha$ H <sub>2</sub> )	A ( $\alpha$ H <sub>3</sub> )	g
23.67	24.56	13.25	2.0031
15.53	15.49	9.64	2.0025
7.39	7.25	4.82	2.0021

The powder spectrum of cytidine is shown in Figure 13. Bernhard *et al.*<sup>159</sup> suggest that the structure of this allyl-type radical is slightly altered between cytidine and 3'-CMP. This statement is based on the fact that they discovered two small  $\beta$ (H) splittings in 3'-CMP which were absent in cytidine. One of these splittings has an isotropic value of 2.7 G and is attributed to interaction with the C<sub>1</sub>' proton (via resonance delocalisation) whilst the other coupling is very small (< 1G)

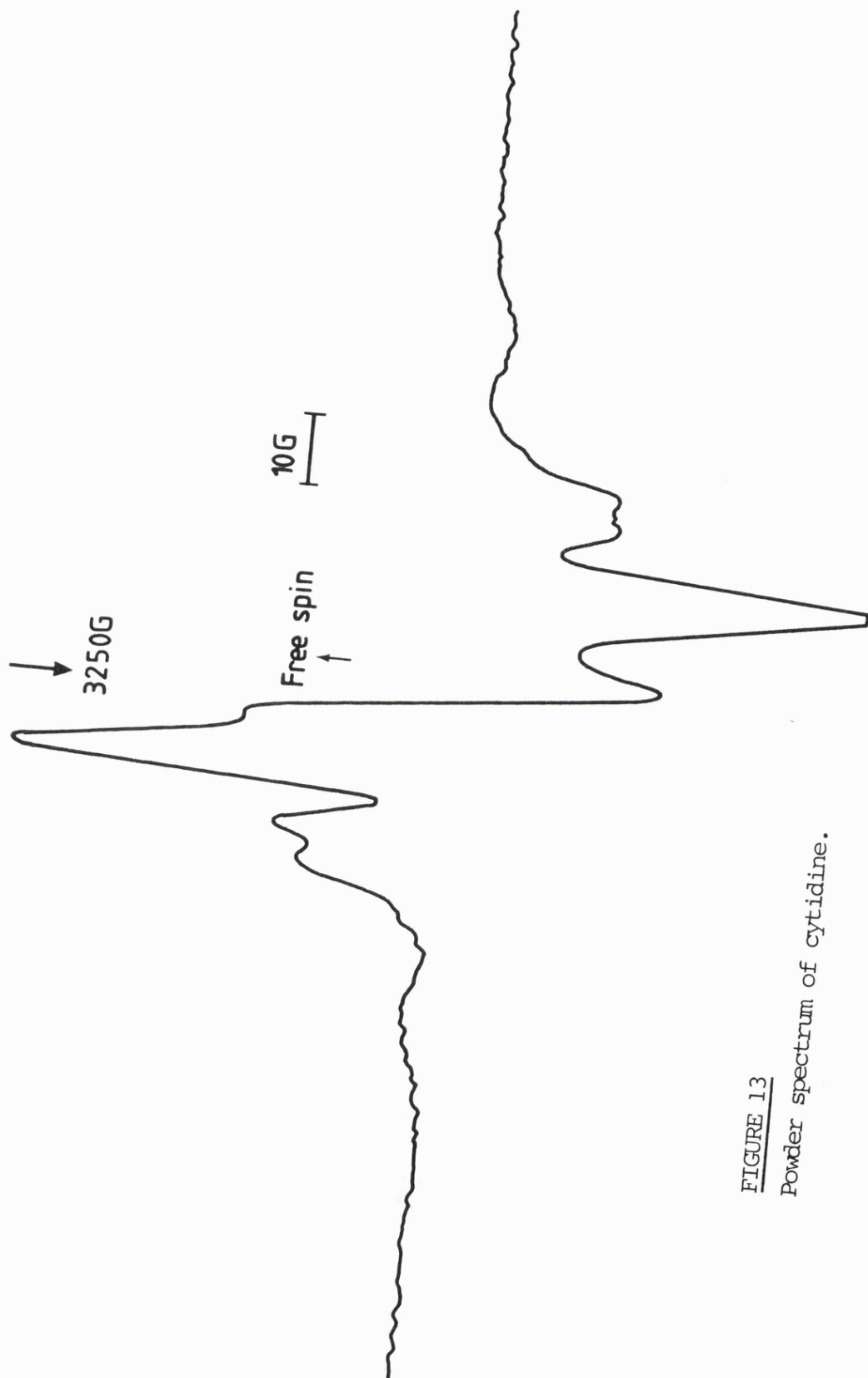
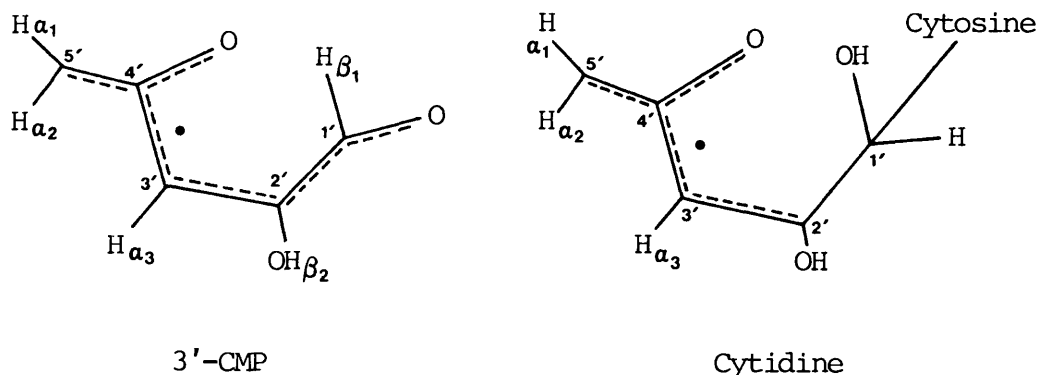


FIGURE 13  
Powder spectrum of cytidine.

and is suggested to result from interaction with the proton of the hydroxyl group on C<sub>2</sub>'.

The suggested allyl radicals in CMP and cytidine have the following structures according to Bernhard et al.



The delocalisation around the sugar explains the interaction with the two  $\beta(\text{H})$ s in 3'-CMP which does not occur in cytidine. Furthermore, the delocalisation of the spin-density onto C<sub>2</sub>' and O explains the reduced value of  $A(\text{H}\alpha_3)$  as compared to that of the equivalent  $A(\text{H}\alpha_1$  and  $\text{H}\alpha_2)$ . Bernhard et al. proposed<sup>159</sup> that these allyl radicals are decay products of the  $\text{ROC}_5'\text{H}$  radical ( $\text{R}=\text{H}$  in 3'-CMP) which is formed by hydrogen abstraction from C<sub>5</sub>'. Such a conversion provides an explanation for the formation of strand breaks and for the release of free base<sup>161</sup> in irradiated aqueous solutions of DNA. A possible precursor of the  $\dot{\text{C}}_5'$  is the  $\dot{\text{C}}_1'$  radical. This radical could be produced by hydrogen abstraction from the  $\dot{\text{C}}_6\text{H}$  radical of the cytosine base, which in turn is formed from the cytosine anion. This postulated sequence of events offers a possible mechanism for the conversion of base damage into strand breaks (i.e. cleavage of the phosphodiester bond) in  $\gamma$ -irradiated DNA.

The X spectrum has also been seen in other DNA systems. Firstly, it can be detected in large quantities in DNA that has been denatured or degraded as a result, for instance, of long-term storage at ambient

temperatures. Consequently, it is vitally important to run control samples in tandem with each experiment. Notably, Rotlevi et al.<sup>162</sup> have published a paper on "the effects of metal ions on radical formation in  $\gamma$ -irradiated DNA in the solid state" in which they show spectra of additive-free DNA comprising predominantly of features clearly attributable to the radical X.

Secondly, Wren et al.<sup>163</sup> have shown that X-like radicals are produced in samples of DNA containing iodoacetamide. By use of perdeuterated iodoacetamide they showed that the decay product,  $\dot{C}D_2CONH_2$ , abstracts a proton from DNA producing an X-like spectrum at 200 K.

#### SUMMARY AND CONCLUSIONS

The four compounds were all found to be effective in reducing overall DNA radical yields as judged by ESR. The order of protection against damage afforded by each compound was as follows:  $CuCl_2 \cdot 2H_2O > HgCl_2 > NaI > cis Pt$ . A reduction in DNA damage resulted from the fact that the additive centres underwent redox reactions with the radiation products, verified by changes in metal ion signals. As well as reducing the overall DNA radical yield certain of the additives, namely cis Pt and  $HgCl_2$ , gave rise to the formation of a novel radical denoted X.

The protective effect of  $CuCl_2 \cdot 2H_2O$  was very significant due to the fact that it was the only additive to reduce both  $[T^-]$  and  $[G^+]$ , resulting in a near complete loss of DNA signal at high  $Cu^{2+}$ /nucleotide ratios.  $HgCl_2$  was a less effective radioprotective additive than  $CuCl_2 \cdot 2H_2O$  as it only underwent oxidation reactions. At high temperatures and high relative  $[HgCl_2]$  the radical X was discovered after the decay of the guanine cation. The effect of the other two additives was less dramatic. NaI, which does not bind to DNA, acted as a hole trap reducing

[G<sup>+</sup>] by 70% at high [I<sup>-</sup>]. Cis Pt, which is known to bind to DNA forming inter- and intrastrand crosslinks, only had a weak effect on DNA radical yields reducing [G<sup>+</sup>] by some 30% as well as slightly affecting the [T<sup>-</sup>]. At higher temperatures the radical X is produced and the protonation of the thymine anion is largely inhibited.

The radical X was discovered both in denatured DNA samples and in samples that had been incubated with cis Pt or HgCl<sub>2</sub>. Both of the compounds are known to significantly alter the DNA structure, lowering the T<sub>m</sub> and intrinsic viscosity, thus I conclude that this radical is produced as a result of the rearrangement of the DNA structure through partial denaturation. As I discussed earlier the radical X has at least two possible structures; a sugar radical in CMP or a base radical in TMP. The latter structure would mean that partial denaturation of the DNA increases the electro-positive nature of the thymine base forming the cation, T<sup>+</sup>, which subsequently decays into the allylic radical T<sub>4</sub>. The lack of evidence for the formation of the thymine cation rules against the likelihood of T<sub>4</sub> being the structure of radical X.

The other possible radical is a delocalised sugar based one. A mechanism has been put forward for the formation of such a radical from the primary DNA irradiation products (base radicals) which covers the formation of single strand breaks in  $\gamma$ -irradiated DNA (inherent in the production of such a radical). The fact that this radical is produced in significant amounts implies that the two additives (particularly HgCl<sub>2</sub>) had more of a sensitizing effect than a protective one. However, it must be borne in mind that this radical may well have a greater thermal stability (due to resonance delocalisation) than those found in unaltered DNA.

As a follow-up to this work experiments should be done on RNA samples,

incubated with  $\text{HgCl}_2$ , to verify the nature of radical X (as RNA contains no thymine).

## REFERENCES FOR CHAPTER 5

1. Nucleic Acid - Metal Ion Interactions, ed. T. G. Spiro, 1980, Wiley, N.Y.
2. Podder, S.K., J. Magn. Res., 1974, 15, 254.
3. Mansy, S., Tobias, R.S., J. Am. Chem. Soc., 1974, 96, 6874.
4. Yamane, T., Davidson, N., Biochim. Biophys. Acta, 1962, 55, 609.
5. Katz, S., J. Am. Chem. Soc., 1952, 74, 2238.
6. Yamane, T., Davidson, N., J. Am. Chem. Soc., 1961, 83, 2599.
7. Williams, M.N., Crothers, D.M., Biochem., 1975, 14, 1944.
8. Gruenwedel, D.W., Davidson, N., J.M.B., 1966, 21, 129.
9. Gruenwedel, D.W., Davidson, N., Biopolymers, 1967, 5, 847.
10. Richard, H., Schreiber, J.P., Daune, M., Biopolymers, 1973, 12, 1.
11. Shin, Y.A., Biopolymers, 1973, 12, 2459.
12. Shin, Y.A., Heim, J.M., Eichhorn, G.L., Bioinorg. Chem., 1972, 1, 149.
13. Zimmer, Ch., Luck, G., Triebel, A., Biopolymers, 1974, 13, 425.
14. Beerman, T.A., Lebowitz, J., J.M.B., 1973, 79, 451.
15. Arya, S.K., Yang, J.T., Biopolymers, 1975, 14, 1847.
16. Clark, P., Eichhorn, G.L., Biochem., 1974, 13, 5098.
17. Dimitri, K., Ukarov, L., Bio fizika, 1980, 25, 615.
18. Axel, W., Luck, G., Nucl. Acid Res., 1977, 4, 539.
19. Walter, A., Stud. Biophys., 1980, 81, 81.
20. Johnson, N.P., Middle Atlantic Regional Meeting, American Chemical Society, 1978.
21. Stone, P.J., Kelman, A.D., Sinex, F.M., Nature, 1974, 251, 736.
22. Howe-Grant, M., Wu, K.C., Bauer, W.R., Lippard, S.J., Biochem., 1976, 15, 4339.
23. Butour, J.L., Macquet, J.P., Eur. J. Biochem., 1977, 78, 455.
24. Thomson, A.J., Williams, R.J.P., Reslova, S., Structure and Bonding, 1972, 11, 1.
25. Chu, G.Y.H., Mansy, S., Duncan, R.E., Tobias, R.S., J. Am. Chem. Soc., 1978, 100, 593.
26. Harder, H.C., Chem-Biol. Int., 1975, 10, 27.
27. Shooter, K.V., Merrifield, R.K., Biochim. Biophys. Acta, 1972, 287, 16.
28. Cohen, G.L., Bauer, W.R., Barton, J.K., Lippard, S.J., Science, 1979, 203, 1014.
29. Macquet, J.P., Theophanides, T., Bioinorg. Chem., 1975, 5, 59.
30. Millard, M.M., Macquet, J.P., Theophanides, T., Biochim. Biophys. Acta, 1975, 402, 166.

31. Dehand, J., Jordanov, J., J.C.S. Chem. Comm., 1976, 598.
32. Goodgame, D.M.L., Jeeves, I., Phillips, F.L., Skapski, A.C., Biochim. Biophys. Acta, 1978, 378, 153.
33. Friedman, M.E., Tiggins, J.E., Fed. Proc., 1976, 35, 623.
34. Friedman, M.E., Melius, P., Tiggins, J.E., McAuliffe, C.A., Bioinorg. Chem., 1978, 8, 341.
35. Rosenberg, B., Van Camp, L., Krigas, T., Nature, 1965, 205, 698.
36. Rosenberg, B., Van Camp, L., Grimley, E.B., Thomson, A.J., J. Biol. Chem., 1967, 242, 1347.
37. Rosenberg, B., Van Camp, L., Trosko, J.E., Mansour, V.H., Nature, 1969, 222, 385.
38. Cisplatin. Current Status and New Developments, eds. Prestayko, A.W., Crooke, S.T., Carter, S.K., Academic Press, New York, 1980.
39. Van Kralingen, C.G., Reedijk, J., Biochimie, 1978, 60, 1057.
40. Van Kralingen, C.G., Ph.D. Thesis, Delft University of Technology, 1979.
41. Reslova, S., Chem. Biol. Interact., 1971, 4, 66.
42. Rosenberg, B., Biochimie, 1978, 60, 859.
43. Turnball, D., Popescu, N.C., DiaPaolo, J.A., Myhr, B.C., Mutat. Res., 1979, 66, 267.
44. Wiencke, J.K., Cervenka, J., Paulus, H., Mutat. Res., 1979, 68, 69.
45. Lecointe, P., Macquet, J.P., Butour, J.L., Paoletti, C., Mutat. Res., 1977, 48, 139.
46. Lecointe, P., Macquet, J.P., Butour, J.L., B.B. Res. Comm., 1979, 90, 209.
47. Andersen, K.S., Mutat. Res., 1979, 67, 209.
48. Johnson, N.P., Hoeschele, J.D., Rahn, R.O., O'Neill, J.P., Hsie, A.W., Cancer Res., 1980, 40, 1463.
49. Leopold, W.R., Batzinger, R.P., Miller, E.C., Miller, J.A., Earhart, R.H., Cancer Res., 1981, 41, 4368.
50. Cocchiarella, L., Mattern, I.E., Van Kralingen, C.G., Mutat. Res., 1980, 74, 252.
51. Konishi, H., Usui, T., Sawada, H., Uchino, H., Kidani, Y., Gann., 1981, 72, 627.
52. Brouwer, J., van de Putte, P., Fichtinger-Schepman, A.M.J., Reedijk, J., PNAC USA, 1981, 78, 7010.
53. Harder, H.C., Rosenberg, B., Int. J. Cancer, 1970, 6, 207.
54. Harder, H.C., Smith, R.G., Leroy, A.F., Cancer Res., 1976, 36, 3821.
55. Pascoe, J.M., Roberts, J.J., Biochem. Pharmacol., 1974, 23, 1345.
56. Johnson, N.P., Hoeschele, J.D., Kuemmerle, N.B., Masker, W.E., Rahn, R.O., Chem. Biol. Interact., 1978, 23, 267.

57. Rahn, R.O., Johnson, N.P., Hsie, A.W., Lemont, J.F., Masker, W.E., Regan, J.D., Dunn, W.C. Jr., in "The Scientific Basis of Toxicity Assessment" (ed. H. Witschi), Elsevier/North Holland Biomedical Press, New York, 1980, p.153.
58. Srivastava, R.C., Froelich, J., Eichhorn, G.L., Biochimie, 1978, 60, 879.
59. Hermann, D., Houssier, C., Guschlbauer, W., Biochim. Biophys. Acta, 1979, 564, 456.
60. Munchausen, L.L., Rahn, R.O., Biochim. Biophys. Acta, 1975, 414, 242.
61. de Pauw-Gillet, M.C., Houssier, C., Fredericq, E., Chem. Biol., 1979, 25, 87.
62. Macquet, J.P., Butour, J.L., Biochimie, 1978, 60, 901.
63. Mong, S., Huang, C.H., Prestayko, A.W., Crooke, S.T., Cancer Res., 1980, 40, 3313.
64. Horacek, P., Drobnik, J., Biochim. Biophys. Acta, 1971, 254, 341.
65. Ganguli, P.K., Theophanides, T., Eur. J. Biochem., 1979, 101, 377.
66. Mansy, S., Rosenberg, B., Thomson, A.J., J. Am. Chem. Soc., 1973, 95, 1633.
67. Drobnik, J., Horacek, P., Chem-Biol. Interact., 1973, 7, 223.
68. Barton, J.K., Lippard, S.J., Ann. N.Y. Acad. Sci. (USA), 1978, 313, 686.
69. Voet, D., Rich, A., Prog. Nucl. Acid Res. Mol. Biol., 1970, 10, 183.
70. Izatt, R.M., Christiensen, J.J., Rytting, J.H., Chem. Rev., 1971, 71, 439.
71. Conner, T.O., Johnson, C., Scovell, W.M., Biochim. Biophys. Acta, 1976, 447, 484.
72. Markowski, V., Sullivan, G.R., Roberts, J.D., J. Am. Chem. Soc., 1977, 99, 714.
73. Cochran, W., Acta Cryst., 1951, 4, 81.
74. Krant, J., Jensen, L.H., Acta Cryst., 1963, 16, 79.
75. Sundaralingsham, M., Acta Cryst., 1966, 21, 495.
76. Lewin, S., J. Chem. Soc., 1964, 792.
77. Roberts, B.W., Lambert, J.B., Roberts, J.D., J. Am. Chem. Soc., 1965, 87, 5439.
78. Kong and Theophanides, Inorg. Chem., 1974, 13, 1167.
79. Kong and Theophanides, Inorg. Chem., 1974, 13, 1981.
80. Kong and Theophanides, Inorg. Chem. Bioinorg. Chem., 1975, 5, 51.
81. Chu, G.Y.H., Tobias, R.S., J. Am. Chem. Soc., 1976, 98, 2641.
82. Gellert, R.W., Bau, R., J. Am. Chem. Soc., 1975, 97, 7379.
83. Cramer, R.E., Dahlstrom, P.L., J. Clin. Hematol. Oncol., 1977, 7, 330.

84. Cramer, R.E., Dahlstrom, P.L., J. Am. Chem. Soc., 1979, 101, 3679.
85. Kistenmacher, T.J., Chiang, C.C., Chalilpoyil, P., Marzilli, L.G., J. Am. Chem. Soc., 1979, 101, 1143.
86. Terzis, A., Hadjiliades, N., Rivest, R., Theophanides, T., Inorg. Chim. Acta, 1975, 12, L5.
87. Terzis, A., Inorg. Chem., 1976, 15, 793.
88. Marcelis, A.T.M., Van Kralingen, C.G., Reedijk, J., J. Inorg. Biochem., 1980, 13, 213.
89. Marcelis, A.T.M., Ph.D. Thesis, State University of Leiden, 1982.
90. Roberts, J.J., Pascoe, J.M., Nature, 1972, 235, 282.
91. Munchansen, L.L., PNAC USA, 1974, 71, 4519.
92. Shooter, K.V., Howse, R.W., Merrifield, R.K., Robins, A.B., Chem. Biol. Interact., 1972, 5, 289.
93. Pera, M.F., Rawlings, C.R., Shackleton, J., Roberts, J.J., Biochim. Biophys. Acta, 1981, 655, 152.
94. Roberts, J.J., Friedlos, F., Biochim. Biophys. Acta, 1981, 655, 146.
95. Laurent, G., Erickson, L.C., Sharkey, N.A., Kohn, K.W., Cancer Res., 1981, 41, 3347.
96. Zwelling, L.A., Anderson, T., Kohn, K.W., Cancer Res., 1979, 39, 365.
97. Zwelling, L.A., Michaels, S., Swartz, H., Dobson, P.P., Kohn, K.W., Cancer Res., 1981, 41, 640.
98. Erickson, L.C., Zwelling, L.A., Ducore, J.M., Sharkey, N.A., Kohn, K.W., Cancer Res., 1981, 41, 2791.
99. Pera, M.F., Rawlings, C.J., Roberts, J.J., Chem. Biol. Interact., 1981, 37, 245.
100. Kelman, A.D., Peresie, H.J., Stone, P.J., J. Clin. Hematol. Oncol., 1976, 7, 440.
101. Stone, P.J., Kelman, A.D., Sinex, F.M., Bhargava, M.M., Halvorson, H.O., J. Mol. Biol., 1976, 104, 793.
102. Tullius, T.D., Lippard, S.J., J. Am. Chem. Soc., 1981, 103, 4620.
103. Royer-Pokora, B., Gordon, L.K., Haseltine, W.A., Nucl. Acid. Res., 1981, 9, 4595.
104. Cohen, G.L., Ledner, J.A., Bauer, W.A., Ushay, H.M., Caravana, C., Lippard, S.J., J. Am. Chem. Soc., 1980, 102, 2487.
105. Ushay, H.M., Tullius, T.D., Lippard, S.J., Biochem., 1981, 20, 3744.
106. Chottard, J.C., Girault, J.P., Chottard, G., Lallemand, J.Y., Mansuy, D., Nouv. J. Chim., 1978, 2, 551.
107. Girault, J.P., Chottard, G., Lallemand, J.Y., Chottard, J.C., Biochem., 1982, 21, 1352.

108. Chottard, J.C., Girault, J.P., Chottard, G., Lallemand, J.Y., Mansuy, D., J. Am. Chem. Soc., 1980, 102, 5565.
109. Jordanov, J., Williams, R.L.P., Bioinorg. Chem., 1978, 8, 77.
110. Inagaki, K., Kidani, Y., J. Inorg. Biochem., 1979, 11, 39.
111. den Hartog, J.H.J., Altona, C., Chottard, J.C., Girault, J.P., Lallemand, J.Y., de Leeuw, F.A.A.M., Marcelis, A.T.M., Reedijk, J., Nucl. Acid. Res., 1982, 10, 4715.
112. Fichtinger-Schepman, A.M.J., Lohman, P.H.M., Reedijk, J., Nucl. Acid. Res., 1982, 10, 5345.
113. Lippard, S.J., Hoeschele, J.D., PNAC USA, 1979, 76, 6091.
114. Macquet, J.P., Theophanides, T., Biopolymers, 1975, 14, 781.
115. Macquet, J.P., Theophanides, T., Inorg. Chim. Acta, 1976, 18, 189.
116. Macquet, J.P., Theophanides, T., Biochim. Biophys. Acta, 1976, 442, 142.
117. Sletten, E., J.C.S. Chem. Comm., 1971, 558.
118. Barton, J.K., Lippard, S.J., Metal Ions in Biology, 1980, 1, 31.
119. Hadjiliadis, N., Theophanides, T., Inorg. Chim. Acta, 1976, 16, 77.
120. Kistenmacher, T.J., Marzilli, L.G., Szalda, D.J., Acta Cryst., 1976, B32, 186.
121. Szalda, D.J., Kistenmacher, T.J., Marzilli, L.G., Inorg. Chem., 1975, 14, 2623.
122. Sletten, E., Thorstensen, B., Acta Crystal., 1974, B30, 2483.
123. Sletten, E., Ruud, N., Acta Cryst., 1975, B31, 982.
124. Sletten, E., Flogstad, N., Acta Cryst., 1976, B32, 461.
125. Acki, K., Clark, G.R., Orbell, J.D., Biochim. Biophys. Acta, 1976, 425, 369.
126. Berger, N.A., Eichhorn, G.L., Biochem., 1971, 10, 1847.
127. Szalda, D.J., Marzilli, L.G., Kistenmacher, T.J., B.B. Res. Comm., 1975, 63, 601.
128. Szalda, D.J., Marzilli, L.G., Kistenmacher, T.J., Inorg. Chem., 1975, 14, 2076.
129. Szalda, D.J., Marzilli, L.G., Kistenmacher, T.J., Acta Cryst., 1975, B31, 2416.
130. Nelson, H.C., Villa, J.F., J. Inorg. Nucl. Chem., 1980, 42, 1669.
131. Kistenmacher, T.J., Sorrel, T., Marzilli, L.G., Inorg. Chem., 1975, 14, 2479.
132. Zimmer, C., Luck, G., Fritzsche, H., Triebel, H., Biopolymers, 1971, 10, 441.
133. Rifkind, J.M., Skin, Y.A., Heim, J.M. Eichhorn, G.L., Biopolymers, 1976, 15, 1879.
134. Kosturko, L.D., Folzer, C., Stewart, R.F., Biochem., 1974, 13, 3949.

135. Authier-Martin, M., Beauchamp, A.L., Can. J. Chem., 1977, 55, 1213.
136. Authier-Martin, M., Hubert, J.H., Rivest, R., Beauchamp, A.L., Acta Cryst., 1978, B34, 273.
137. Young, P.R., Nandi, U.S., Kallenbach, N.R., J. Am. Chem. Soc., 1982, 21, 62.
138. Eichhorn, G.L., Clark, P., J. Am. Chem. Soc., 1963, 85, 4020.
139. Ding, D., Allen, F.S., Biochim. Biophys. Acta, 1980, 610, 72.
140. Yamane, T., Davidson, N., J. Am. Chem. Soc., 1961, 83, 2599.
141. Nandi, U.S., Wang, J.C., Davidson, N., Biochem., 1965, 4, 1687.
142. Katz, S., J. Am. Chem. Soc., 1952, 74, 2238.
143. Moore, A.M., Anderson, S.M., Can. J. Chem., 1959, 37, 590.
144. Adams, G.E., Cooke, M.S., Int. J. Rad. Biol., 1969, 15, 457.
145. Boon, P.J., Cullis, P.M., Symons, M.C.R., Wren, B.W., J. Chem. Soc., Perkin Trans. 2, 1984, 1393.
146. Hofer, H., Altmann, H., Int. J. Rad. Biol., 1971, 19, 459.
147. Gregoli, S., Olast, M., Bertinchamps, A.J., Rad. Res., 1982, 89, 238.
148. Wren, B.W., Cullis, P.M., Symons, M.C.R., unpublished results.
149. Gräslund, A., Ehrenberg, A., Rupprecht, A., Ström, G., Cresp, H., Int. J. Rad. Biol., 1975, 28, 313.
150. Nazhat, N., Weiss, J., Trans. Faraday Soc., 1970, 66, 1302.
151. Herak, J.N., McDowell, C.A., J. Magn. Res., 1979, 16, 434.
152. Pruden, B., Snipes, W., Gordy, W., PNAC, 1965, 53, 917.
153. Hüttermann, J., Int. J. Rad. Biol., 1971, 17, 249.
154. Gregoli, S., Olast, M., Bertinchamps, A.J., Rad. Res., 1976, 65, 202.
155. Sevilla, M.D., Van Paemel, C., Nichols, C., J. Phys. Chem., 1972, 76, 3571.
156. Sevilla, M.D., Engelhardt, M.L., Faraday Disc. Chem. Soc., 1977, 63, 255.
157. Myers, L.S., Hollis, M.L., Theard, L.M., Peterson, F.C., Warnick, A., J. Am. Chem. Soc., 1970, 92, 2875.
158. Hampton, D.A., Alexander, C., J. Chem. Phys., 1973, 58, 4891.
159. Bernhard, W.A., Hüttermann, J., Müller, A., Close, D.M., Fouse, G.W., Rad. Res., 1976, 68, 390.
160. Herak, J.N., Krilov, D., McDowell, C.A., J. Magn. Res., 1976, 23, 1.
161. Ullrich, M., Hagen, U., Int. J. Rad. Biol., 1971, 19, 507.
162. Rotlevi, E., Moss, H.M., Kominami, S., Riesz, P., Ann. N.Y. Acad. Sci., 1973, 222, 387.
163. Wren, B.W., Symons, M.C.R., Cullis, P.M., Gregoli, S., J. Chem. Soc., Perkin Trans. II, 1985, 1819.

# An ESR Study of $\gamma$ -Irradiated Haemoglobin and DNA

Nick Bartlett

---

## ABSTRACT

The first half of this thesis is concerned with studying the mechanism of autoxidation of haemoglobin and myoglobin. The paramagnetic  $\gamma$ -irradiated forms were used in this ESR study as the native protein is diamagnetic. On irradiation of haemoglobin distinct radical centres are seen representing the  $\alpha$  and  $\beta$  subunits formed by electron addition to the  $\text{FeO}_2$  unit. The radical yields are found to be both pH and solvent dependent. A similar centre is formed on irradiation of myoglobin which is pH but not solvent dependent.

Warming these centres above 77 K results in conversion into new centres with  $g$ -values approaching those of low-spin Fe(III). This conversion is interpreted mechanistically in terms of proton transfer from the distal histidine to the  $(\text{FeO}_2)^-$  unit [assuming that the  $(\text{FeO}_2)^-$  unit is hydrogen-bonded to the distal histidine]. Further anneal results in the loss of signal in the  $g=2$  region and the growth of the high-spin Fe(III) signal at  $g=6$  as a result of loss of  $\text{HO}_2^-$ .

To substantiate this theory experiments were done using haemoglobin *Glycera* which has a distal leucine instead of histidine (i.e. there are no hydrogen bonding sites available). The primary centre formed in this case has a  $g$ -value which is close to that of superoxide. This indicates that the centres formed in haemoglobin and myoglobin have more spin-density on iron which would result if the centres were hydrogen bonded.

The second half of the thesis concerns the mechanism of  $\gamma$ -irradiation damage in DNA. In irradiated frozen samples of DNA two ESR signals are found at 77 K. One has been shown to be the guanine cation, the other the thymine anion. Annealing these samples, in the absence of oxygen, results in the protonation of the anion and loss of the cation. Further anneal results in loss of signal altogether. As  $\gamma$ -irradiation produces strand breaks in DNA it is surprising that no sugar radicals are detected.

By incorporation of different additives I found that this mechanism of radical interconversion can be altered. Addition of electron scavengers such as  $\text{CuCl}_2$  prevented the formation of the thymine radicals without affecting the guanine cation yield. Addition of  $\text{I}^-$  had the reverse effect reducing the formation of guanine cations. However, addition of soft heavy metal compounds such as  $\text{HgCl}_2$  and  $\text{cis Pt}(\text{NH}_3)_2\text{Cl}_2$  resulted in the formation of a new radical which has identical parameters with radicals previously found in the sugar moiety of dCMP and in the thymine base moiety of dTMP.